Impact of Frailty on Cardiac Contractile Function in an Aging Mouse Model

by

Michael H. Sun

Submitted in partial fulfilment of the requirements
for the degree of Master of Science

at

Dalhousie University
Halifax, Nova Scotia
August 2014

Table of Contents

List of Tables

List of Figures

Abstract

This study quantified frailty in a longitudinal study in the mouse model and investigated whether frailty was a better predictor of changes in cardiac morphology and function than chronological age. Frailty scores progressively increased as mice aged. Echocardiography showed *in vivo* that left ventricular internal diameter increased as frailty increased while contractile function declined. Individual ventricular myocytes hypertrophied with increasing age and especially frailty, while peak contractions declined in myocytes from moderately frail mice in comparison to the least frail mice. By contrast, calcium transient amplitudes declined slightly with age but not frailty. Interestingly, intracellular Ca^{2+} levels in myocytes were similar between all frailty groups, even when Ca^{2+} overload was induced by β-adrenergic agonist. These results suggest that age-associated changes in cardiac structure and function are more prominent in animals with high frailty scores and that frailty is a better predictor of these changes than chronological age.

List of Abbreviations and Symbols Used

°C	Degree Celsius
AC	Adenylyl cyclase
ANOVA	Analysis of variance
ATP	Adenosine triphosphate
ATPase	Adenosine triphosphatase enzyme
bpm	Beats per minute
Ca^{2+}	Calcium ion
$CaCl_2$	Calcium chloride
cAMP	Cyclic adenosine monophosphate
CGA	Comprehensive geriatric assessment
CICR	Calcium induced calcium release
CRP	C-reactive protein
CVD	Cardiovascular disease
DMSO	Dimethyl sulfoxide
EC	Excitation-contraction
ECG	Electrocardiography
EF	Ejection fraction
EGTA	Ethylene glycol tetraacetic acid
FI	Frailty index
FS	Fractional shortening
g	Gram
Hz	Hertz
$I_{Ca,L}$	L-type Ca^{2+} current
IGF	Insulin-like growth factor
IL-6	Interleukin-6
IL-10	Interleukin-10
ISO	Isoproterenol
I_{TO}	Transient outward K^+ current

IVS	Interventricular septum
K^+	Potassium ion
KCl	Potassium chloride
KH_2PO_4	Potassium dihydrogen phosphate
L	Liter
LV	Left ventricle
LVID	Left ventricular internal diameter
LVPW	Left ventricular posterior wall
mA	Milliamp
mg	Milligram
$MgCl_2$	Magnesium chloride
$MgSO_4$	Magnesium sulfate
min	Minute
ml	Milliliter
mM	Millimolar
ms	Millisecond
mV	Millivolt
nm	Nanometer
Na^+	Sodium Ion
NaCl	Sodium chloride
NaH_2PO_4	Sodium dihydrogen phosphate
NaOH	Sodium hydroxide
NCX	Na^+/Ca^{2+} exchanger
O_2	Oxygen
PCI	Percutaneous coronary intervention
PCR	Polymerase chain reaction
PKA	Protein kinase A
PLB	Phospholamban
PTI	Photon Technology International
RyR	Ryanodine receptor

SD	Standard deviation
SEM	Standard error mean
SERCA	Sarcoplasmic endoplasmic reticulum Ca^{2+}-ATPase
SNS	Sympathetic nervous system
SR	Sarcoplasmic reticulum
TnI	Troponin I
β_1-AR	β_1-andrenergic receptor
µg	Microgram
µl	Microliter
µm	Micrometer
µM	Micromolar

Acknowledgements

First and foremost, I would like to thank my supervisor, Dr. Susan Howlett, for all her guidance, support, and encouragement throughout this project. Thank you for giving the opportunity to develop as a scientist and gain important life skills. You always pushed me to step outside my comfort zone and encouraged me to always think critically. It was been a privilege to learn from such a passionate and motivated scientist. I will always appreciate everything you've done for me.

I would also like to thank Peter Nicholl, Dr. Jie-quan Zhu, and Rick Livingston for all your help and training throughout my time in the lab. Thank you for giving so much of your time for me and I truly enjoyed the many conversations we shared. My experience with you has helped me become more attentive and focus the small details. Without you guys, I would not have been able to complete my experiments.

I would also like to thank my family, friends, and lab mates for all their support and encouragement. Your friendship has made every day in the lab enjoyable and not stressful.

Finally, I would like to give my appreciation to Luisa Vaughan, Sandi Leaf, and Cheryl Bailey for all their help with administrative tasks. You are always willing to answer any questions and your assistance has been invaluable over the past two years.

Chapter 1: Introduction

1.1 Broad overview

Population aging is a growing problem in Canada and around the world. Indeed, by 2006 13.7% of our population was over the age of 65, and by 2011 it had grown to 14.8% (Statistics Canada, 2011). As the average life expectancy has lengthened over the past century, the proportion of older individuals in the population is expected to continue to increase substantially. The incidence of cardiovascular diseases, including heart failure, hypertension, and cardiac arrhythmias, increases markedly with age (Lakatta & Levy, 2003). For example, 37.7% of adults 65 years or older reported having heart disease in 2009 (Public Agency of Canada, 2009). Therefore, as the population ages the incidence of cardiovascular diseases is expected to rise dramatically. Understanding the factors that modify the structure and function of the aging heart in the absence of overt cardiovascular diseases may help us understand why some older adults have an increased risk of developing these diseases.

There is a growing body of literature that shows that people age at different rates (Rockwood *et al.*, 2000; Mitnitski *et al.*, 2001). Thus, individuals of the same chronological age may not share the same "biological age". In other words, one individual may be much healthier, or fitter than the other, even though they share the same chronological age. Over the past twenty years, the term frailty has been used to describe a person's biological age, and account for the differences in health between two age-matched individuals. Frailty, from the French word *frêle*, meaning of little resistance, is defined as a state of reduced physiological reserve and increased vulnerability to stressors (Bergman *et al.*, 2007). When exposed to stressors, frail individuals are at much higher risk for

adverse outcomes, procedural complications, disability, and mortality (Shamliyan *et al.*, 2012). With an aging population, researchers are increasingly interested in frailty because heterogeneity in health status is most evident in older adults. Technological innovations have enabled clinicians to treat a wider array of patients and cardiovascular diseases (Afilalo *et al*., 2014). Nonetheless, there is growing evidence that frail older adults are much more likely to be harmed by these medical approaches. Although information is limited, frailty has been used to help identify risks and benefits of treatments for cardiovascular diseases and may be useful to guide patients towards personalized treatment plans that will maximize their likelihood of a positive outcome (Afilalo *et al.*, 2014). Still, little is known about the biology of frailty partly because, until recently, frailty has not been quantified in an animal model.

Several cross-sectional studies have proposed novel methods to quantify frailty in the mouse model. Parks *et al.* (2012) developed an invasive mouse frailty index based on the idea of deficit accumulation. More recently, Whitehead *et al.* (2014) developed a non-invasive, reproducible clinical frailty index to assess frailty in mice. These cross-sectional studies demonstrate that frailty can be quantified in animal models. Still, longitudinal studies in animals have not yet been conducted. Such studies have the potential to translate into clinical settings, where understanding the development of frailty may help determine whether frailty can be reversed. Parks *et al.* (2012) also investigated the relationship between frailty and ventricular myocyte morphology and function, suggesting that frailty can predict changes in cardiac function at the cellular level. Whether such changes develop as frailty progresses and whether they occur in the intact heart is not yet clear. The overall goals of this thesis are: 1) to examine the relationship between age and frailty in a

longitudinal study, and 2) to determine whether frailty is a better predictor of changes in cardiac morphology and contractile function than chronological age in the mouse model.

1.2 Age-related changes in cardiac structure and function

1.2.1 Impact of age on heart morphology

The process of aging has been shown to affect the morphology of the heart even in the absence of cardiovascular diseases (CVDs). For example, studies in healthy subjects without any signs of cardiovascular disease show that left ventricular (LV) wall thickness progressively increases with age (Lakatta & Levy, 2003). In addition, there is an age-dependent increase in both collagen deposition and fibrous tissue, which contributes to the thickening of the LV (Lakatta & Levy, 2003). This age-dependent remodeling of cardiac structure may increase the susceptibility of older adults to various CVDs (Lakatta & Levy, 2003). For example, LV hypertrophy is an independent risk factor for the development of heart failure, coronary heart disease, and stroke (Meijis *et al.*, 2007; Gradman & Alfayoumi, 2006). The cardiac fibrosis and increased collagen deposition that occur in aging are also known to adversely affect the heart. Increased fibrous tissue can cause cardiac stiffness and may alter the contractility of the heart, leading to heart failure (Biernacka & Frangogiannis, 2011). These data suggest that hearts from older adults undergo cardiac remodelling, which may increase the risk of developing various CVDs.

Changes in heart structure have also been investigated in aged rodent models. Based on survival data, the 50% mortality rate for humans occurs around the age of 85 years (Grundy, 2003), while in mice and rats the 50% mortality rate occurs near 24 months

of age (Turturro *et al.*, 1999). Based on these observations, 24 month old rodents can be used as a model for 85-year-old humans. Studies in the rat model have shown an age-dependent increase in LV mass in 24 month old rats when compared to younger adults (Hacker *et al.*, 2006). The mouse model shows similar age-dependent changes in LV mass as well as an increase in left atrial dimensions (Dai & Rabinovitch, 2009). These structural changes in the heart may contribute to age-associated changes in cardiac function, as discussed in the next section.

1.2.2 Changes in cardiac function in the aging heart

Age-associated changes in cardiac function in the absence of overt cardiovascular diseases have been investigated in humans. While the resting heart rate does not change significantly with age, the maximal heart rate during exercise is slower in aged hearts compared to younger hearts (Lakatta & Levy, 2003; Dai *et al.*, 2011). This may partially account for the impaired ability to increase ejection fraction in response to exercise in older adults (Lakatta & Levy, 2003). This age-dependent decline in maximal heart rate also helps explain the smaller increase in cardiac output during exercise in aged people compared to younger adults (Lakatta & Levy, 2003; Dai *et al.*, 2011). In addition to changes in force development, studies have shown that the duration of cardiac contraction is prolonged and cardiac relaxation is incomplete in aged hearts when compared to the hearts of young adults (Lakatta & Sollott, 2002; Lakatta & Levy, 2003).

Cardiac contractile function also appears to change with age in animal models. Although there are no consistent changes in heart rate in relation to age (Xing *et al.*, 2009),

Dai & Rabinovitch (2009) found that fractional shortening declined and LV diastolic function slowed with age in the mouse model. Similar changes were observed in the rat model (Hacker *et al.*, 2006). In addition, aged rat hearts showed a much smaller increase in contractile force in response to β-adrenergic stimulation than young hearts (Hacker *et al.*, 2006). The morphological and functional changes observed in aged hearts from both humans and animals may reflect, at least in part, age-associated changes at the cellular level. Therefore, the age-dependent decrease in cardiac contractile function may arise from modifications in individual cardiomyocytes. The next section provides an overview of the ventricular myocyte and the mechanisms involved in initiation and regulation of cardiac contractions at the cellular level.

1.3 Myocyte contractile function

1.3.1 The ventricular myocyte and membrane potentials

Cardiomyocytes are individual cardiac muscle cells that make up the heart, comprising approximately 75% of the mass of the ventricle (Loscalzo *et al.*, 2012). Human ventricular myocytes are normally 60 – 140 μm in length and 17 – 25 μm in diameter and have a striated appearance due to the presence of sarcomeres (Loscalzo *et al.*, 2012). As with all other cells in the body, the concentrations of ions inside a ventricular myocyte differ dramatically when compared to the ion concentrations outside the cell. Inside the ventricular myocyte, concentrations of Na^+, K^+, and Ca^{2+} are 10 mM, 135 mM, and 0.1 mM, respectively (Ten Eick *et al.*, 1981). By contrast, the extracellular concentrations of Na^+, K^+, and Ca^{2+} are 145 mM, 4 mM, and 2 mM, respectively (Ten Eick

et al., 1981). These electrochemical gradients, along with the resting permeability of the cell to K^+, result in a membrane potential that is about 80 mV lower inside than outside the cell (Bers, 2001).

When the resting membrane potential is depolarized to its threshold (approximately -65 mV), a propagated action potential occurs (Berne & Levy, 1997). The voltage changes recorded from a typical human ventricular myocyte during an action potential are illustrated in Figure 1.1A. Each phase of the myocyte action potential arises from specific changes in ion concentrations across the cell membrane. These changes are mediated by the opening of voltage-gated ion channels. Phase 0 marks the beginning of the action potential. The cell membrane rapidly depolarizes as a result of a large influx of Na^+, which gives rise to the upstroke of the action potential (Berne & Levy, 1997). Immediately after the upstroke, the Na^+ channels quickly inactivate and an efflux of K^+ occurs via potassium voltage-gated channels as the transient outward current (I_{to}), resulting in a slight repolarization (Birkeland *et al.*, 2005). This represents phase 1 of the action potential. As the Na^+ channels close, an influx of Ca^{2+} occurs via Ca^{2+} channels, predominantly the L-type Ca^{2+} channels (Bers, 2001). The influx of Ca^{2+} ions temporarily balances the outflow of K^+ through the potassium voltage-gated channels, resulting in a plateau in the action potential (phase 2). In phases 3 and 4, the cell repolarizes upon further extrusion of K^+, returning the membrane potential to rest until another action potential occurs. The Na^+-K^+ ATPase pumps 3 Na^+ out of the cell in exchange for 2 K^+ entering the cell, to help restore ion concentrations to resting values (Apell & Karlish, 2001).

Mice have much faster heart rates than humans and much shorter action potential durations (Knollmann *et al.*, 2006). A representation of a mouse ventricular action

potential is shown in Figure 1.1B. As with human action potentials, mouse action potentials show a rapid upstroke due to Na^+ influx during phase 0. However, phases 1, 2, and 3 of mouse action potentials are not as well defined. There is a lack of plateau in phase 2, due to the predominance of rapidly activating outward K^+ currents (Knollmann *et al.*, 2006). During the repolarization phase, there is a slight plateau at approximately -40 mV (Knollmann *et al.*, 2001). The low plateau is produced by the inward current generated by the Na^+/Ca^{2+} exchanger during the extrusion of Ca^{2+} from the cytosol (Knollmann *et al.*, 2003). Furthermore, repolarization in the mouse action potential is considerably faster than humans. This is a result of the rapid activation of repolarizing K^+ currents, primarily the transient outward current (Knollmann *et al.*, 2006). In both mice and humans, the action potential triggers cardiac contraction, as discussed in the next section.

1.3.2 Cardiac EC-Coupling

Cardiac contraction is initiated by the cardiac action potential. Contraction arises when Ca^{2+} is released from the sarcoplasmic reticulum (SR) as a result of a sequence of events known as excitation-contraction (EC) coupling (Bers, 2001). A schematic of the EC-coupling pathway is shown in Figure 1.2. In ventricular myocytes, the EC-coupling pathway is initiated when an action potential propagates along the cell membrane and invades the cell interior via the T-tubules, which are invaginations in the sarcolemma. This causes depolarization of the cell membrane and activates voltage-sensitive L-type Ca^{2+} channels, resulting in an influx of Ca^{2+} into the cytosol (Bers, 2001). This influx of Ca^{2+} is known as the L-type Ca^{2+} current ($I_{Ca,L}$). The L-type Ca^{2+} channels on the cell membrane are closely associated with Ca^{2+} release channels on the SR. These SR Ca^{2+} release

A)

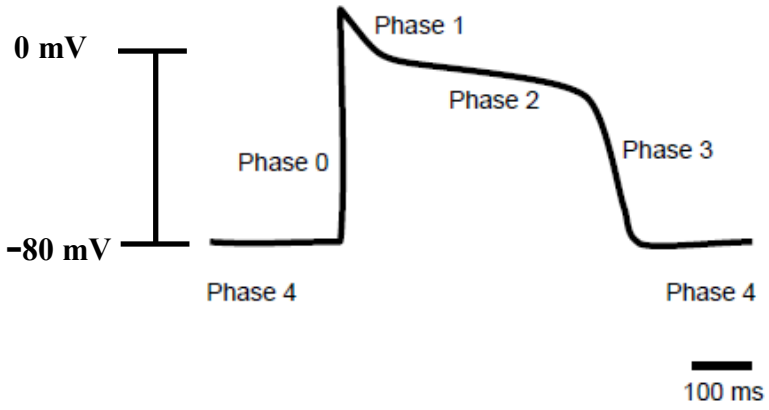

B)

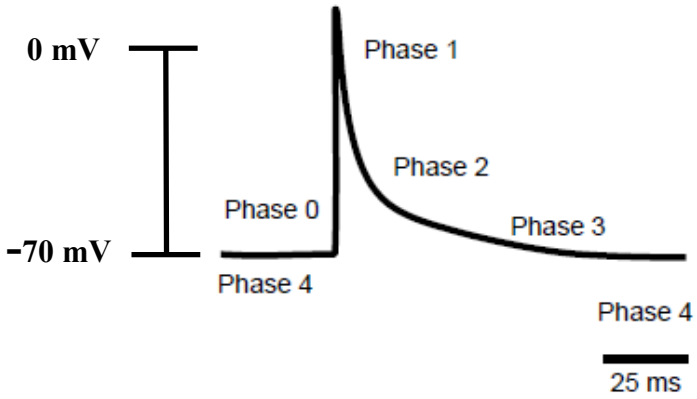

Figure 1.1 Schematic of the human and mouse ventricular myocyte action potentials. A) Human ventricular myocyte action potential. Phase 0 marks depolarization of the membrane resulting in a rapid influx of Na^+. Na^+ channels quickly inactivate, and a slight repolarization occurs as a result of K^+ efflux through the transient outward current (I_{TO}) (Phase 1). As Na^+ channels close, an influx of Ca^{2+} via the L-type Ca^{2+} channels characterizes the plateau in phase 2. Further extrusion of K^+ allows the cell to repolarize (phase 3), returning the cell to its resting membrane potential (phase 4). **B)** Mouse ventricular myocyte action potential. Ion movement is similar in a mouse action potential to that seen in human ventricular myocytes. Mouse action potentials lack a plateau in phase 2. Repolarization in mouse ventricular myocytes is much faster than those in humans.

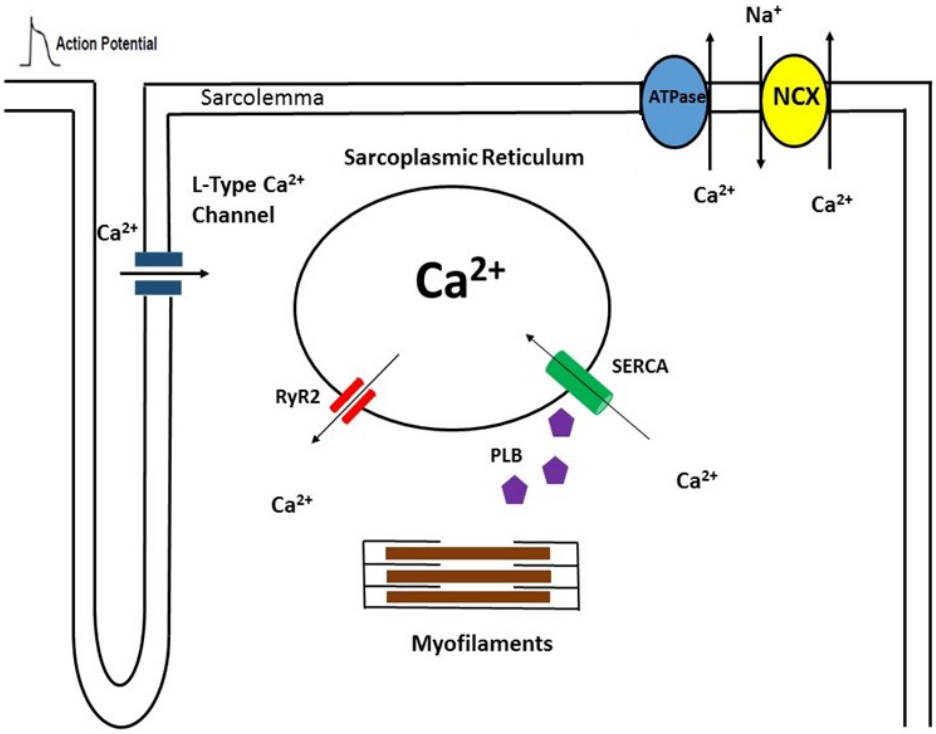

Figure 1.2. Schematic of the excitation-contraction coupling pathway. An action potential depolarizes the sarcolemma and promotes Ca^{2+} influx through the L-type Ca^{2+} channels. The incoming Ca^{2+} interacts with ryanodine receptors (RyRs) on the sarcoplasmic reticulum (SR) and triggers Ca^{2+}-induced-Ca^{2+}-release (CICR). This gives rise to the Ca^{2+} transient. The Ca^{2+} released from the SR interacts with myofilaments to induce a contraction. Myocyte relaxation occurs when the Ca^{2+} is taken back up into the SR via the sarcoplasmic endoplasmic reticulum Ca^{2+}-ATPase (SERCA) and extruded from the cell, primarily via the Na^{+}/Ca^{2+} exchanger (NCX).

channels are known as ryanodine receptors (RyR; Scriven *et al.*, 2000). The Ca^{2+} that enters as $I_{Ca,L}$ interacts with RyR and causes these receptors to activate and open, leading to Ca^{2+}-induced Ca^{2+} release (CICR) from the SR (Fabiato, 1985). The amount of Ca^{2+} released from the SR is much greater than the Ca^{2+} that enters the cell via the $I_{Ca,L}$, resulting in amplification of the initial Ca^{2+} influx signal and producing a large Ca^{2+} transient. The Ca^{2+} released from the SR increases the intracellular Ca^{2+} concentration, allowing Ca^{2+} to bind to myofilaments, causing myocyte contraction (Bers, 2002).

Cardiomyocyte relaxation occurs when Ca^{2+} is removed from the cytosol. The majority of Ca^{2+} released from the SR is transported back into the SR by a sarco/endoplasmic reticulum Ca^{2+}-ATPase (SERCA). The primary isoform expressed in the heart, SERCA2a, is regulated by the phosphoprotein, phospholamban (PLB) (Rodriguez & Kranias, 2005). PLB is an endogenous SERCA2a inhibitor that controls the rate of Ca^{2+} reuptake into the SR. When phosphorylated, PLB prevents the inhibition of SERCA2a, thus increasing its activity and allowing more Ca^{2+} to move back into the SR (Bers, 2002). In addition to SERCA, some Ca^{2+} is removed from the cell through the electrogenic Na^{+}/Ca^{2+} exchanger (NCX), with a much smaller amount removed by the Ca^{2+}-ATPase located on the cell membrane. In rodent cardiomyocytes, SERCA and NCX are responsible for approximately 92% and 7% of Ca^{2+} removal from the cytosol, respectively (Hove-Madsen & Bers, 1993; Li *et al.*, 1998). A minimal amount of Ca^{2+} is also taken up by the mitochondria through a uniporter, especially under conditions of Ca^{2+} overload and a small amount of Ca^{2+} is removed by the sarcolemmal Ca^{2+}-ATPase (Bers, 2002). At steady pacing rates, the amount of Ca^{2+} removed from the cell is proportional to

the amount of Ca^{2+} that enters the cell via $I_{Ca,L}$, ensuring that a steady concentration of intracellular Ca^{2+} is maintained inside the cell (Bers, 2008).

The cardiac action potential and EC-coupling pathway are normally tightly regulated processes, and disruptions in Ca^{2+} movement within the cardiomyocyte are associated with various cardiovascular diseases (Katz & Reuter, 1979). For example, Frommeyer *et al.* (2012) showed that Ca^{2+} overload within the heart is a key factor in the development of ventricular arrhythmias. Ischemia and reperfusion injury may occur as a result of Ca^{2+} overload (Wang *et al.*, 2002). A decrease in peak Ca^{2+} release can lead to a decline in LV performance, a characteristic of systolic heart failure (Sjaastad *et al.*, 2003). If components of the EC-coupling pathway are disrupted by the aging process, this could lead to Ca^{2+} dysregulation and increased susceptibility to CVDs in older hearts.

1.3.3 β-adrenergic Signalling in Cardiomyocytes

As discussed in the previous section, the EC-coupling pathway is tightly regulated to prevent disruptions in Ca^{2+} homeostasis. One important regulator of cardiac EC-coupling is the sympathetic nervous system (SNS). The effects of sympathetic activation in the heart are primarily mediated by a family of G-protein coupled receptors called the β-adrenergic receptors. β_1-adrenergic receptor (β_1-AR) stimulation causes positive inotropic effects, resulting in increased cardiac contractile force (Bers, 2002). In addition, β_1-AR activation has positive lusitropic effects, increasing the speed of myocardial relaxation through rapid reduction in cytosolic Ca^{2+} (Li *et al.*, 2000). The binding of catecholamines to the β_1-AR activates the heterotrimeric G-protein, G_s (Bers, 2002). This causes the α-

subunit of G_s to dissociate from the βγ-subunit and subsequently activate adenylyl cyclase (AC). AC then stimulates the conversion of ATP into cyclic AMP (cAMP), which in turn activates protein kinase A (PKA). Activation of PKA phosphorylates various targets in the EC-coupling pathway such as L-type Ca^{2+} channels, RyR, and PLB, as well as troponin I (TnI) on the myofilaments (Bers, 2002; Li *et al.*, 2000).

The phosphorylation of EC-coupling targets by PKA profoundly affects cardiac EC-coupling. PKA phosphorylation increases the open probability of L-type Ca^{2+} channels, allowing a greater influx of Ca^{2+} into the cell upon depolarization (Valdivia *et al.*, 1995; Marx *et al.*, 2000). In addition, phosphorylation of RyRs augments CICR, resulting in larger Ca^{2+} transients (Valdivia *et al.*, 1995; Marx *et al.*, 2000). Phosphorylation of PLB speeds the re-uptake of Ca^{2+} into the SR and increase the rate of myocyte relaxation by causing PLB to dissociate from SERCA2a (Li *et al.*, 2000). Moreover, phosphorylation of TnI reduces myofilament sensitivity, causing a more rapid dissociation of Ca^{2+} from the myofilaments and enhancing myocardial relaxation (Kentish *et al.,* 2001). Overall, phosphorylation of key components of the EC-coupling pathway by PKA results in positive inotropy and faster relaxation in cardiomyocytes. Disruption of this pathway can cause Ca^{2+} dysregulation and lead to cardiovascular disease.

1.4 Age-related changes in morphology and function in ventricular myocytes

The age-associated decline in cardiac function may be attributable to changes in morphology and contractile function in individual cardiomyocytes. In both humans and animals, the number of ventricular myocytes declines with age, causing the remaining

myocytes to increase in size (Lakatta & Levy, 2003; Olivetti *et al.*, 1992). This increase in myocyte size is thought to contribute to left ventricular wall thickening (Olivetti *et al.*, 1992). At slow pacing rates (< 1 Hz), ventricular myocytes from rodents do not show any age-associated changes in contractile function (Farrell & Howlett, 2008; Lim *et al.*, 2000; Xiao *et al.*, 1994). However, when myocytes are paced at faster, more physiological rates (> 2 Hz), there is an age-associated decline in fractional shortening in cells from aged animals (Lim *et al.*, 2000; Grandy & Howlett, 2006). The relaxation time for contractions is also prolonged in myocytes from aged mice (Lim *et al.*, 2000). This is attributable to changes in the underlying Ca^{2+} transients. Studies have shown that Ca^{2+} transients are much smaller and the rates of decay are slower in aged myocytes when compared to myocytes from younger mice (Lim *et al.*, 2000). Ventricular myocytes from aged rodents also show a reduction in their ability to increase contractions and Ca^{2+} transients in response to β-adrenergic stimulation (Farrell & Howlett, 2007; Farrell & Howlett, 2008). Furthermore, relaxation of contractions and decay of Ca^{2+} transients are prolonged in aged myocytes under β-adrenergic stimulation (Xiao *et al.*, 1994). This suggests that the contractile ability of individual ventricular myocytes declines with age, in particular under conditions of stress such as rapid pacing or β-adrenergic stimulation.

To understand the mechanisms behind the decline in ventricular myocyte function in aging hearts, studies have evaluated whether components of the EC-coupling pathway are affected by age in rodent models. Studies have shown that the action potential duration is prolonged in aged ventricular myocytes compared to myocytes from younger animals (Liu *et al.*, 2000; Walker *et al.*, 1993). This may be due to age-related changed in transmembrane currents. In fact, it has been shown that aging causes a reduction in both

the peak density and the rate of inactivation of I_{TO} (Liu *et al.*, 2000; Walker *et al.*, 1993). Moreover, the rate of inactivation of $I_{Ca,L}$ is much slower in aged ventricular myocytes (Liu *et al.*, 2000; Walker *et al.*, 1993). These changes in transmembrane currents would be expected to prolong depolarization and increase action potential duration. An increase in action potential duration would allow greater influx of Ca^{2+}, which would increase in CICR resulting in larger Ca^{2+} transients and contractions. However, studies have shown that peak $I_{Ca,L}$ density actually declines with age (Grandy & Howlett, 2006; Howlett, 2010). Furthermore, Howlett & Nicholl (1992) showed that the expression of L-type Ca^{2+} cannels declines with age. This smaller $I_{Ca,L}$ may counteract the increase in action potential duration and help explain the decrease in peak contractions and Ca^{2+} transients in aged myocytes.

The prolonged relaxation in aged ventricular myocytes may be due to changes in Ca^{2+} removal mechanisms in the EC-coupling pathway. In theory, an age-associated decrease in SERCA2a activity could account for prolonged Ca^{2+} transient decay and relaxation. Indeed, Lim *et al.* (1999) showed that levels of PLB expression were increased in aged hearts. This increased expression of PLB would be expected to promote inhibition of SERCA2a, resulting in slower Ca^{2+} reuptake. Additionally, phosphorylation of PLB by PKA declines with age (Xu & Narayanan, 1998). This decline in phosphorylation of PLB would lower PLB inhibition and thereby slow SERCA2a activity in the aging heart. This inhibition of SERCA2a could account for prolonged relaxation of myocytes from aged hearts.

In summary, changes in the EC-coupling pathway at the level of the ventricular myocyte may underlie the age-associated decline in heart function discussed previously. This decline in contractile function may be due to changes in the expression and regulation

of important proteins in the EC-coupling pathway. While the impact of age on cardiac function has been relatively well-characterized, little is known about the impact of frailty on the heart both *in vivo* and at the cellular level. The next section will discuss the concept of frailty and will highlight what little is known about the effect of frailty on the heart.

1.5 The concept of frailty

Chronological age is widely regarded as an important determinant of health and survival. However, people age at different rates, thus chronological age does not necessarily reflect biological age. Indeed, there is growing evidence that individuals of the same chronological age differ dramatically with respect to their health status (Rockwood *et al.*, 2000). For example, a sixty-five year-old individual may live a very active lifestyle and may not require any medications or assistance. By contrast, another individual of the same age may be bed-ridden, require frequent hospitalization, and suffer from numerous diseases. Although these two people have the same chronological age, their biological health differs dramatically. Therefore, the health status of older adults can vary from fit to frail (Mitnitski *et al.*, 2001; Howlett & Rockwood, 2013).

The concept of frailty was developed to account for heterogeneity of health outcomes in older individuals of the same age. Frailty can be regarded as a dynamic state of balance between assets and deficits covering physical, functional, psychological, nutritional, and social domains (Rockwood *et al.*, 1994; de Vries *et al.*, 2011). Assets such as health, resources, and caregivers are balanced against deficits such as illnesses, dependency on others, and support burden (Rockwood *et al.*, 1994). Frailty occurs when

the deficits outweigh the assets, resulting in a diminished ability to respond to stress (Rockwood *et al.*, 1994). Stressors can be classified as environmental factors, acute or chronic illnesses (e.g. myocardial infarction), or iatrogenic factors (e.g. cardiac surgery) (Afilalo *et al.*, 2014). When exposed to these stressors, frail patients are at much higher risk for adverse events, procedural complications, prolonged recovery, functional disability, and death (Shamliyan *et al.*, 2013). Interestingly, even relatively minor stressors, such as a new medication prescription, can have profound adverse effects on frail older adults (Clegg & Trust, 2011).

Frailty poses a major challenge in health care because frail individuals have higher mortality and use more health care services than do fit people (Clegg *et al.*, 2013). Still, the causes of frailty are not fully understood. A pathway that is similar, but not identical, to the aging process has been suggested (de Vries *et al.*, 2011). For example, inflammatory markers such as interleukin-6 (IL-6) and C-reactive protein (CRP) are elevated with normal aging, with values doubling between the ages of 40 and 65 (Ferucci *et al.*, 2002). Several studies have suggested that chronic inflammation is also linked to frailty (Collerton *et al.*, 2012; Li *et al.*, 2011; Visser *et al.*, 2002). High levels of cytokines such as IL-6 and CRP can induce sarcopenia and neuroendocrine dysregulation, which are both major contributors to frailty (Visser *et al.*, 2002). In addition, elevated levels of these markers are associated with adverse cardiovascular events and mortality (Cesari *et al.*, 2003). Clinical studies have also investigated the role of hormones in frailty. In longitudinal studies of aging, low levels of free testosterone and insulin-like growth factor (IGF) were found to be predictors of muscle mass degeneration (Baumgartner *et al.*, 1999; Waters *et al.*, 2000). However, hormone replacement therapies have not been shown to be useful.

Testosterone supplementation in humans increased lean body mass but did not affect functional status or cognitive function (Ottenbacher *et al.*, 2006). Although frailty has been linked to numerous health-associated changes including inflammation, impaired immunity, neuroendocrine dysregulation, and metabolic alteration, little is still known about the pathway or pathways that lead to frailty (Fulop *et al.*, 2010).

Frailty is universally regarded as a multidimensional concept comprised of several inter-related physiological systems that include physical, psychological, social, and environmental factors (Clegg *et al.*, 2013). This idea of frailty as increased vulnerability arising from dysregulation of multiple physiological systems is reasonably non-controversial (Koller & Rockwood, 2013). However, there are still conflicting views on how to systematically quantify frailty in those who are at increased risk of adverse outcomes. There are currently more than 20 different instruments used to quantify frailty clinically (de Vries *et al.*, 2011). The next section will discuss two of the more widely used methods to assess frailty.

1.6 Quantification of frailty

1.6.1 Measuring frailty in humans

Clinical studies have shown that frailty can be quantified in a number of ways, although how to best measure frailty in people is controversial (Heuberger, 2011). de Vries *et al.* (2011) identified eight risk factors in three domains that are important to the concept of frailty. These factors include, in the physical domain: nutritional status, physical activity, mobility, strength, and energy; in the psychological domain: cognition and mood;

and in the social domain: lack of social contacts/support (de Vries *et al.*, 2011). A practical frailty measurement instrument should be multidimensional and incorporate these eight factors in its assessment. One popular method to assess frailty is based on Fried's operational definition of frailty. Fried *et al.* (2001) defined frailty as a clinical syndrome in which three or more of the following five characteristics are present: unintentional weight-loss, self-reported exhaustion, weakness (low grip strength), slow walking speed, and low levels of physical activity. Subjects are assessed using questionnaires, standardized interviews and physical examinations. Based on this so-called Fried "phenotype" approach, a person is considered frail if three or more of these characteristics are present. Those with one or two characteristics are regarded as pre-frail, and those with no characteristics are deemed robust, or fit (Fried *et al.*, 2001). Fried's model has been praised for its reproducibility and consistency (Bergman *et al.*, 2007). In addition, Fried's method of frailty assessment is easy to administer. Therefore, it is not limited to hospitalized or nursing home patients and can be used in community-dwelling persons (Fried *et al.*, 2001). However, critics of Fried's frailty measurement note that it is a one-dimensional approach to a multidimensional concept (Hogan *et al.*, 2003). Its focus on weakness and physical wasting, and exclusion of the psychological domain (cognition and mood) and social domain (social relationships and social support), have been particularly controversial (de Vries *et al.*, 2011; Bergman *et al.*, 2007).

Another notable approach to assess frailty is by evaluating frailty based on the accumulation of deficits (Rockwood *et al.*, 2011; de Vries *et al.*, 2011; Mitnitski *et al.*, 2001). The concept of deficit accumulation is centred on the idea that as people age, the number of deficits that are manifest in the individual increases. As a consequence, older

adults are at an increased risk of adverse health outcomes and have a diminished ability to respond to stress (Rockwood & Mitnitski, 2011). The Frailty Index (FI) score is calculated using a range of deficits based on symptoms, signs, disabilities, diseases, and laboratory measurements (Rockwood and Mitnitski, 2007; Singh *et al.*, 2014; Rockwood and Mitnitski, 2011; Mitnitski *et al.*, 2001). For example, a standard Comprehensive Geriatric Assessment (CGA) records approximately 40 items, in which some are self-reported (*e.g.* How would you rate your health?), while others are assessed by tests (*e.g.* Mini-Mental State Examination), clinical evaluation (*e.g.* signs and symptoms), or laboratory measurement (*e.g*. diabetes mellitus) (Rockwood and Mitnitski, 2007; Singh *et al.*, 2014). A score is given for each deficit measured (*e.g.* good = 0, fair = 0.5, poor = 1). The number of deficits present is summed and expressed as a proportion of the total number of deficits possible to yield a FI score between 0 and 1 (a theoretical score of 1 would indicate that all possible deficits are present) (Rockwood and Mitnitski, 2007). For example, if a patient has 8 of the 40 measured deficits (8/40 = 0.20), the patient would have a FI score of 0.20. One concern regarding the FI is the specific nature of the variables measured (Rockwood and Mitnitski, 2007). However, Rockwood and Mitnitski (2011) showed that a FI can be generated from almost any set of health-associated variables, as long as a few criteria are met. The criteria for an item to be considered as a deficit are that the item needs to be acquired, age-related, associated with an adverse outcome, and does not saturate too early (Rockwood and Mitnitski, 2011). When a sufficiently large number of variables are measured (> 30), the nature of the specific variables that make up the index are no longer considered. Indeed, variables can be selected at random and still yield a FI that predicts the risk of adverse outcomes (Rockwood *et al.*, 2006).

The FI is commended for being the only instrument that includes all eight factors in the three domains (de Vries *et al.*, 2011), but assessment of a large number of variables may seem daunting and time consuming to clinicians (Hubbard *et al.*, 2008). It is currently unclear which method of frailty assessment is preferred in clinical studies (De Vries *et al.*, 2011). Each frailty measurement instrument has its advantages and disadvantages, dependent on the setting, aim of the measurement, availability, and accessibility of the instrument. At this point, the Frailty Index seems to be the most suitable instrument to assess frailty due to its comprehensiveness (de Vries *et al.*, 2011). Developing a standardized frailty assessment method can accelerate our understanding of frailty and identify relationships between frailty and various diseases such as cardiovascular disease. Understanding the biology of frailty would be advanced by the development of animal models of frailty. However, whether frailty can be modelled and quantified in animals has only recently been investigated.

1.6.2 Measuring frailty in the animal model

Recent clinical studies have suggested that increased inflammatory mediators and decreased muscle-related hormones are correlated with frailty (Collerton *et al.*, 2012; Li *et al.*, 2011; Visser *et al.*, 2002). Therefore, Walston *et al.* (2008) proposed an IL-10 knockout mouse as a model of frailty. The genetically altered IL-10 deficient mice, like frail humans, are more susceptible to inflammatory pathway activation (Walston *et al.*, 2008). Walston *et al.* (2008) compared IL-10 deficient mice to normal C57BL/6J mice to determine physical and biological changes that may be associated with being frail. Weight, activity levels, and strength of mice were compared monthly beginning at 40 weeks of age up to 18

months. Serum IL-6 levels were compared at 8 weeks of age and again when mice were 50 weeks old. In addition, polymerase chain reaction (PCR) assays were performed to compare skeletal gene expression. Walston *et al.* (2008) found that hair loss was more apparent in IL-10 deficient mice. Muscle strength also declined at a much faster rate in the IL-10 deficient mice. Moreover, IL-6 levels were higher in IL-10 deficient mice compared to age-matched C57BL/6J control mice, suggesting an increase in pro-inflammatory cytokines in "frail" mice. PCR analyses showed that many genes related to apoptosis were up-regulated in IL-10 deficient mice compared to controls. In addition, genes associated with protein transport, regulation of cell growth, and maintenance were down-regulated compared to control mice. This study provided some insight into the biological basis of frailty, identifying certain physical and biological changes that may be associated with frailty. However, Walston *et al.* (2008) noted that mice used in this study were genetically altered, and the loss of the IL-10 gene may lead to changes different than those observed in natural aging. In addition, these IL-10 knockout mice are widely used to model Crohn's disease, an inflammatory bowel disease (Herfarth & Scholmerich, 2002; Yuan *et al.*, 2013). Therefore, the mice were kept in barrier conditions to prevent illness, and are not likely to be representative of free-living adults.

Parks *et al.* (2012) conducted a cross-sectional pilot study to develop an approach to quantify frailty in a C57BL/6J mouse model of natural aging, based on the idea of deficit accumulation. Using specialized equipment, a FI was constructed by measuring thirty-one parameters that reflect different aspects of health in adult (~12 months) and aged (~30 months) mice (Parks *et al.*, 2012). These parameters included activity levels, hemodynamic measures, body composition, and basic metabolic status and were selected to model known

age-related changes in aging C57BL/6J mice (Parks *et al.*, 2012). Activity levels were determined by measuring parameters such as the distanced the mouse moved, velocity of movement, and rearing frequency. Heart rate, systolic and diastolic blood pressures, and blood volume were used to assess hemodynamic status. Body composition was evaluated by body mineral content, percent body fat, and percent lean tissue. Basic metabolic status was determined by measuring levels of electrolytes (sodium, potassium, chloride) and other blood components (*e.g.* pH, glucose, and hemoglobin). A score was given for each deficit based on standard deviation (SD) from the mean reference value (Parks *et al.*, 2009). Values that were 1 SD above or below the mean reference value were given a frailty value of 0.25. Values that differed by 2 SD were given a score of 0.5. Values that differed by 3 SD were scored 0.75, and values more than 3 SD above or below the mean were given a maximal value of 1. As with the FI used in clinical studies in people, the total number of deficits present were summed and divided by the total number of parameters measured (31) to yield a FI score for each animal. Parks *et al.* (2012) found that aged mice had higher FI scores than younger animals, suggesting that an FI can be developed for use in murine models. However, the need for specialized equipment to measure health parameters may limit the ability to implement this approach in other labs. Furthermore, this frailty index cannot be used in longitudinal studies of frailty in mice due to the invasive nature of some of the methods used (*e.g.* exposure to x-rays, volume of blood taken, etc.) (Whitehead *et al.*, 2014).

To address this concern, Whitehead *et al.* (2014) developed a simplified, non-invasive method to quantify frailty through clinical assessment of more than 30 potential deficits in aging mice. This clinical FI assessment evaluated readily apparent signs of

clinical deterioration in aging mice. The parameters and potential deficits measured are described in Table 1.1 (Whitehead *et al.*, 2014). For each deficit, a score of 0 is given if the deficit is absent, a score of 0.5 if the deficit is mild, and a score of 1 if the deficit is severe. Again, the total number of deficits present in an individual is divided by the total number of deficits measured to yield a unique FI score for each animal. Whitehead *et al.* (2014) showed that this simplified approach could be used to create a FI and characterize frailty in aging mice. When normalized, the relationship between FI scores and age was virtually identical in mice and humans (Whitehead *et al.*, 2014). The development of a simple, reproducible FI provides a standardized method of assessing frailty in animal models and may be useful in experimental studies designed to investigate the mechanisms involved in frailty and in the assessment of novel treatments for frailty. In addition, the non-invasive nature of this clinical FI makes it suitable for longitudinal studies of frailty involving multiple assessments over a mouse's entire lifespan. Still, longitudinal studies of frailty have not yet been conducted in animal models.

1.7 Association between frailty and cardiovascular disease

As CVDs are the leading cause of death and hospitalization in older adults (Singh *et al.*, 2014), there is growing interest in the link between frailty and CVD. As average life expectancy has lengthened over the past century, there has been an increase in the age of the population and a corresponding increase in the incidence of CVD. In Canada, 14.8% of adults age 65 to 74 report having heart disease, with the proportion climbing to 22.9% for adults over 75 years of age (Public Health Agency of Canada, 2009). Current treatments for CVDs emphasize treatment of the underlying condition or conditions. However,

Table 1.1. Clinical signs of deterioration in aging C57BL/6J mice

System and Parameter	Potential Deficit	References
Integument		
Alopecia	Hair loss due to age-related balding and/or barbering (fur trimming)	30
Loss of fur color	Change in fur color from black to grey or brown	30
Dermatitis	Inflammation, over-grooming, barbering or scratching causing skin erosion. Can result in open sores anywhere on body	16, 35
Loss of whiskers	Loss of vibrissae (whiskers) due to aging and/or whisker trimming	103, 113
Coat condition	Ruffled fur and/or matted fur. Un-groomed appearance. Coat does not look smooth, sleek, and shiny	35, 110
Physical/musculoskeletal		
Tumors	Development of tumors or masses anywhere on the body	13, 16, 35
Distended abdomen	Enlarged abdomen. May be due to tumor growth, organ enlargement, or intraperitoneal fluid accumulation	110
Kyphosis	Exaggerated outward curvature of the lower cervical/thoracic vertebral column. Hunched back or posture	30, 35, 110
Tail stiffening	Tail appears stiff, even when animal is moving in the cage. Tail does not wrap freely when stroked	30
Gait disorders	Lack of coordination in movement including hopping, wobbling, or uncoordinated gait. Wide stance. Circling or weakness	35
Tremor	Involuntary shaking at rest or during movement	35
Forelimb grip strength	A decline in forelimb grip strength	30
Body condition score	Visual signs of muscle wasting or obesity based on the amount of flesh covering bony protuberances	30, 35, 110
Vestibulocochlear/auditory		
Vestibular disturbance	Disruption in the ability to perceive motion and gravity. Reflected in problems with balance, orientation, and acceleration	97, 98
Hearing loss	Failure to respond to sudden sound (e.g. clicker) indicative of hearing loss or impairment	16, 97
Ocular/nasal		
Cataracts	Clouding of the lens of the eye. An opaque spot in the center of the eye	16, 121, 130
Corneal opacity	Development of white spots on the cornea. Cloudy cornea	35, 114
Eye discharge/swelling	Eyes are swollen or bulging (exophthalmia). They may exhibit abnormal secretions and/or crusting	35, 110, 113
Microphthalmia	Eyes are small and/or sunken. May involve one or both eyes	16, 35
Vision loss	Vision loss, indicated by failure to reach toward the ground when lowered by tail	16, 65
Menace reflex	Rapid eye blink and closure of the palpebral fissure in response to a non-tactile visual threat to the eye. Measures the integrity of the entire visual pathway including cortical components	40
Nasal discharge	Signs of abnormal discharge from the nares	110
Digestive/urogenital		
Malocclusions	Incisor teeth are uneven or overgrown. Top teeth grow back into the roof of the mouth or bottom teeth are long and easily seen	35
Rectal prolapse	Protrusion of the rectum just below the tail	1, 35
Vaginal/uterine/penile prolapse	Vagina or uterus protrudes through the vagina and vulva. Penis cannot re-enter the penile sheath	1, 15, 35, 83
Diarrhea	Feces on the walls of the home cage. Bedding adheres to feces in cage. Feces, blood, or bedding around the rectum	35
Respiratory		
Breathing rate/depth	Difficulty breathing (dyspnea), pulmonary congestion (rales), and/or rapid breathing (tachypnea)	35, 108
Discomfort		
Mouse Grimace Scale	Measure of pain/discomfort based on facial expression. Assessment of five facial features: orbital tightening, nose bulge, cheek bulge, ear position (drawn back), or whisker change (either backward or forward)	26, 62
Piloerection	Involuntary bristling of the fur due to sympathetic nervous system activation	113
Other		
Temperature	Increase or decrease in body temperature	105, 113
Weight	Increase or decrease in body weight	30, 105, 113, 122

*numbers denote reference number

incorporation of frailty into risk prediction models and management of frailty may help improve care of frail, older patients with CVD (Singh *et al.*, 2014). Studies have shown that frailty is present in 25% to 50% of all patients with CVD (Purser *et al.*, 2006, Afilalo, 2011), and frail patients with CVD have much worse prognosis than non-frail patients (Newman *et al.*, 2001; Cacciatore *et al.*, 2005). In fact, a study by Lee *et al.* (2009) showed that over 63% of frail cardiac surgery patients either died or ended up in long-term care facilities compared to only 13.5% of non-frail patients. In a study of 628 patients over the age of 65 who underwent percutaneous coronary intervention (PCI), the 3-year mortality rate was 28% for frail patients compared to only 6% for non-frail patients determined using the Fried frailty score (Singh *et al.*, 2011). Therefore, frail patients with CVD who are undergoing invasive procedures are much more likely to suffer adverse outcomes than their non-frail age-matched counterparts. Incorporation of frailty assessment in these patients may improve risk assessment and help develop personalized treatment plans that will maximize their likelihood of a positive outcome.

Despite the observed differences in the outcomes between frail and non-frail patients undergoing cardiovascular interventions, there is currently little evidence on how treatment and management should be altered to account for frailty. Because frail patients have an increased vulnerability to adverse outcomes from procedures (Lee *et al.*, 2009; Singh *et al.*, 2011), a less invasive strategy may be preferred. For example, as frailty advances, it may be more appropriate to shift the focus of care to palliation, with the goal of optimizing quality of life and easing of pain and discomfort, rather than undergoing invasive procedures (Boockvar & Meier, 2006). The emergence of technological innovations has enabled clinicians to treat a wider array of patients. Frailty offers valuable

prognostic insights essential to existing risk assessment models and can assist clinicians to define optimal care pathways for their patients (Afilalo *et al.*, 2014). Recognizing frailty is an important factor in patient care, contributing to the organization and delivery of health care.

Given the influence of frailty on patients with CVDs, and the appreciable difficulties in performing biological studies in frail humans, the development of animal models for frailty is essential to improve our understanding of the relationships between frailty and CVD. Although information is limited, one study did examine the effects of frailty on contractile function in ventricular myocytes isolated from mice. A study by Parks *et al.* (2012) showed that the detrimental effects of aging on the morphology and function of individual ventricular myocytes were highly correlated with the FI. As the FI score increased, there was an increase in myocyte hypertrophy accompanied by a decrease in peak contractions (Parks *et al.*, 2012). This suggests that age-associated changes in myocytes are more prominent in animals with high FI score. This small-scale cross-sectional study was an important first step in investigating the association between frailty, cardiovascular morphology and function at the cellular level. Still, whether frailty is a better predictor of these cellular changes than chronological age has not been investigated and the impact of these cellular changes on *in vivo* morphology and function remains to be clarified.

1.8 Objectives

The objectives of the present study were to: 1) quantify frailty in the mouse model in a longitudinal study; 2) determine if frailty can predict changes in heart structure and function independently of age *in vivo*; 3) determine whether frailty can predict myocyte hypertrophy and changes in contractile function at the cellular level better than age; and 4) determine whether myocytes from frail mice are more sensitive to stimuli that provoke intracellular Ca^{2+} overload.

1.9 Hypotheses

1. Frailty increases with age in mice in a longitudinal study involving multiple assessment throughout their lifespan.
2. Frailty can predict changes in heart morphology and function *in vivo* independently of age.
3. Frailty can predict changes in ventricular myocyte morphology and contractile ability independently of age.
4. Acute application of β-adrenergic agonist, isoproterenol, promotes Ca^{2+} overload and augments contractile dysfunction in frail cardiomyocytes.

Chapter 2: Methods

2.1 Animals

All experimental protocols involving animals were performed in accordance with the guidelines of the Canadian Council on Animal Care (CCAC; Ottawa, ON: Vol.1, 2nd edition, 1993; Vol. 2, 1984) and approved by the Dalhousie University Committee on Laboratory Animals. All C57BL/6 mice were obtained from Charles River Laboratories (St. Constant, QC) and aged in micro-isolator cages in the Carlton Animal Care Facility at Dalhousie University. For the longitudinal study, male mice were purchased at 3 weeks of age, housed in groups of five mice per cage and maintained on a 12-hour light/dark cycle with free access to food and water. Additional male and female mice that were not part of the longitudinal cohort were included in some experiments.

2.2 Survival curve

Mice survival data was collected from 257 male C57BL/6 mice used in the longitudinal study of frailty. Mortality was recorded as sudden death or when animals had to be euthanized as a humane endpoint, such as in cases of illness determined by the university veterinarian. Mice that were voluntarily used in experiments were censored and were included in the analysis as censored data. Mice were followed over a period of approximately 22 months and a Kaplan-Meier survival curve was generated from the data.

2.3 Quantification of frailty using a clinical frailty index

To quantify frailty in mice in a longitudinal study, frailty examinations were performed on each mouse at approximately 6 month intervals and prior to euthanasia. Frailty was assessed using a 31-item frailty index based on established clinical signs of deterioration in mice that was previously developed in the Howlett lab (Whitehead *et al.*, 2014). Frailty was measured as deficit accumulation. An example of the frailty assessment form developed by Whitehead *et al.* (2014) is shown in Table 2.1. Clinical assessment included evaluation of deficits in the integument, the physical/musculoskeletal system, the vestibulocochlear/auditory systems, the ocular and nasal systems, the digestive and urogenital systems, the respiratory system, and signs of discomfort. Deviations from the mean body weight (g) and body surface temperature (°C) were also recorded as deficits, as described in the following paragraph.

To assess frailty, mice were taken to a quiet assessment room in the animal care facility and allowed 15 minutes to acclimatize to their new surroundings. The mice were then assessed with a clinical exam to evaluate parameters described in Table 2.2 (Whitehead *et al.*, 2014). The severity of each deficit was rated on a scale of 0, 0.5, or 1. A score of 0 indicated there was no signs of a deficit, a score of 0.5 was given if the deficit was mild, and a score of 1 was given for a severe deficit (Whitehead *et al.*, 2014). Details and parameters of the scoring scheme used for clinical assessment are outlined in Table 2.2 (Whitehead *et al.*, 2014). A clicker similar to ones used to train dogs was used to evaluate hearing loss. Following clinical evaluation, mice were weighed (g) and body surface temperature (°C) was recorded with an infrared temperature probe (Infrascan; La Crosse

Table 2.1. Mouse frailty assessment form.

Mouse #: _____ **Date of Birth: _____** **Sex:** F M
Body weight (g) _____ **Surface body temperature (°C) _____**

Mouse Frailty Assessment Form

Rating: 0 = absent 0.5 = mild 1 = severe

➢ **Integument:**					**NOTES:**
❖	Alopecia (hair loss)	**0**	**0.5**	**1**	_____
❖	Loss of fur colour	**0**	**0.5**	**1**	_____
❖	Dermatitis	**0**	**0.5**	**1**	_____
❖	Loss of whiskers	**0**	**0.5**	**1**	_____
❖	Coat condition	**0**	**0.5**	**1**	_____
➢ **Muscoskeletal system:**					
❖	Tumours	**0**	**0.5**	**1**	_____
❖	Distended abdomen	**0**	**0.5**	**1**	_____
❖	Kyphosis/hunched posture	**0**	**0.5**	**1**	_____
❖	Tail stiffening	**0**	**0.5**	**1**	_____
❖	Gait	**0**	**0.5**	**1**	_____
❖	Tremor	**0**	**0.5**	**1**	_____
❖	Forelimb grip strength	**0**	**0.5**	**1**	_____
❖	Body condition score	**0**	**0.5**	**1**	_____
➢ **Vestibulocochlear/Auditory:**					
❖	Head tilt	**0**	**0.5**	**1**	_____
❖	Hearing loss	**0**	**0.5**	**1**	_____
➢ **Ocular/Nasal:**					
❖	Cataracts	**0**	**0.5**	**1**	_____
❖	Discharge/swollen/ squinting	**0**	**0.5**	**1**	_____
❖	Microphthalmia	**0**	**0.5**	**1**	_____
❖	Corneal opacity	**0**	**0.5**	**1**	_____
❖	Vision loss	**0**	**0.5**	**1**	_____
❖	Menace reflex	**0**	**0.5**	**1**	_____
❖	Nasal discharge	**0**	**0.5**	**1**	_____
➢ **Digestive/Urogenital system:**					
❖	Malocclusions	**0**	**0.5**	**1**	_____
❖	Rectal prolapse	**0**	**0.5**	**1**	_____
❖	Penile/Uterine prolapse	**0**	**0.5**	**1**	_____
❖	Diarrhoea	**0**	**0.5**	**1**	_____
➢ **Respiratory:**					
❖	Breathing rate/depth	**0**	**0.5**	**1**	_____
➢ **Discomfort:**					
❖	Mouse Grimace Scale	**0**	**0.5**	**1**	_____
❖	Piloerection	**0**	**0.5**	**1**	_____

Total Score/ Max Score:

Table 2.2. Clinical assessment of deficits in aging mice to create a frailty index.

System/Parameter	Clinical assessment of deficit	Scoring
Integument		
Alopecia	Gently restrain the animal and inspect it for signs of fur loss	0 = normal fur density 0.5 = < 25% fur loss 1 = > 25% fur loss
Loss of fur color	Note any chance in fur color from black to grey or brown	0 = normal color 0.5 = focal grey/brown changes 1 = grey/brown throughout body
Dermatitis	Document skin lesions	0 = absent 0.5 = focal lesions (e.g. neck, flanks, under chine) 1 = widespread/multifocal lesions
Loss of whiskers	Inspect the animal for signs of a reduction in the number of whiskers	0 = no loss 0.5 = reduced number of whiskers 1 = absence of whiskers
Coat condition	Inspect the animal for signs of poor grooming	0 = smooth, sleek, shiny coat 0.5 = coat is slightly ruffled 1 = unkempt and un-groomed, matted appearance
Physical/ Musculoskeletal		
Tumors	Observe the mice to look for symmetry. Hold the base of the tail and manually examine mice for visible or palpable tumors	0 = absent 0.5 = < 1.0 cm 1 = > 1.0 cm or multiple smaller tumors
Distended abdomen	Hold the mouse vertically by the base of the tail and tip backwards over your hand. Excess fluid visible as a bulge below the rib cage	0 = absent 0.5 = slight bulge 1 = abdomen clearly distended
Kyphosis	Inspect the mouse for curvature of the spine or hunched posture. Run your fingers down both sides of the spine to detect abnormalities	0 = absent 0.5 = mild curvature 1 = clear evidence of hunched posture
Tail stiffening	Grasp the base of the tail with one hand, and stroke the tail with a finger of the other hand. The tail should wrap freely around the finger when mouse is relaxed	0 = no stiffening 0.5 = tail responsive but does not curl 1 = tail completely unresponsive
Gait disorders	Observe the freely moving animal to detect abnormalities such as hopping, wobbling, circling, wide stance and weakness	0 = no abnormality 0.5 = abnormal gait but animal can still walk 1 = marked abnormality, impairs ability to move
Tremor	Observe the freely moving animal to detect tremor, both at rest and when the animal is trying to climb up an incline	0 = no tremor 0.5 = slight tremor 1 = marked tremor; animal cannot climb
Forelimb grip strength	Hold the mouse. Allow it grip the bars on the cage lid. Life animal by the base of the tail and assess grip strength	0 = sustained grip 0.5 = reduction in grip strength 1 = no strength, no resistance

Body condition score	Place mouse on flat surface, hold tail base and manually assess the flesh/fat that covers the sacroiliac region (back and pubic bones)	0 = bones palpable, not prominent 0.5 = bones prominent or barely felt 1 = bones very prominent or not felt due to obesity
Vestibulocochlear/ Auditory		
Vestibular disturbance	Hold the base of the tail and lower mouse towards a flat surface. Inspect for head tilt, spinning, circling, head tuck or trunk curling	0 = absent 0.5 = mild head tilt and/or slight spin when lowered 1 = severe disequilibrium
Hearing loss	Test startle reflex. Hold a clicker ~ 10 cm from mouse, sound it 3 times and record responses	0 = always reacts (3/3 times) 0.5 = reacts 1/3 or 2/3 times 1 = unresponsive (0/3 times)
Ocular/ Nasal		
Cataracts	Visual inspection of the mouse to detect opacity in the center of the eye	0 = no cataracts 0.5 = small opaque spot 1 = clear evidence of opaque lens
Eye discharge/ swelling	Visual inspection of the mouse to detect ocular discharge and swelling of the eyes	0 = normal 0.5 = slight swelling and/or secretions 1 = obvious bulging and/or secretions
Microphthalmia	Inspect eyes	0 = normal size 0.5 = one or both eyes slight small or sunken 1 = one or both eyes very small or sunken
Corneal opacity	Visual inspection of the mouse for superficial white spots and/or clouding of the cornea	0 = normal 0.5 = minimal changes in cornea 1 = marked clouding and/or spotting of cornea
Vision loss	Lower mouse towards a flat surface. Evaluate the height at which the mouse reaches towards the surface	0 = reaches >5 cm above surface 0.5 = reaches 2-5 cm above surface 1 = reaches <2 cm above surface
Menace reflex	Move an object towards the mouse's face 3 times. Record whether the mouse blinks in response	0 = always responds 0.5 = no response to 1 or 2 approaches 1 = no response to 3 approaches
Nasal discharge	Visual inspection of the mouse to detect nasal discharge	0 = no discharge 0.5 = small amount of discharge 1 = obvious discharge, both nares
Digestive/ Urogenital		
Malocclusions	Grasp the mouse by the neck scruff, invert and expose teeth. Look for uneven, overgrown teeth	0 = mandibular longer than maxillary incisors 0.5 = teeth slightly uneven 1 = teeth very uneven and overgrown
Rectal prolapse	Grasp the mouse by the base of the tail to detect signs of rectal prolapse	0 = no prolapse 0.5 = small amount of rectum visible below tail 1 = rectum clearly visible below tail
Vaginal/ uterine/ penile prolapse	Grasp the mouse by the base of the tail to detect signs of vaginal/ uterine or penile prolapse	0 = no prolapse 0.5 = small amount of prolapsed tissue visible 1 = prolapsed tissue clearly visible

Diarrhea	Grasp the mouse and invert it to check for signs of diarrhea. Also look for fecal smearing in home cage	0 = none 0.5 = some feces or bedding near rectum 1 = feces + blood and bedding near rectum, home cage smearing
Respiratory		
Breathing rate/ depth	Observe the animal. Not the rate and depth of breathing as well as any gasping behavior	0 = normal 0.5 = modest change in breathing rate and/or depth 1 = marked changes in rate/depth, gasping
Discomfort		
Mouse grimace scale	Note facial signs of discomfort: 1) orbital tightening, 2) nose bulge, 3) check bulge, 4) ear position (drawn back) or 5) whisker change (either backward or forward)	0 = no signs present 0.5 = 1 or 2 signs present 1 = 3 or more signs present
Piloerection	Observe the animal and look for signs of piloerection, in particular on the back of the neck	0 = no piloerection 0.5 = involves fur at base of neck only 1 = widespread piloerection
Other		
Temperature	Measure surface body temperature with an infrared thermometer directed at the abdomen (average of 3 measures). Compare with reference values from sex-matched adult animals	0 = differs by <1 SD from reference value 0.25 = differs by 1 SD 0.5 = differs by 2 SD 0.75 = differs by 3 SD 1 = differs by >3 SD
Weight	Weight the mouse. Compare with reference values from sex-matched adult animals	0 = differs by <1 SD from reference value 0.25 = differs by 1 SD 0.5 = differs by 2 SD 0.75 = differs by 3 SD 1 = differs by >3 SD

Technology) directed at the lower abdomen. Three measurements of body surface temperature were taken and the average of the three readings was used. Deficits in body weight and body surface temperatures were determined based on deviation from the mean values for all mice of the same age (Parks *et al*., 2012; Whitehead *et al.*, 2014). Values that differed from the mean reference values by less than 1 standard deviation (SD) were given a score of 0. Values that were ± 1 SD with respect of the mean values were given a score of 0.25. Values that differed by ± 2 SD were scored as 0.5, those that differed by ± 3 SD were given a score of 0.75, and values that were greater than 3 SD from the reference value received a maximal score of 1. Following frailty assessment, the frailty index of each mouse was determined by summing all the deficit scores, and the total was divided by the number of parameters measured (31) to provide a frailty index score between 0 (no deficits present) and 1 (all possible deficits present).

2.4 Measurement of *in vivo* heart function using echocardiography

Two-dimensional guided echocardiography was performed on mice in this study to assess *in vivo* heart function. All echocardiography experiments were performed using a Vivid 7 imaging system (GE Medical Systems, Horten, Norway). Mice were anesthetized under 1.5% isoflurane in oxygen (1 L/min) and placed in a supine position on a heated platform (~37°C). The hair on the chest area of each mouse was removed with depilatory cream to minimize interference. Ultrasound transmission gel (Parker Laboratories Inc., NJ, USA) was applied to the chest to maximize image quality. Electrocardiography (ECG) electrodes (Grass technologies, RI, USA) were inserted subcutaneously to obtain

electrocardiographic measurements. A high-resolution linear transducer (il3L, GE ultrasound, Horten, Norway) was used to collect images of the mouse heart. Two-dimensional guided M-mode images of the heart in the short axis orientation were used to measure left ventricular dimensions in systole and diastole. The measurements made included left ventricular internal diameter (LVID), interventricular septum (IVS), and left ventricular posterior wall (LVPW). Ejection fraction (EF), which is the fraction of blood pumped from the heart with each beat, and fractional shortening (FS), which is the percentage change in ventricular diameter from diastole to systole, were calculated using the following equations: $EF = [(\text{end-diastolic}^3 - \text{end-systolic}^3) / \text{end-diastolic}^3] \times 100\%$ and $FS = [(\text{end-diastolic} - \text{end-systolic}) / \text{end-diastolic}] \times 100\%$. Mouse heart rate was determined from ECG traces. Following echocardiography, mice were placed on a heating pad for approximately 20 minutes to allow the anesthetic to wear off and permit the animals to recover. Mice were returned to their home cages once they regained their motor function. Mice that underwent echocardiography were given at least 4 days to recover before euthanization for cell isolation.

2.5 Ventricular myocyte isolation

To determine the contractile function of ventricular myocytes, cells were isolated by enzymatic digestion as described previously in our lab (Grandy & Howlett, 2006). To anaesthetize the mice and prevent blood coagulation during myocyte isolation, sodium pentobarbital (220 mg/kg; Pharmaceutical Partners of Canada, Richmond, ON) and heparin (3000 U/kg; CDMV, Saint-Hyacinthe, QC) were co-administered via intraperitoneal

injection. Anaesthesia was confirmed by the absence of pedal withdrawal and corneal reflexes.

Following anaesthesia, each animal was weighed, and then placed on the surgical table in a supine position. Forelimbs were secured with clamps to maintain position during surgery. The thoracic cavity was exposed using a sternal incision. The rib cage was cut laterally on both sides and folded back to expose the heart. The aorta was severed before removing the heart from the chest cavity. The aorta was then cannulated *ex-vivo*, secured with a suture, and the heart was retrogradely perfused at 2.2 ml/min with oxygenated nominally Ca^{2+}-free buffer containing (mM): 105 NaCl, 5 KCl, 1 $MgCl_2$, 0.33 NaH_2PO_4, 25 HEPES, 20 glucose, 3 Na-pyruvate, 1 lactic acid (pH 7.4 with NaOH). Following 10 minutes of perfusion, the heart was then enzymatically digested by perfusing with same Ca^{2+}-free buffer supplemented with 50 μM $CaCl_2$, collagenase type I (8.0 mg/30ml; Worthington, Lakewood, NJ), dispase II (3.4 mg/30ml; Roche Diagnostics, Laval, QC), and trypsin (0.5 mg/30ml; Sigma Aldrich, Oakville, ON) for approximately 8 minutes. All isolation buffers were bubbled with 100% O_2 (Praxair, Dartmouth, NS) and warmed to 37°C using a heating coil (Radnoti Glass Technology Inc. Monrovia, CA) heated by a circulating water bath (Haake; Scientific, Ottawa, ON). A peristaltic pump (Piper model P; Fred A. Dungey Inc., Agincourt, ON) was used to deliver the solution through the perfusion apparatus to the heart, and any air bubbles were collected by a bubble trap located within the heating coil.

Following enzymatic digestion, the ventricles were isolated from the atria and cut into small pieces in a high potassium buffer containing (mM): 45 KCl, 3 $MgSO_4$, 30 KH_2PO_4, 50 L-glutamic acid, 20 taurine, 0.5 EGTA, 10 HEPES, 10 glucose (pH 7.4 with

KOH). The ventricular tissue was rinsed with this buffer three times to ensure removal of all enzyme containing solution. Individual ventricular myocytes were dissociated from the tissue by gentle swirling, and the cell suspension was passed through a 225 μm polyethylene mesh to filter out any large pieces of tissue.

2.6 Field stimulation: Intracellular Ca^{2+} and contraction measurements

Following ventricular myocyte isolation, Ca^{2+} transients and cell shortening were measured in cells paced with field stimulation electrodes. A schematic of the field stimulation setup is shown in Figure 2.1. Myocytes were incubated in the dark with fura-2 AM (2.5 μM) for approximately 20 minutes in a plexiglass chamber with a glass bottom mounted to the stage of an inverted microscope (Nikon Eclipse TE200; Nikon Canada, Mississauga, ON). The microscope was placed in a Faraday cage covered with black vinyl to prevent light from interfering with the fluorescence recordings. In addition, the microscope was supported by a custom-made air table to reduce vibrations. Following incubation, myocytes were superfused at 3 ml/min with a buffer solution containing (mM): 135 NaCl, 10 glucose, 10 HEPES, 4 KCl, 1 $MgCl_2$, and 2 $CaCl_2$ (pH 7.4 with NaOH). The buffer was kept at a constant temperature of 37°C using a circulating water bath (Polystat, Model # 12112-10, Cole Parmer, Vernon Hills, IL).

Myocytes were visualized using an oil immersion 40x lens (Nikon S-Fluor, numerical aperture 1.30, Nikon Canada Inc.). Fluorescence and cell shortening were measured simultaneously by dividing the microscope light between a photomultiplier tube (Photon Technologies International (PTI), Birmingham, NJ) and a video camera (Philips,

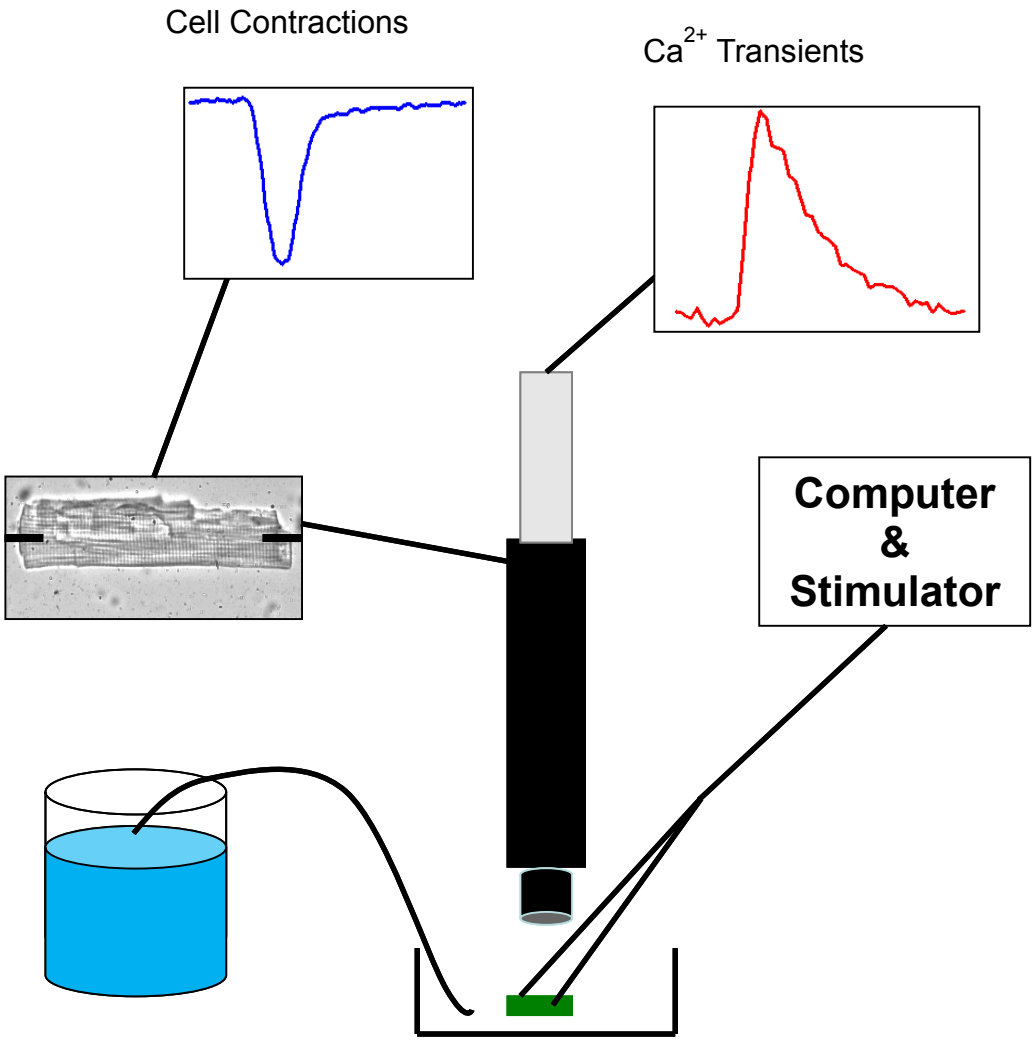

Figure 2.1. Schematic of the field stimulation setup. Each component is described in detail in the methods section.

Markham, Ontario) using a dichroic cube (Chroma Technology Corp., Rockingham, VT). Fluorescence measurements from healthy myocytes (rectangular shaped with clear striations) were obtained by closing the photomultiplier aperture to fit the precise size of the cell observable through the viewing window. A DeltaRam fluorescence system (PTI) was used to excite myocytes with light alternating between 340 nm and 380 nm. Fluorescence emitted at 510 nm was recorded for both 340 nm and 380 nm wavelengths at a rate of 200 samples/second with Felix software (PTI). Fluorescence was recorded for a period of 10 seconds. Following the fluorescence recordings, a background fluorescence reading was taken for each cell from an area close to the cell that was free of myocytes and cell fragments.

Cell shortening was measured by a video edge detector at a rate of 120 samples/second (Model #105; Crescent Electronics, Sandy, UT). Two platinum electrodes were placed in the plexiglass chamber with one electrode just above and the other electrode just below the microscope field of view. Bipolar pulses (3 ms, 30-70 mA) were generated by a stimulus isolation unit (Model #SIU-102; Warner Instruments, Hamden, CT). The pacing rate was controlled by pClamp 8.2 software (Molecular Devices, Sunnyvale, CA). Myocytes were stimulated at 2 Hz and cell shortening as well as cell length and width were recorded with pClamp 8.2 software.

2.7 Treatment of ventricular myocytes with isoproterenol

To determine whether ventricular myocytes from frail animals were more sensitive to stress induced by Ca^{2+} overload than non-frail animals, in some experiments cells were

exposed to the non-selective β-adrenergic agonist, isoproterenol. For each experiment, a fresh 1 μM working solution was made by diluting a 1 mM isoproterenol stock solution with the buffer described in Section 2.6. The working solution was administered for 5 min at 3 ml/min by the same perfusion method described previously. Following drug administration, Ca^{2+} transients and cell shortening were measured simultaneously.

2.8 Chemicals

Fura-2 AM was obtained from Invitrogen (Burlington, ON). Stock solutions of Fura-2 AM were prepared by dissolving 50 μg of fura-2 AM in 20 μl of anhydrous DMSO, with a final concentration of 0.2% DMSO. Isoproterenol was dissolved in water to make a 1 mM stock solution, which was stored at -20°C. All chemicals used to make buffer solutions were purchased from Sigma Aldrich (Oakville, ON).

2.9 Statistical Analysis

Echocardiography data were analyzed using the Vivid 7 imaging system (GE Medical Systems, Horten, Norway). Field stimulation data were analyzed using Clampfit 8.2 (Molecular Devices, Sunnyvale, CA). All graphs and tables were constructed using Sigma Plot 12.0 (Systat Software, Inc., Point Richmond, CA). Sigma Plot 12.0 was also used to perform statistical analyses. Contraction was measured as the difference between resting cell length and the cell length at peak contraction. Ca^{2+} transients were measured by subtracting the background fluorescence from the fluorescence measured at each

wavelength. The fluorescence signals were converted to an emission ratio (340/380 nm) using Felix software (PTI). Ratios were then transformed to Ca^{2+} concentrations and Ca^{2+} transients were measured as the difference between diastolic Ca^{2+} and systolic Ca^{2+}.

Survival in the cohort was illustrated using a Kaplan-Meier survival curve. Comparisons of mouse frailty indices for each assessment were evaluated with a one-way ANOVA. To evaluate the relationship between age and the frailty index, the curve was fitted with an exponential function ($y = a^{b*x}$). The effects of age and frailty on *in vivo* and cellular structure and function were assessed with linear regression analysis ($f = y_0 + a*x$). In addition, mice were divided into groups based on either age or frailty. With age, mice were divided into 3 groups: young mice that were less than 365 days old, middle-aged mice that were between 365 and 730 days old, and old mice that were older than 730 days. With FI scores, mice were divided so that the least frail group had a FI score of less than 0.15, the moderately frail group had FI scores between 0.15 and 0.30, and the frailest group had FI scores greater than 0.30. Differences between the groups were evaluated using a one-way ANOVA test against the control, with the youngest and least frail mice as control groups. Findings were reported as significant if $p < 0.05$. The effects of isoproterenol treatment in ventricular myocytes were assessed using a two-way ANOVA test. Incidence of spontaneous contractile activity and cell death were evaluated using a chi-squared test.

Chapter 3: Results

3.1 Quantification of frailty in a longitudinal study of aging mice

Frailty was assessed at regular intervals in a large cohort of male C57BL/6J mice (n = 257). Survival in the cohort was followed throughout the study from 1 month of age to approximately 15 months. Figure 3.1 illustrates a Kaplan-Meier survival curve for the mice investigated in this study. Mortality occurred when animals died unexpectedly or were euthanized due to illness. Arrows in Figure 3.1 indicate the approximate ages of the mice when frailty assessments were performed.

To examine the relationship between frailty and age, a FI was determined in each mouse with the clinical frailty assessment tool described in the Methods section. Mice were purchased at 3 weeks of age and the first frailty assessment was performed at approximately 1 month of age. Each subsequent frailty assessment was conducted at intervals of approximately 6 months. Figure 3.2A shows that the average FI scores progressively increased with age. The FI scores were significantly higher at 6 months and 12 months of age when compared to scores at 1-month of age (values were 0.016 ± 0.001, 0.085 ± 0.003, and 0.212 ± 0.002 at 1-, 6-, and 12-months of age, respectively; mean ± SEM; $p < 0.05$). Furthermore, FI scores were significantly higher when the mice were 12 months of age compared with the same mice at 6 months of age (Figure 3.2A). Figure 3.2B shows FI scores plotted as a function of age; each point represents the FI score of a mouse at that age. These longitudinal data indicate that frailty increased exponentially with age ($r^2 = 0.84$; $p < 0.05$), as shown previously in a cross-sectional study of a small cohort of mice using the same frailty assessment tool (Whitehead *et al*., 2014).

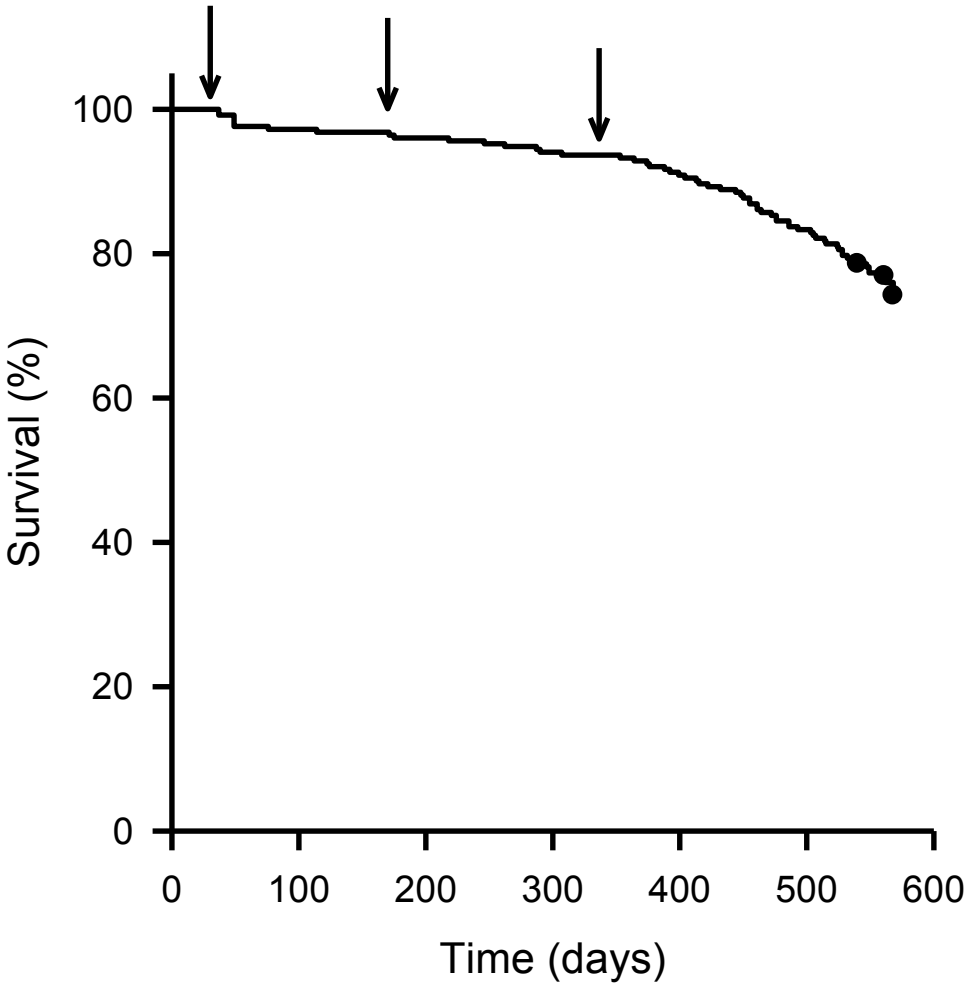

Figure 3.1. Kaplan-Meier survival curve for mortality in the mice used in this study. Survival in the cohort was followed throughout this study. Mortality occurred when animals died unexpectedly or were euthanized due to illness. Arrows above indicate approximate ages of mice when frailty assessment was performed (n = 257).

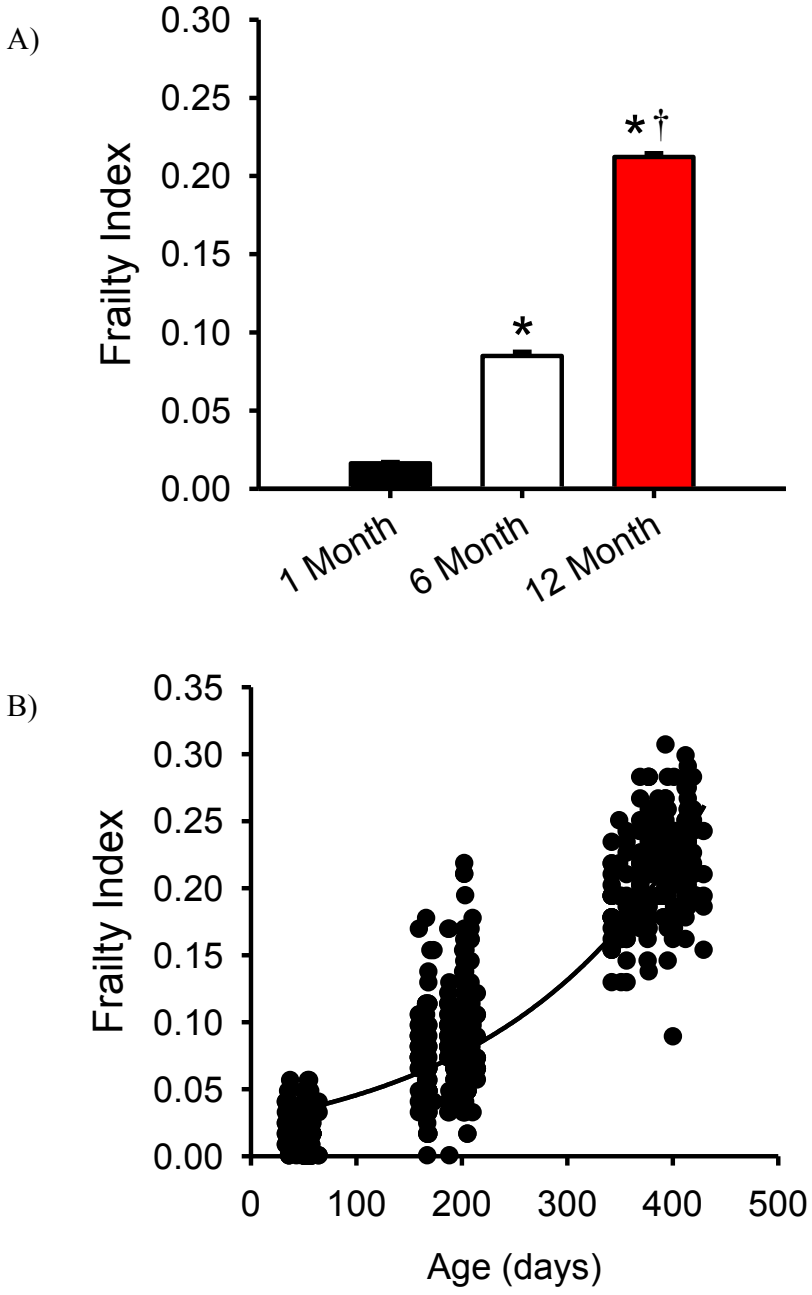

Figure 3.2. Average FI scores progressively increased with age. Frailty assessment was performed at 6 month intervals. **A)** FI scores were significantly higher at 6 months and 12 months of age when compared to scores at 1 month of age. FI scores at 12 months were significantly higher than at 6 months of age ($n = 257$; $^*p < 0.05$). **B)** FI scores were plotted as a function of age. Frailty increased exponentially with age ($r^2 = 0.84$; $p < 0.05$).

To determine whether age-matched male and female mice had different FI scores, males and females were compared in young (approximately 6 months old) and old (approximately 27 months old) mice. Figure 3.3 shows that FI scores were similar between young female and male mice (values were 0.094 ± 0.002 and 0.085 ± 0.003 for female and male mice, respectively; $p < 0.05$). FI scores did not differ between old female and male mice either (values were 0.290 ± 0.039 and 0.234 ± 0.020 for females and males, respectively; $p < 0.05$). These results suggest that there are no sex differences in FI scores in mice, and justifies using some female mice in some *in vivo* and cellular experiments conducted and pooling male and female data.

3.2 Impact of frailty and age on *in vivo* ventricular morphology and function

To investigate the relationship between frailty, age, and *in vivo* ventricular morphology and function, two-dimensional guided M-mode echocardiography was performed. Echocardiography images were obtained from anesthetized mice with a high-resolution linear transducer (il3L, GE ultrasound, Horten, Norway) attached to a Vivid 7 imaging system (GE Medical Systems, Horten, Norway). Figure 3.4A and 3.4B illustrates representative M-mode images from a mouse with a low FI score and a mouse with a higher FI score, respectively. Figure 3.4C and 3.4D show M-mode images from a young and an old mouse, respectively. M-mode images showed that the mouse with a higher FI score had a noticeably larger LV internal diameter compared to the less frail mouse. In addition, contractility of the heart seemed to decline in the frailer mouse. By contrast, there were no marked differences evident in LV internal diameter and the contractile function between the younger mouse and the older mouse with similar FI scores.

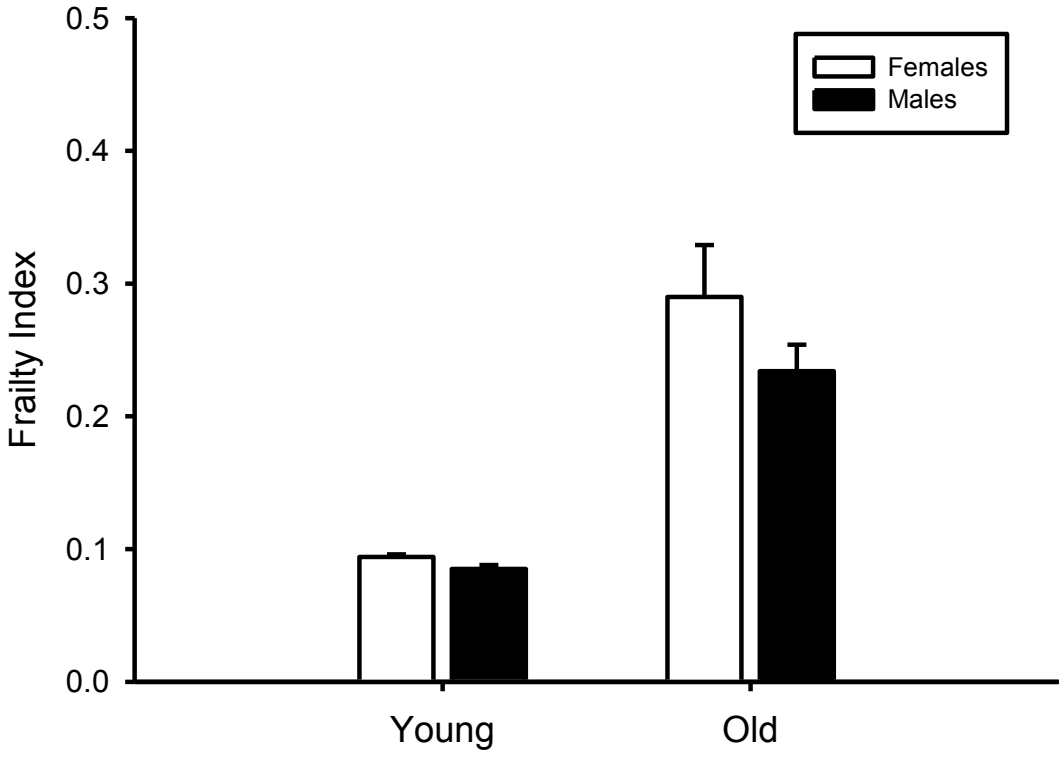

Figure 3.3. There were no differences in FI scores between age-matched female and male mice. FI scores were similar between young (~6 months) females and males (n = 15 young females, n = 249 young males). There were no signifcant differences in FI scores between old (~ 27 months) females and males either (n = 4 old females, n = 6 old males).

A)

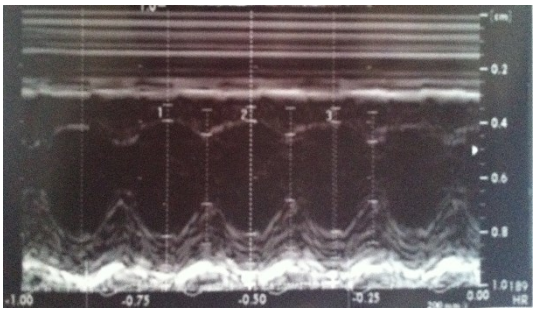

B)

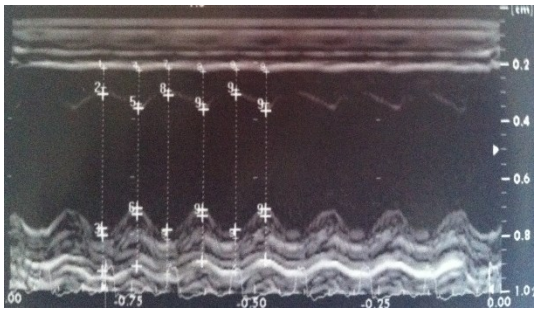

C)

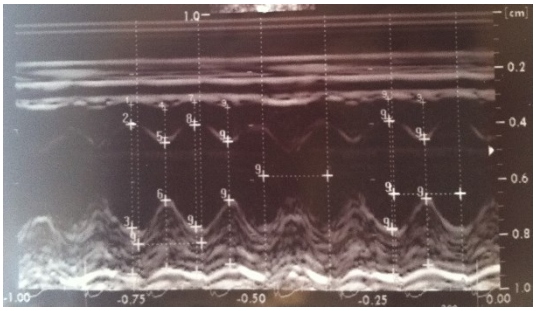

D)

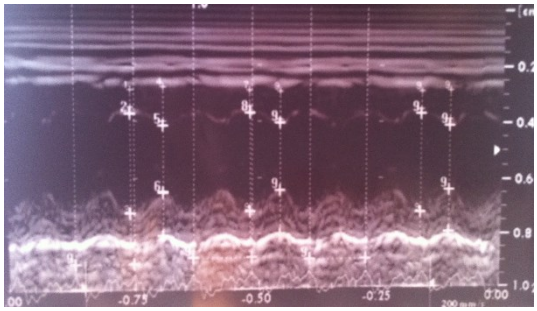

Figure 3.4. Representative M-mode images of *in vivo* cardiac function. A) M-mode image from a mouse with a low FI score (FI = 0.105). **B)** M-mode image from a mouse with a higher FI score (FI = 0.290). **C)** M-mode image from a young mouse (age = 148 days). **D)** M-mode image from an old mouse (age = 821 days).

Ventricular morphology and function were assessed based on age and FI score using linear regression analysis as well as differences between groups described in the Methods section. Briefly, mice were divided into three groups based on age or FI score. With FI scores, mice in the control group had FI scores of less than 0.15; the moderately frail group had FI scores between 0.15 and 0.30; and the frail group had FI scores greater than 0.30. With age, the control group consisted of mice less than 365 days of age; the second group were middle-aged mice that were between 365 and 730 days old; and the third group were old mice that were older than 730 days. First, ventricular morphology was compared between groups. Figure 3.5A-D shows that interventricular septum thickness in systole and diastole did not show any correlation or differ between the three frail groups or the three age groups. LV posterior wall thickness in systole and diastole was also unaffected by either frailty or age (Figure 3.6A-D). Figure 3.7A shows that LV internal diameter during systole was significantly greater in both frail groups when compared to the group with the lowest FI scores (values were 0.307 ± 0.020 cm, 0.338 ± 0.010 cm, and 0.243 ± 0.015 cm for least frail, moderately frail, and frail groups, respectively; $r^2 = 0.22$, $p < 0.05$). There were no significant differences in LV internal diameter during systole between the moderately frail group and the very frail group. By contrast, LV internal diameter during systole was not correlated with age and did not differ between the 3 age groups (Figure 3.7B). Figure 3.7C shows that the LV internal diameter during diastole was significantly increased in both frail groups compared to the control group, but there were no significant differences between the two frail groups (values were 0.360 ± 0.016 cm, 0.410 ± 0.015 cm, and 0.415 ± 0.010 cm for control, moderately frail, and frail groups, respectively; $r^2 = 0.21$, $p < 0.05$). Interestingly, there were no correlations or significant differences in LV internal diameter during diastole when comparing the three different age groups (Figure 3.7D).

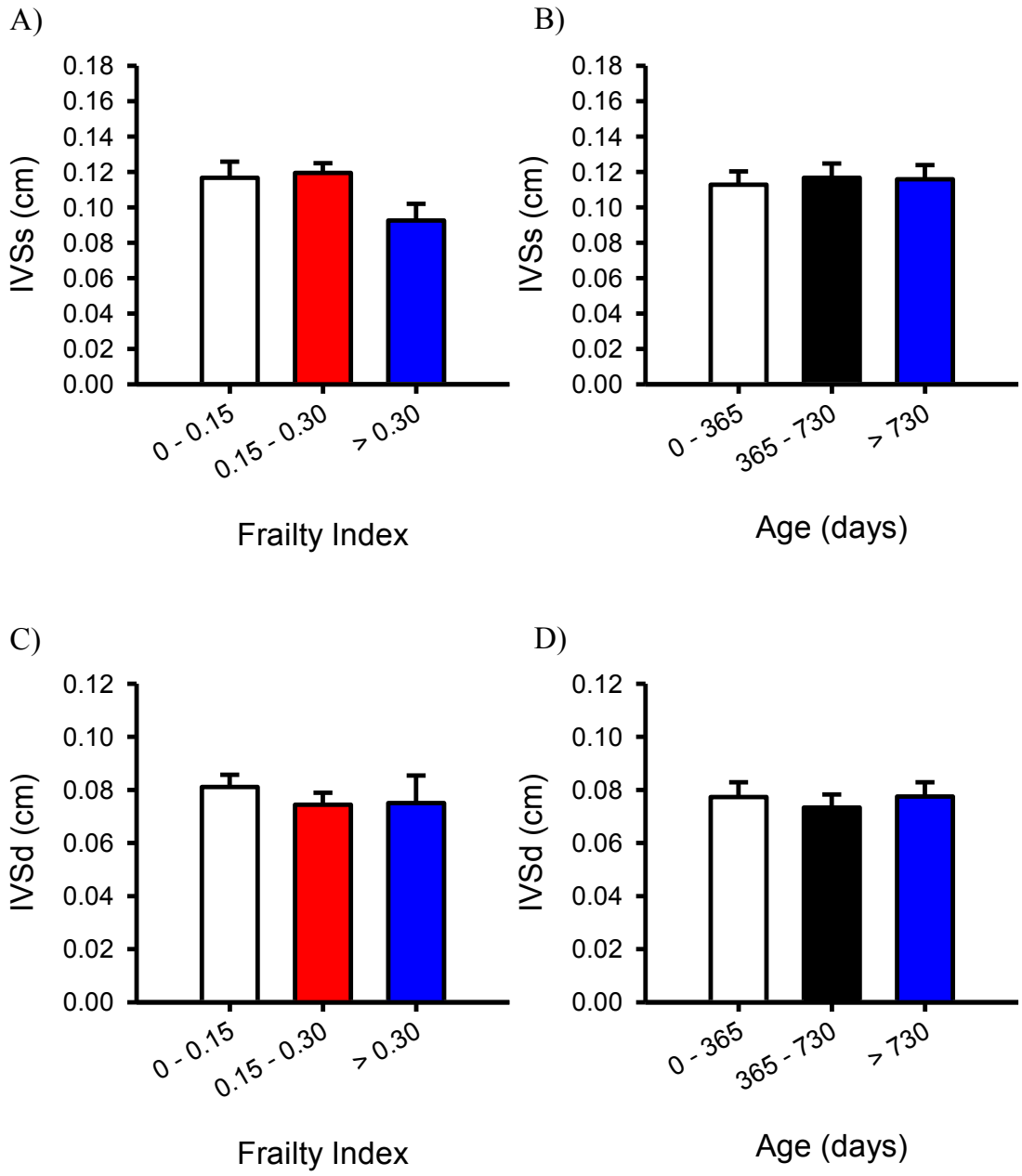

Figure 3.5. Interventricular septum thickness (IVS) was not affected by frailty or age in either systole or diastole. A,B) IVS in systole was similar in all 3 frail groups (n = 9, 16, and 4 animals for least frail, moderately frail, and frail groups, respectively) and all 3 age groups (n = 11, 6, and 12 animals for young, middle-aged, and oldest groups, respectively). **C,D)** IVS during diastole also was unaffected by either frailty or age (n = 9, 16, and 4 animals for least frail, moderately frail, and frail groups, respectively; n = 11, 6, and 12 animals for young, middle-aged, and oldest groups, respectively).

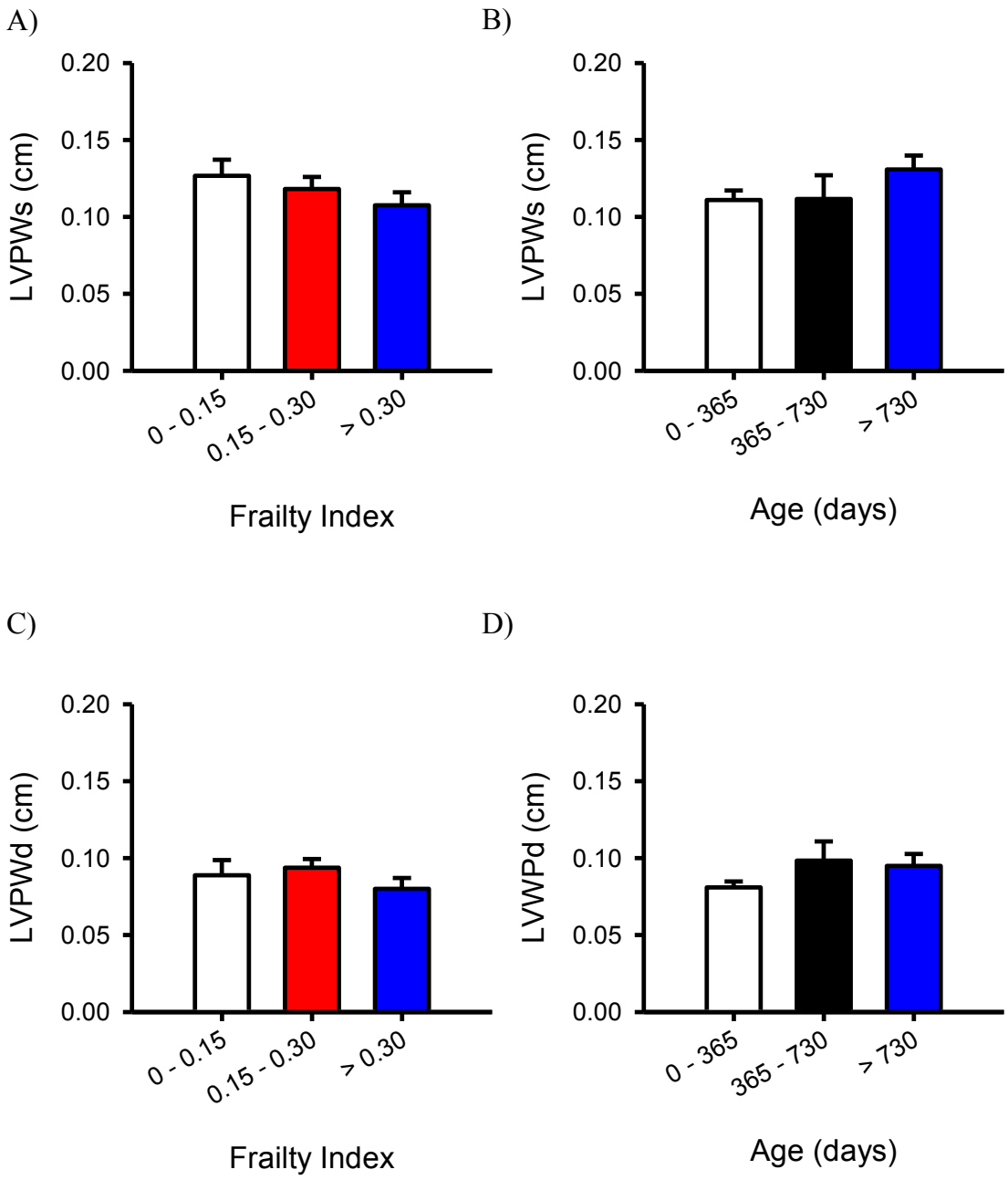

Figure 3.6. LV posterior wall thickness (LVPW) was not affected by frailty or age during systole or diastole. A,B) LVPW during systole was similar in all 3 frail groups and all 3 age groups (n = 9, 16, and 4 animals for least frail, moderately frail, and frail groups, respectively; n = 11, 6, and 12 animals for young, middle-aged, and oldest groups, respectively). **C,D)** LVPW during diastole was also unaffected by either frailty or age (n = 9, 16, and 4 animals for least frail, moderately frail, and frail groups, respectively; n = 11, 6, and 12 animals for young, middle-aged, and oldest groups, respectively)

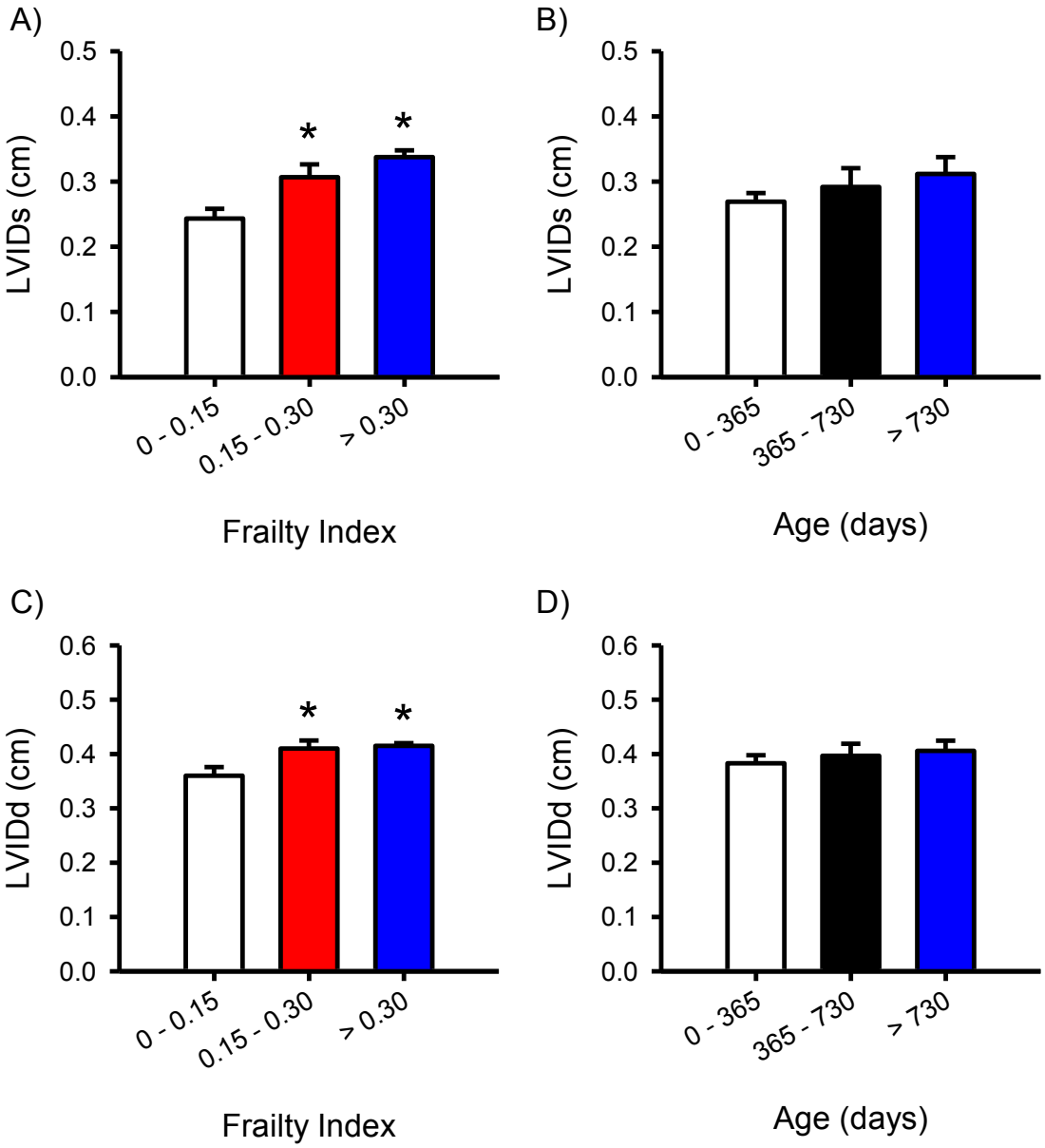

Figure 3.7. LV internal diameter increased with frailty but not age. A) LV internal diameter during systole (LVIDs) was significantly higher in the two frail groups when compared to least frail group (n = 9, 16, and 4 animals for least frail, moderately frail, and frail groups, respectively; *p < 0.05). **B)** LVIDs did not differ between the 3 age groups (n = 11, 6, and 12 animals for young, middle-aged, and oldest groups, respectively). **C)** LV internal diameter during diastole (LVIDd) was significantly higher in both frail groups compared to the least frail group (n = 9, 16, and 4 animals for least frail, moderately frail, and frail groups, respectively; *p < 0.05). **D)** LVIDd did not differ between the 3 age groups (n = 11, 6, and 12 animals for young, middle-aged, and oldest groups, respectively).

These data demonstrate that hearts are enlarged in frail mice compared to mice that are less frail. However, these changes are not evident with age.

To assess the relationship between frailty and heart function, heart rate, LV fractional shortening, and ejection fraction were measured. Electrocardiogram measurements obtained during echocardiography were used to compare heart rate. Figure 3.8A shows that heart rates was not correlated to frailty and did not differ amongst the three frailty groups. There were also no correlation or significant differences in heart rate between the three age groups (Figure 3.8B). Figure 3.9A shows that fractional shortening declined as frailty increased, and fractional shortening in the most frail group was significantly less than the control group (values were 32.7 ± 3.5 % and 18.2 ± 2.7 % for control and frail groups, respectively; $r^2 = 0.14$, $p < 0.05$). By contrast, mice from all three age groups showed a similar degree of LV fractional shortening (Figure 3.9B). Ejection fraction was also significantly lower in the most frail group compared to the control group (values were 67.1 ± 3.5 % and 43.3 ± 5.2 % for control and frail groups, respectively; $r^2 = 0.17$, $p < 0.05$) (Figure 3.9C). By contrast, ejection fraction was similar at all ages (Figure 3.9D). These data suggest that there is a decline in *in vivo* cardiac contractile function associated with increasing frailty. Again, these changes were not observed when aged mice were compared to young mice.

3.3 Influence of frailty and age on ventricular myocyte morphology

To investigate the relationship between frailty, age, and myocyte size at the cellular level, ventricular myocyte lengths and widths were measured in each cell as described in

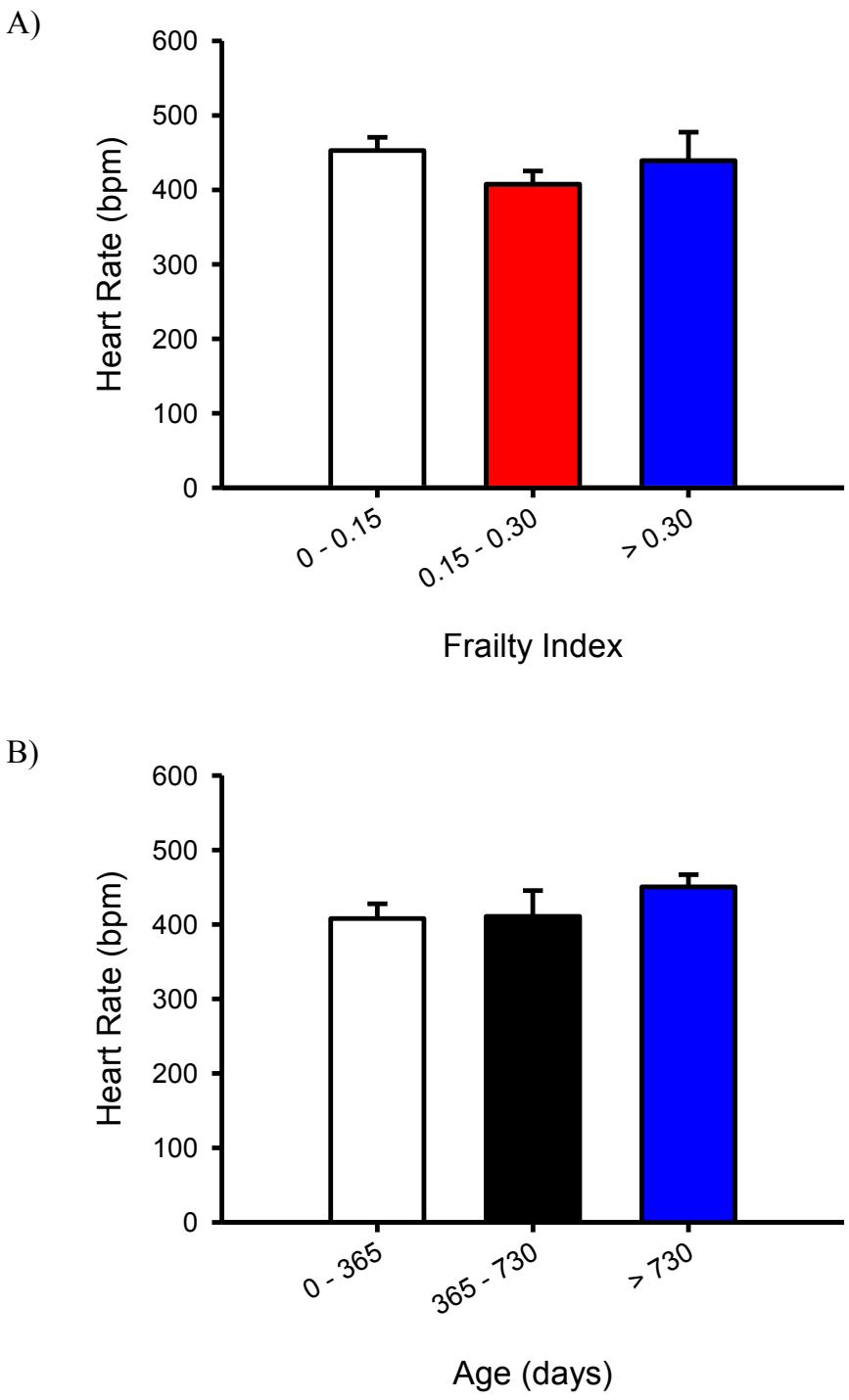

Figure 3.8. Heart rate was unaffected by frailty or age. A) Heart rate did not differ between the 3 frailty groups (n = 9, 16, and 4 animals for least frail, moderately frail, and frail groups, respectively). **B)** Heart rate also was unaffected by age (n = 11, 6, and 12 animals for young, middle-aged, and oldest groups, respectively).

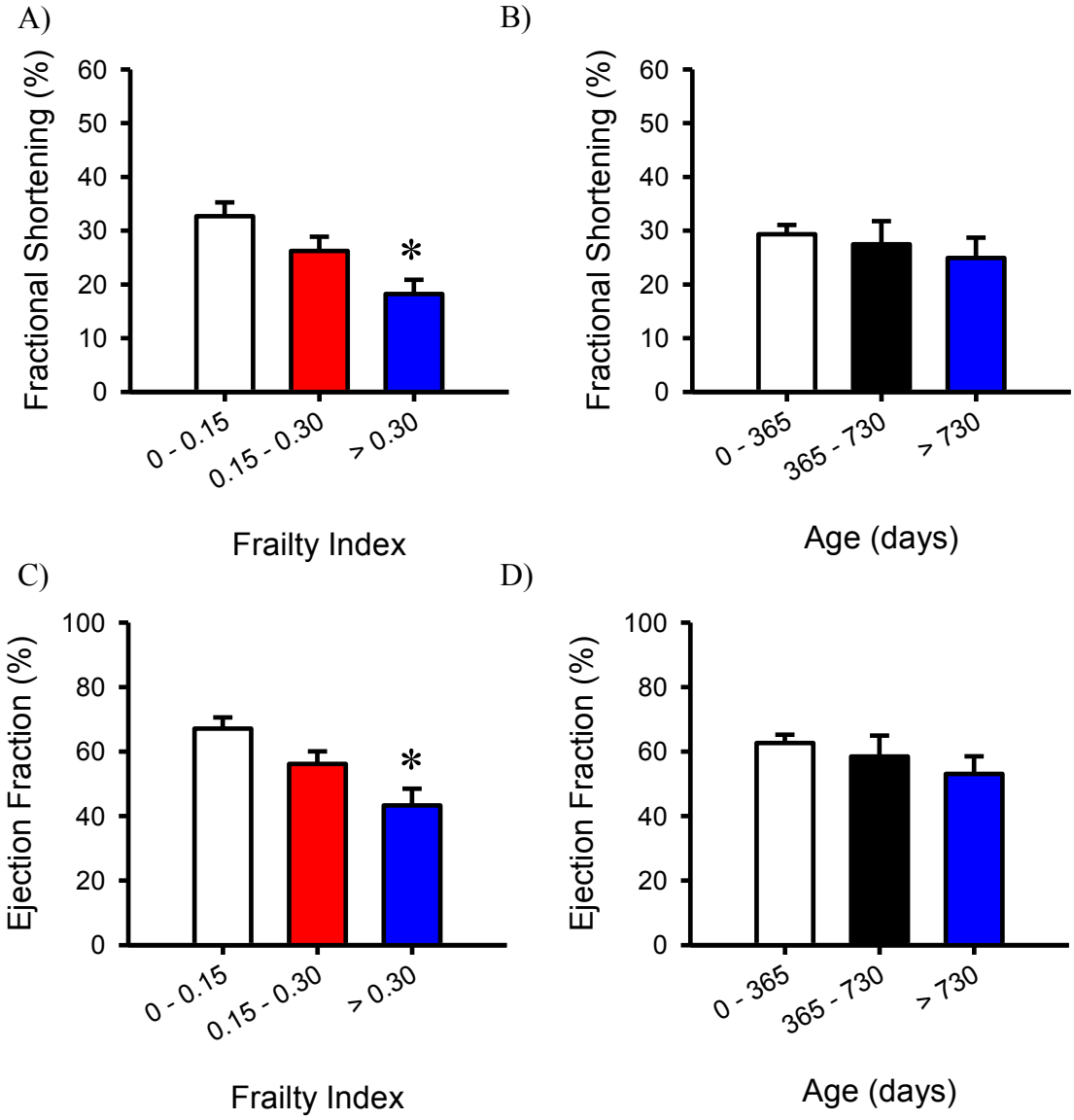

Figure 3.9. ***In vivo*** **contractile function declined with increasing frailty but now with increasing age.** **A)** Fractional shortening was significantly lower in the most frail group when compared to the control group (n = 9, 16, and 4 animals for least frail, moderately frail, and frail groups, respectively; *p < 0.05). **B)** Fractional shortening was unaffected by age (n = 11, 6, and 12 animals for young, middle-aged, and oldest groups, respectively). **C)** Ejection fraction was lower in the most frail group compared to the control group (n = 9, 16, and 4 animals for least frail, moderately frail, and frail groups, respectively; *p < 0.05). **D)** Ejection fraction did not differ between the 3 age groups (n = 11, 6, and 12 animals for young, middle-aged, and oldest groups, respectively).

the Methods section. Since ventricular myocytes are roughly rectangular in shape, the cell area was estimated by multiplying the cell length by cell width. To determine the relationship between FI, age, and cell morphology, mice were graded by FI as described earlier. Figure 3.10A shows that mean cell length increased as the FI increased, where the two frail groups had significantly longer cells than the control group (values were: 123.7 ± 3.0 μm, 134.7 ± 3.3 μm, and 156.1 ± 6.0 μm for control, moderately frail and frail groups, respectively; $r^2 = 0.06$, $p < 0.05$). In addition, the most frail group had significantly longer cell lengths than the moderately frail group (Figure 3.10A). Figure 3.10B shows that mean cell lengths were significantly shorter in cells from middle-aged mice compared to the youngest mice. By contrast, mean cell length from the oldest mice was greater than the youngest group (values were: 133.1 ± 2.6 μm, 115.9 ± 4.7 μm, and 144.1 ± 3.7 μm for youngest, middle aged, and oldest groups, respectively; $p < 0.05$). Figure 3.10C shows that cell width also increased as the FI increased; the cells were significantly wider in the two frail groups compared to control (values were: 25.3 ± 0.8 μm, 29.8 ± 1.0 μm, and 32.6 ± 2.1 μm for control, moderately frail and frail groups, respectively; $r^2 = 0.08$, $p < 0.05$). The very frail group also had significantly greater cell widths compared to the moderately frail group (Figure 3.10C). Figure 3.10D shows that cells from the oldest mice were wider than cells from young mice (values were: 26.8 ± 0.8 μm, 28.0 ± 1.7 μm, and 31.2 ± 1.1 μm for youngest, middle aged, and oldest groups, respectively; $r^2 = 0.03$, $p < 0.05$). Figure 3.11A shows ventricular myocytes in the control group had a smaller average cell area compared to the moderately frail and frail groups (values were: 3191.2 ± 136.7 μm^2, 4026.0 ± 177.1 μm^2, and 5210.8 ± 416.4 μm^2 for control, moderately frail and frail groups, respectively; $r^2 = 0.13$, $p< 0.05$). There was also an age-dependent change in cell area, where cells from the oldest mice were larger than cells from youngest mice (values were: 3579.7 ± 130.8

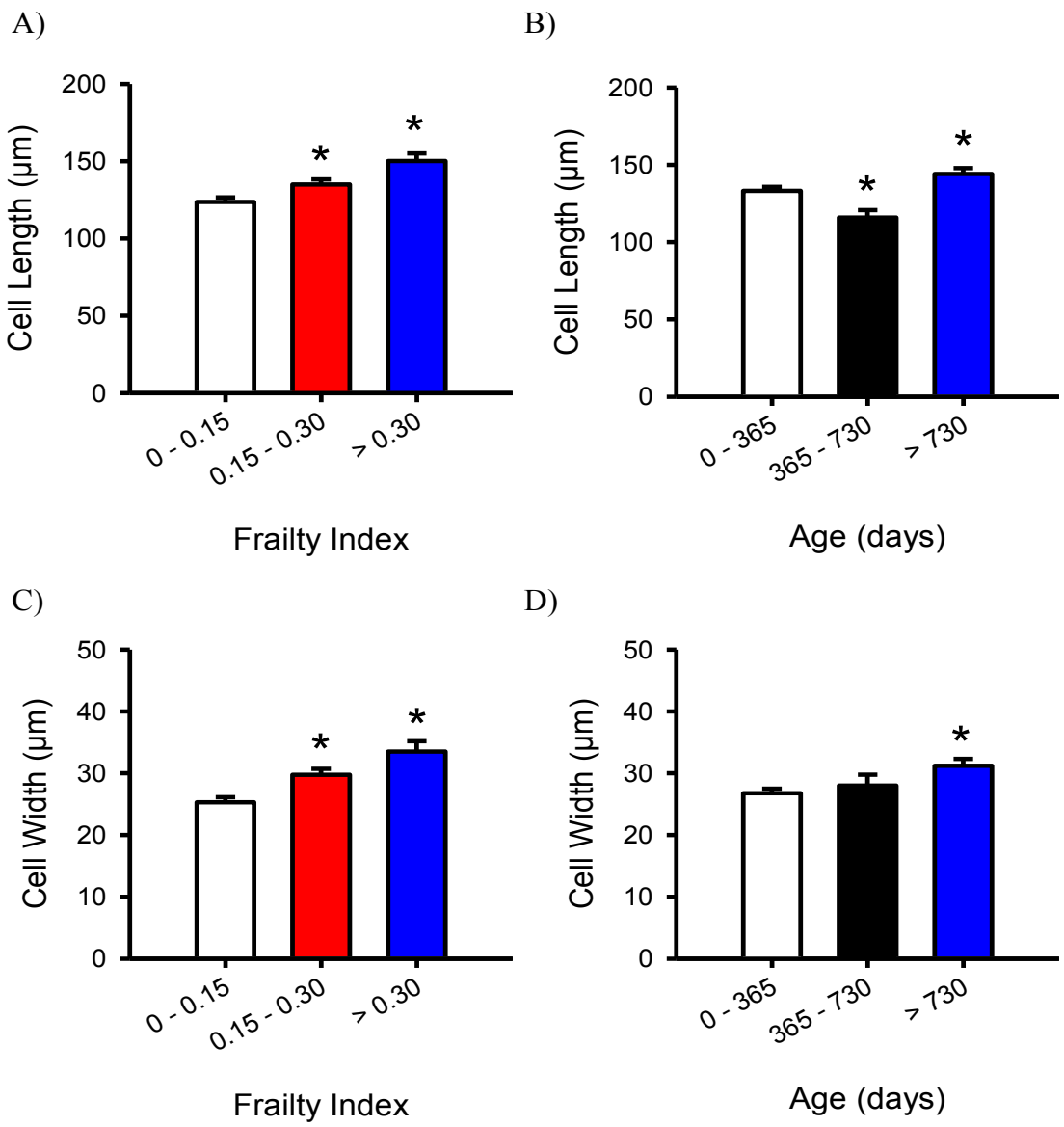

Figure 3.10. Relationship between ventricular myocyte size and frailty or age. A) Mean cell length from both frail groups was significantly longer compared to control (n = 105, 78, and 47 cells for least frail, moderately frail, and frail groups, respectively; *p < 0.05). **B)** While mean cell length from the middle-aged group was shorter than the control group, cell length in aged cells was longer compared to cells from young mice (n = 105, 50, and 75 cells for youngest, middle-aged, and oldest groups, respectively; *p < 0.05). **C)** Mean cell width from both frail groups was wider compared to control (n = 105, 78, and 47 cells for least frail, moderately frail, and frail groups, respectively; *p < 0.05). **D)** Mean width from the aged cells were wider compared to cells from mice in the youngest group (n = 105, 50, and 75 cells for youngest, middle-aged, and oldest groups, respectively; *p < 0.05).

μm, 3427.0 ± 276.8 μm, and 4519.9 ± 209.3 μm for youngest, middle aged, and oldest groups, respectively; $r^2 = 0.05$, $p < 0.05$) (Figure 3.11B). Together, these results show that ventricular myocytes experience both frailty-dependent and age-associated hypertrophy, although myocyte hypertrophy is graded more by FI than by age.

3.4 Impact of frailty and age on ventricular myocyte contractions and Ca^{2+} transients

To determine the relationship between frailty, age, and cardiac contractile function, myocytes were paced at 2 Hz and contractions and the underlying Ca^{2+} transients were measured simultaneously. Figure 3.12A-D shows representative examples of Ca^{2+} transients (top) and contractions (bottom) recorded from isolated myocytes paced at 2 Hz from a mouse with a low FI score, a mouse with a high FI score, a young mouse, and an old mouse, respectively. Ca^{2+} transient amplitudes and contractions were similar in myocytes isolated from a mouse with a low FI score and a mouse with a higher FI score. Contractions were also similar in myocytes from a young mouse and an old mouse. However, the Ca^{2+} transient amplitude was visibly lower in the old mouse compared to the young mouse.

To determine the relationship between FI, age, and contractile function, mice were categorized into groups as described earlier. Contractions were normalized to resting cell length and expressed as fraction of shortening (% cell length). Figure 3.13A shows although there were no significant correlation between frailty and fractional shortening, fractional shortening significantly declined in the moderately frail group, but not in the most frail group, when compared to the control group (values were: 4.0 ± 0.4 %, 3.2 ± 0.3

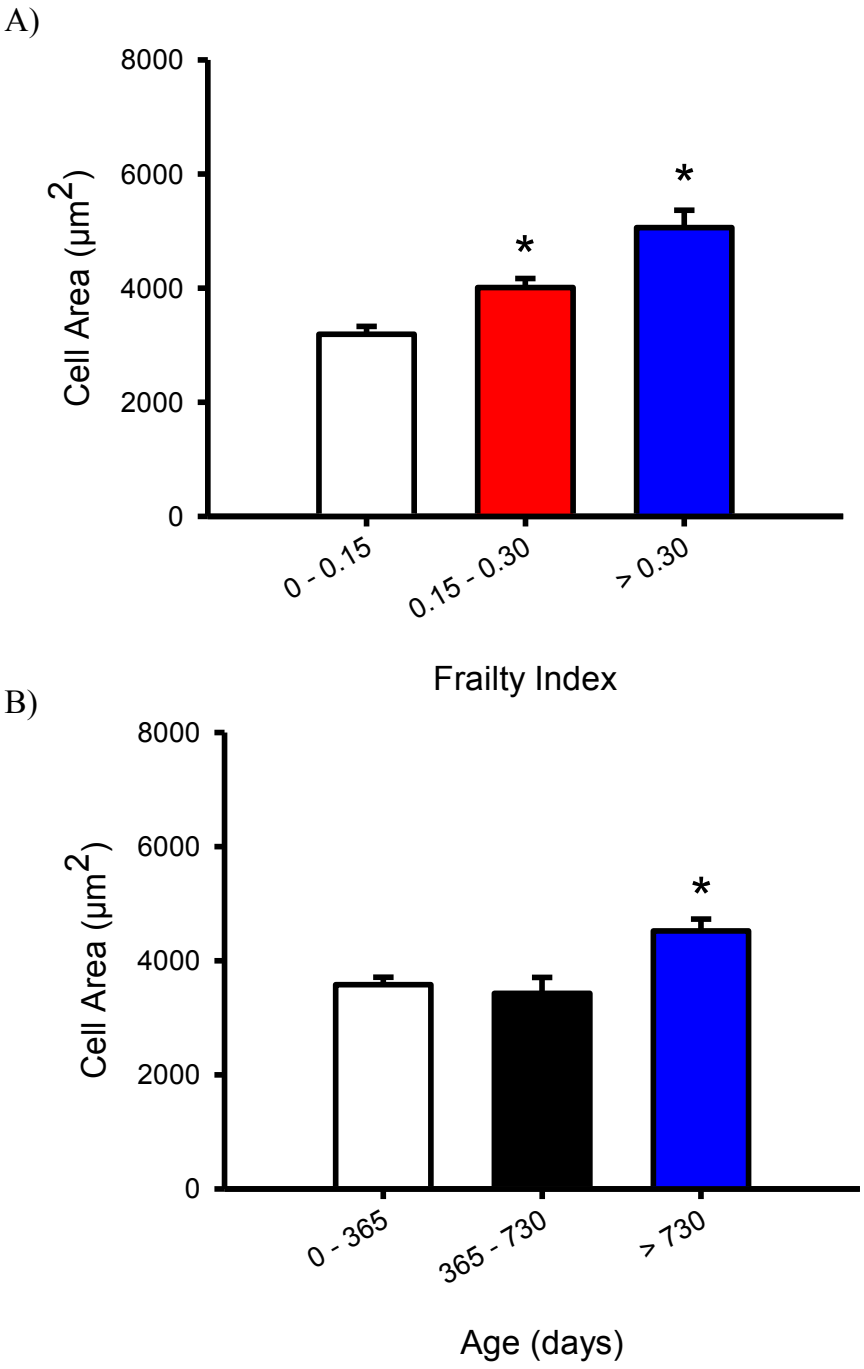

Figure 3.11. Mean cell area increased with frailty and age. A) Mean cell area was significantly increased in both frail groups compared to control group (n = 105, 78, and 47 cells for least frail, moderately frail, and frail groups, respectively; *$p < 0.05$). **B)** Mean cell area was significantly greater in the oldest group compared to cells from the youngest mice (n = 105, 50, and 75 cells for young, middle-aged, and oldest groups, respectively; *$p < 0.05$).

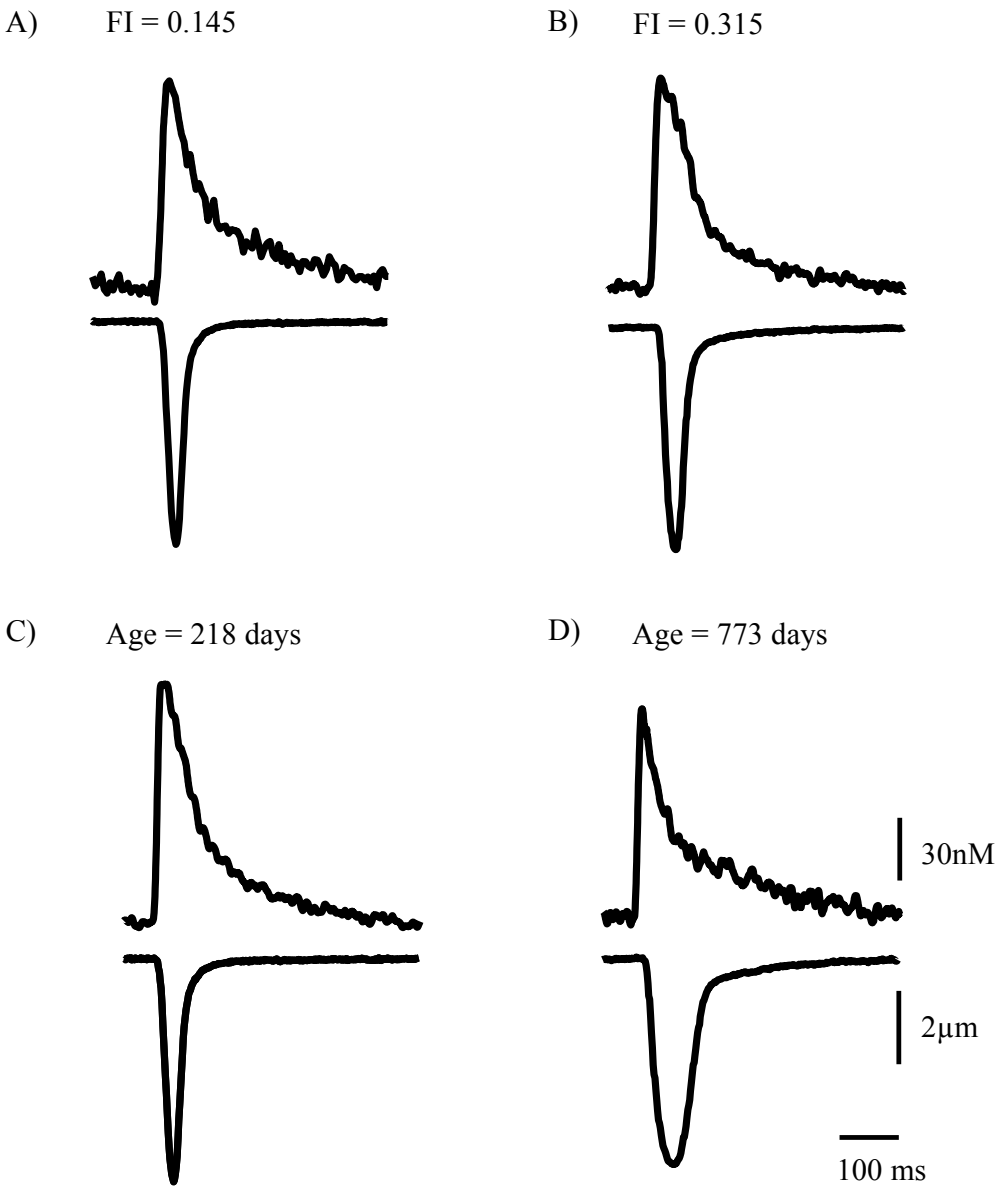

Figure 3.12. Representative examples of Ca^{2+} transients and contractions recorded in myocytes paced a 2Hz. Representative examples of Ca^{2+} transients (bottom) and contractions (top) in myocytes from **A)** mouse with a low FI score, **B)** mouse with a high FI score, **C)** young mouse, **D)** old mouse.

%, and 3.5 ± 0.5 % for control, moderately frail and frail groups, respectively; $p< 0.05$). By contrast, fractional shortening was not correlated or affected by age (Figure 3.13B). There were no correlation or differences in calcium transient amplitude between the three frailty groups (Figure 3.14A). However, Figure 3.14B shows that myocytes from oldest mice had significantly lower calcium transient amplitude when compared to cells from the youngest mice (values were: 223.4 ± 12.5 nM, 231.4 ± 26.2 nM, and 154.2 ± 12.2 nM for youngest, middle aged, and oldest groups, respectively; $r^2 = 0.05$, $p < 0.05$). Interestingly, diastolic calcium levels were not correlated or affected by either frailty or age (Figure 3.14C, D).

3.5 Contractile responses and Ca^{2+} concentrations following acute application of isoproterenol in cardiomyocytes

To determine whether contractile dysfunction occurred in ventricular myocytes from frail mice subjected to Ca^{2+} overload, cells were exposed to 1 μM of isoproterenol, a β-adrenergic agonist. Contractions and Ca^{2+} transients were recorded after 5 minutes of acute drug application. Figure 3.15 shows representative examples of Ca^{2+} transients (top) and contractions (bottom) before and after exposure to 1 μM isoproterenol in ventricular myocytes paced at 2 Hz. Mean data showed that fractional shortening significantly increased following treatment with isoproterenol when compared to untreated myocytes in the moderately frail group (values were 3.7 ± 0.7 % and 7.3 ± 1.1 % for pre- and post-isoproterenol treatment, respectively; $p < 0.05$) (Figure 3.16A). Interestingly, fractional shortening did not significantly increase following isoproterenol treatment in the most frail group (values were 3.2 ± 0.8 % and 5.4 ± 1.5 % for pre- and post-isoproterenol treatment,

A)

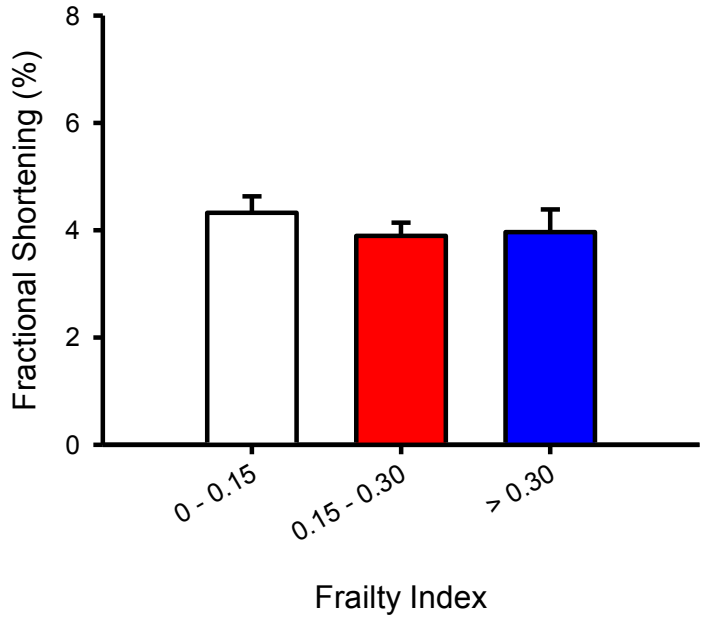

B)

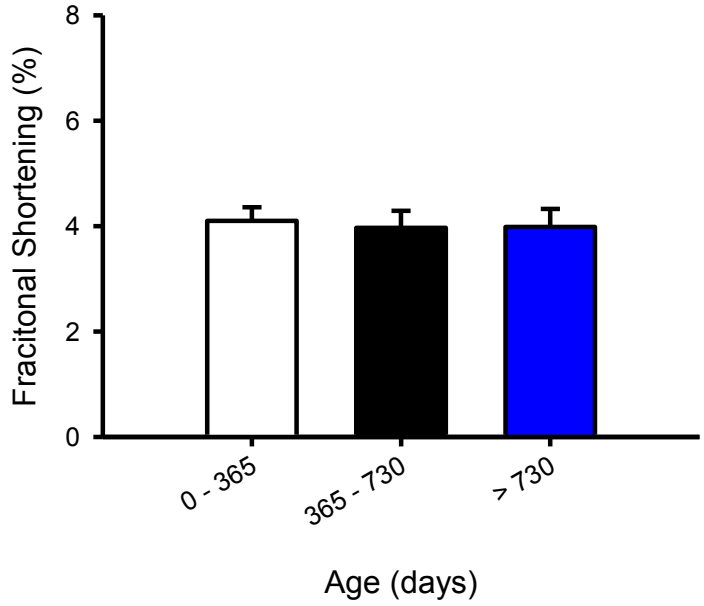

Figure 3.13. Fractional shortening declined in the moderately frail group when compared to the least frail group. A) Fractional shortening was significantly smaller in myocytes from moderately frail mice when compared to the control group (n = 40, 68, and 20 cells for least frail, moderately frail, and frail groups, respectively; *p < 0.05). **B)** Fractional shortening did not differ between the 3 age groups (n = 64, 31, and 33 cells for young, middle-aged, and oldest groups, respectively).

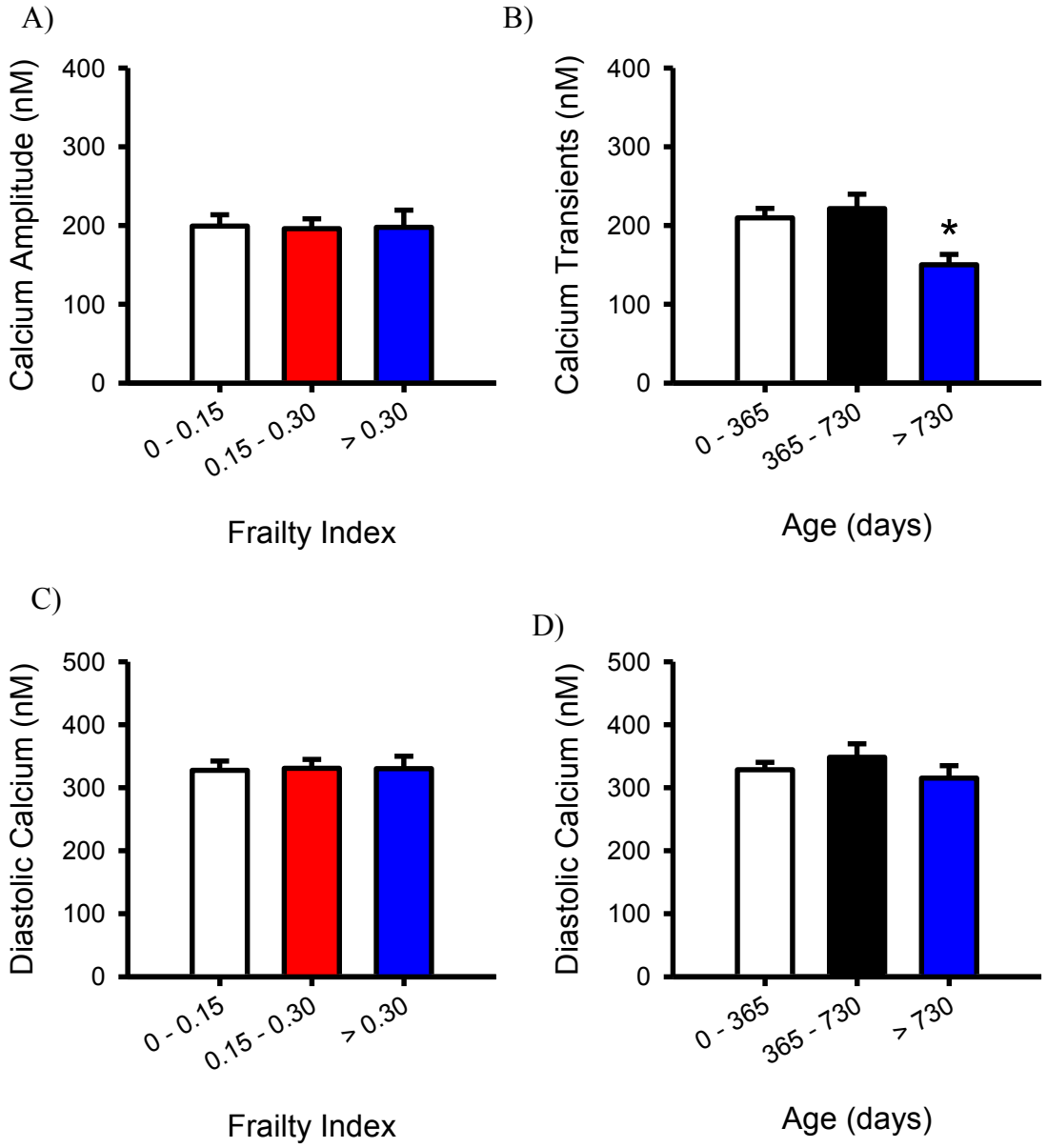

Figure 3.14. Ca^{2+} transients were smaller in the oldest mice when compared to youngest mice. A) Ca^{2+} transients were similar in myocytes from the 3 frail groups (n = 40, 68, and 20 cells for least frail, moderately frail, and frail groups, respectively). **B)** Ca^{2+} transients were significantly smaller in the oldest group when compared to the youngest mice (n = 64, 31, and 33 cells for young, middle-aged, and oldest groups, respectively; *$p < 0.05$). **C, D)** Diastolic Ca^{2+} levels were similar between all frailty groups as well as all age groups (n = 40, 68, and 20 cells for least frail, moderately frail, and frail groups, respectively; n = 64, 31, and 33 cells for young, middle-aged, and oldest groups, respectively).

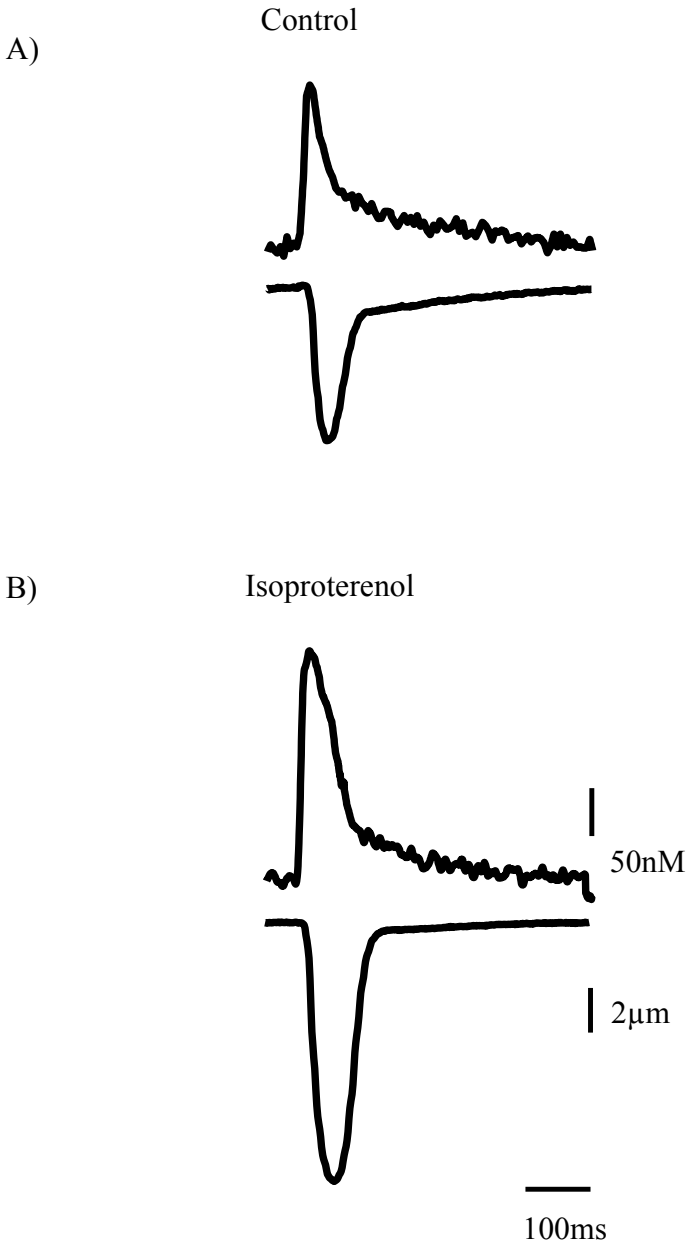

Figure 3.15. Represenstative examples of Ca^{2+} transients and contractions in myocytes stimulated with the ß-adrenergic agonist, isoproterenol. Representative examples of Ca^{2+} transients (top) and contractions (bottom) in myocytes **A)** under normal conditions, and **B)** following acute application of 1 μM isoproterenol.

respectively; $p < 0.05$) (Figure 3.16A). Figure 3.16B shows that Ca^{2+} transient amplitude significantly increased following isoproterenol treatment in both moderately frail and frail groups (values were 144.9 ± 9.1 nM and 227.2 ± 18.8 nM for pre- and post-isoproterenol treatment, respectively in the moderately frail group; values were 158.7 ± 17.0 nM and 262.7 ± 37.2 nM for pre- and post-isoproterenol treatment, respectively in the frail group; $p < 0.05$). However, diastolic Ca^{2+} concentrations did not differ between control and isoproterenol-treated myocytes in either frailty groups (values were 236.6 ± 18.4 nM and 292.4 ± 24.7 nM for pre- and post-isoproterenol treatment, respectively in the moderately frail group; values were 288.3 ± 19.3 nM and 295.6 ± 23.0 nM for pre- and post-isoproterenol treatment, respectively in the frail group; $p < 0.05$) (Figure 3.17A).

Isoproterenol treatment also caused slight increase in spontaneous contractile activity and cell death. Figure 3.17B shows that the incidence of spontaneous contractile activity was slightly higher than control in both frailty groups but did not differ between myocytes from the moderately frail group and the frail group (values were 36.4 % and 30.0 % for the moderately frail group and frail group, respectively). There was also an increase in cell death compared to control, although this was not statistically significant. Cell death was slightly higher in the frail group in comparison to the moderately frail group (values were 9.1 % and 30.0 % for the moderately frail group and frail group, respectively) (Figure 3.17C).

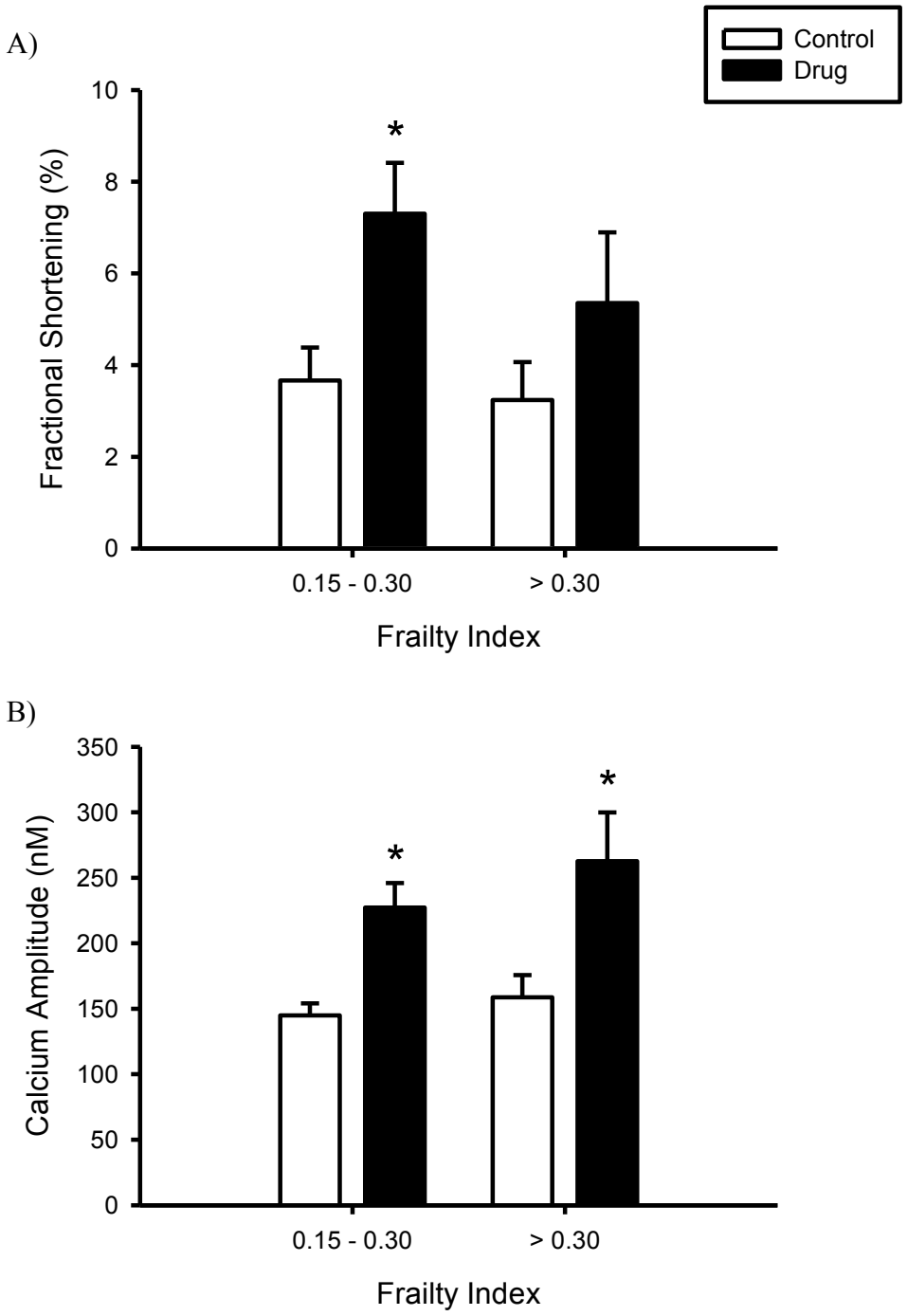

Figure 3.16. Fractional shortening and Ca^{2+} transients increased in the presence of isoproterenol. A) Fractional shortening significantly increased following exposure to isoproterenol in the moderately frail group but not in the frail group (n = 11 and 10 cells for moderately frail and frail groups, respectively; *p < 0.05). **B)** Isoproterenol induced significant increases in Ca^{2+} transients in both moderately frail and frail groups (n = 11 and 10 cells for moderately frail and frail groups, respectively; *p < 0.05).

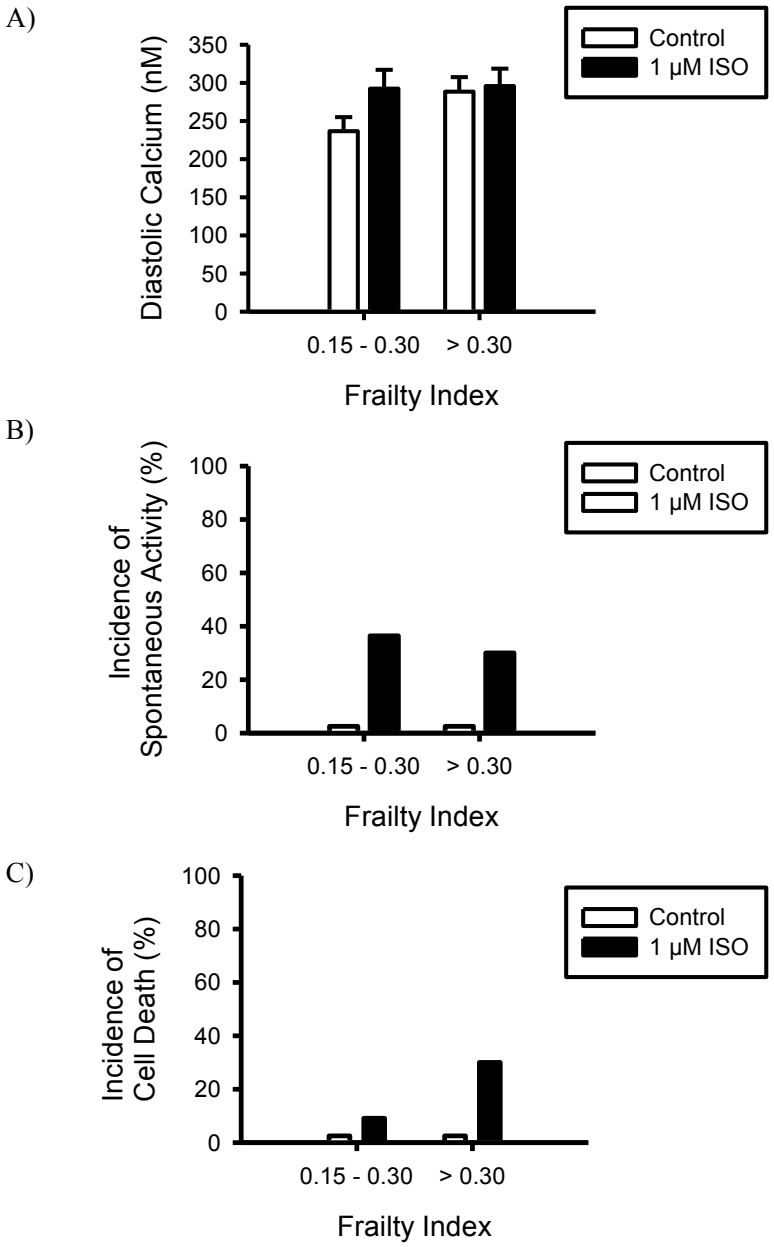

Figure 3.17. Incidence of cell death was slightly higher in myocytes from the frail group than from the moderately frail group. A) Concentrations of diastolic Ca^{2+} were similar in myocytes from all frail groups in the absence and presence of 1 μM ISO (n = 11 and 10 cells for moderately frail and frail groups, respectively; *$p < 0.05$). **B)** Incidence of spontaneous contractile activity was similar between myocytes from the moderately frail group and the frail group following ISO treatment (n = 11 and 10 cells for moderately frail and frail groups, respectively; *$p < 0.05$). **C)** Cells from the frail group had a higher incidence of cell death compared to moderately frail cells in the presence of ISO (n = 11 and 10 cells for moderately frail and frail groups, respectively; *$p < 0.05$).

Chapter 4: Discussion

4.1 Overview of key findings

The first objective of this study was to quantify frailty in a longitudinal study using a large cohort of mice. Using the clinical FI previously established by Whitehead *et al.* (2014), mice were assessed at approximately 6 month intervals. It was shown that frailty significantly increased as age increased. Mean FI scores were lowest at the youngest age and progressively increased through each subsequent assessment. Furthermore, frailty in the cohort increased exponentially with age, similar to previous cross-sectional studies in mice as well as human data (Whitehead *et al.*, 2014; Mitnitski *et al.*, 2005). These findings show that a simple, non-invasive method of frailty assessment can be used to quantify frailty in longitudinal studies of aging animals.

This study also sought to determine whether frailty can predict changes in *in vivo* cardiac structure and function independently of age. Results indicated that, as frailty increased, the LV internal diameter during both systole and diastole increased. By contrast, LV internal diameter did not vary as a function of age. Additionally, fractional shortening and ejection fraction were significantly lower in frail mice compared to control mice, but these parameters did not fluctuate with respect to age. These results suggest that, as frailty develops, the LV becomes hypertrophied and contractile function deteriorates. Furthermore, these changes in cardiac structure and function are better predicted by frailty than chronological age.

The third objective of this study was to determine whether frailty can predict myocyte hypertrophy and contractile dysfunction independently of age. Results showed

that cell length, cell width, and cell area progressively increased as frailty increased. Cell lengths, widths, and area were also greater in oldest mice when compared to the youngest group but cell length was actually lower in the middle-aged group when compared to the youngest group. Taken together, these results suggest that both frailty and age can predict hypertrophy in ventricular myocytes. However, frailty was a better indicator of myocyte hypertrophy than chronological age. This study also provides some evidence that frailty predicts contractile dysfunction in individual myocytes. Changes in contractile function in individual cardiomyocytes were also investigated. When cells were paced at 2 Hz, cells from the moderately frail group showed a decrease in cell shortening when compared to the control group, although these changes were not observed in the most frail group. By contrast, peak contractions were not affected by chronological age. Furthermore, Ca^{2+} transient amplitudes and diastolic Ca^{2+} concentrations were similar between all three frailty groups. However, further experiments using older and more frail mice are required to reinforce these findings.

The final objective of the study was to determine whether cardiomyocytes responded to Ca^{2+} overload induced by β-adrenergic stimulation differently in cells from frail and less frail animals. Treatment with 1 μM isoproterenol showed that Ca^{2+} transient amplitudes were significantly larger in both frailty groups in the presence of isoproterenol. Interestingly, fractional shortening significantly increased in ventricular myocytes from the moderately frail group but not the frail group. Additionally, both frailty groups had a small increase in spontaneous contractile activity following isoproterenol treatment compared to control, although the incidences did not differ between the two groups. Application of isoproterenol also increased cell death in both frailty groups, and induced a slightly higher

incidence of cell death in the frail group compared to the moderately frail group. These findings show that there are no differences in contractile function between myocytes from frail and moderately frail mice in the presence of isoproterenol. However, differences in fractional shortening and slightly higher incidence of spontaneous activity and cell death in frail cells may suggest possible links between frailty and Ca^{2+} handling following β-adrenergic stimulation.

4.2 Quantification of frailty in a longitudinal study using C57BL/6J mice

The concept of frailty has been widely regarded as an increased vulnerability to adverse outcomes for organisms of the same age (Fulop *et al.*, 2010; Rockwood *et al.*, de Vries *et al.*, 2011). However, how to best measure frailty remains controversial (de Vries *et al.*, 2011). Although many different measurement instruments have been proposed, the two most common approaches to assess frailty are the Fried phenotype and deficit accumulation (de Vries *et al.*, 2011). This has translated to the development of methods to assess frailty in animal models based on these two approaches. Parks *et al.* (2012) was the first to quantify frailty in mice based on deficit accumulation. The Frailty Index was developed by assessing deficits from 31 invasive and non-invasive health-associated parameters. The invasive tests required anesthetizing the animal before procedures to assess body composition and euthanizing mice to obtain enough blood to assess metabolic status. Although Park *et al.* (2012) recognized the importance of identifying frailty in animal models, the parameters used to construct the Frailty Index required specialized equipment that may not be readily available in most research laboratories. This, coupled with the invasive nature of the method, limited the implementation of this approach and

could prevent the Frailty Index from being used in longitudinal studies. The clinical FI developed by Whitehead *et al.* (2014) addressed these concerns, focusing on simplified, non-invasive approaches in its assessment, enabling the longitudinal study of frailty presented here to be conducted.

A major objective of the present study was to use the clinical FI previously developed by Whitehead *et al.* (2014) to investigate frailty in a longitudinal study in mice. The results of this study showed that the clinical FI can be used to quantify frailty in a longitudinal study of aging using a large cohort of mice. Assessing mice at approximately 6 month intervals revealed that frailty increased progressively with age. In fact, FI scores were shown to increase exponentially with age. These findings were consistent with the results from the cross-sectional pilot study by Whitehead *et al.* (2014). Moreover, studies of frailty defined by deficit accumulation in humans also revealed that frailty increased exponentially with age (Mitnitski *et al.*, 2005). Indeed, when mouse and human ages were normalized to their respective 90% mortality, the increase in frailty was almost identical between mice and humans (Whitehead *et al.*, 2014). Taken together, these results indicate that the concept of frailty as deficit accumulation, originally developed to quantify frailty in humans (Rockwood *et al.*, 2011; Mitnitski *et al.*, 2001), can also be applied to an aging mouse model. By assessing age-associated deficits specific to the model of interest, a FI may be created by adapting the clinical FI to each species of interest. This may permit researchers to quantify frailty in other mouse strains such as transgenic models and even adopt this approach for use in other animal models. This is the first study to investigate frailty in a longitudinal study using an animal model. Results from this study show that the

clinical FI is ideal for longitudinal studies due to its simplicity and non-invasive nature and may provide the basis for future intervention studies to modify frailty in aging animals.

Liu *et al.* (2013) recently introduced a different approach to quantify frailty in mice by adapting the Fried phenotype that had been developed to assess frailty in humans (Fried *et al.*, 2001). Liu *et al.* (2013) assessed weakness, slow walking speed, low activity levels, and poor endurance. This frailty assessment focused on non-invasive criteria, noting the complexity and specificity of the Frailty Index developed by Parks *et al.* (2012). If a mouse presents with three or more of the frailty criteria, it is then identified as frail (Liu *et al.*, 2013). Although the frailty criteria used in this study are non-invasive and easily reproducible, the authors noted that other frailty criteria require consideration (Liu *et al.*, 2013). For example, measures of cognition, balance, and gait patterns are neglected. The advantage of the clinical FI is that it assesses deficits across several biological systems. Cognitive impairment is evaluated through grooming of the fur coat and abnormalities in balance are determined by vestibular disturbance (Table 1.1; Whitehead *et al.*, 2014). Gait was also observed to indicate lack of coordination (Table 1.1; Whitehead *et al.*, 2014). Therefore, although the methods proposed by Liu *et al.* (2013) and Whitehead *et al.* (2014) to quantify frailty are non-invasive and reproducible, the clinical FI covers a much wider range of parameters across various biological systems.

Previous studies have provided evidence that inflammation is a major component of frailty in humans (Collerton *et al.*, 2012; Li *et al.*, 2011; Visser *et al.*, 2002). Indeed, the IL-10 knockout mouse was proposed by Walston *et al.* (2008) as a model for human frailty. These IL-10 knockout mice were found to exhibit increased inflammation and to develop an age-related decrease in skeletal muscle strength (Walston *et al.*, 2008). This study

provided interesting insights to the biological basis of frailty. However, mice used in this study were genetically engineered and they were actually first developed as a model of Crohn's disease (Herfarth & Scholmerich, 2002; Yuan *et al.*, 2013). This results in changes different than those observed in natural aging. Even so, it would be interesting to apply the current clinical FI to evaluate frailty in these genetically altered mice to determine the link between inflammation, health deficits across various biological systems and frailty. In this current longitudinal study, it is evident that the incidence of dermatitis, which has been linked to inflammation (Dhingra & Guttman-Yassky, 2014), increased markedly with age. To what degree inflammation contributes to frailty still needs to be investigated.

4.3 Sex differences in frailty in the mouse model

This study primarily focused on quantification of frailty in a longitudinal study using male C57BL/6J mice. However, we did evaluate some female mice and our study provided preliminary data to investigate sex differences in frailty in the mouse model. Studies in humans have typically reported that women have a higher frailty index than men (Mitnitski *et al.*, 2002; Yang *et al.*, 2010; Puts *et al.*, 2005). On the other hand, Kulminski *et al.* (2007) showed that sex differences were not present in individuals under 75 years of age and over 95 years of age. In the mouse model, Whitehead *et al.* (2014) found no sex differences in mice evaluated with the clinical assessment tool used in the present study. These findings are consistent with results of Parks *et al.* (2012), who showed that levels of frailty were similar in aged males and females. These previous studies suggest that male-female differences in frailty characteristic of humans may not be present in the mouse model.

This present study used two small cohorts of female mice to assess difference in frailty between age-matched male and female mice. Frailty was compared in young (approximately 6 months old) and old (approximately 27 months old) male and female mice. Males and females had similar frailty scores in both age groups, agreeing with findings by Parks *et al.* (2012) and Whitehead *et al.* (2014). Differences in the results of animal and human studies may be due to the ages of the animals used and/or the limited sample sizes used. Human data suggest that sex differences in frailty are most prominent between the ages of 75 and 95 (Kulminski *et al.*, 2007). Therefore, mice outside of that age range with respect to their lifespan may show little evidence of a male-female distinction. Furthermore, it is important to note that these findings are preliminary, and a larger study of sex differences in frailty in the mouse model is now warranted.

4.4 Changes in *in vivo* cardiac morphology and function in relation to frailty and age

This is the first study to assess changes in *in vivo* cardiac morphology and function in relation to frailty in an animal model. Thus, little is known about the link between frailty and cardiovascular function in mice. The results of this study showed that LV internal diameter was significantly larger during both systole and diastole in frail hearts compared to hearts from less frail mice. Interestingly, there was no relationship between LV internal diameter and age. Previous studies have shown that changes in LV internal diameter have been linked to geometrical and structural remodeling of the LV in humans (Wu *et al.*, 2012). LV remodeling is associated with LV dysfunction and decrease of coronary flow reserve (Zhang & McDonald, 1995). This may predispose towards the development of heart failure and contribute to the worsening of symptoms in those with existing heart failure (Frigerio

& Roubina, 2005; Gradman & Alfayoumi, 2006; Meijis *et al.*, 2007). Taken together, these data show that frailty is a good predictor of LV remodelling in mice independently of age. These observations suggest that frailty may be incorporated into assessments when evaluating the risk of developing heart failure in older adults.

Evaluating contractile function of the heart *in vivo* revealed that both fractional shortening and ejection fraction declined as frailty scores increased. Interestingly however, chronological age did not predict these changes in cardiac function. Fractional shortening is the percentage change in ventricular diameter from diastole to systole, and ejection fraction is the fraction of blood pumped from the heart with each beat. A decrease in fractional shortening coupled an with increase in LV internal diameter suggests that hearts from frail mice are enlarged, but unable to contract in the same manner as hearts from less frail mice. The decline in contractile function is evident as a decrease in ejection fraction, where hearts from frail animals pump less blood out of the LV. In theory, these changes in contractile function could have major clinical implications. A decrease in ejection fraction can result in systolic heart failure, where the heart does not contract effectively and in turn, less oxygenated blood is pumped out to the body (Chatterjee & Massie, 2007). Therefore, frail animals are at increased risk of systolic heart failure, regardless of their chronological age. In summary, changes in the morphology and function of the hearts were associated with higher frailty scores in the mouse model. By contrast, these changes were not evident with respect to age. Although age-associated changes in cardiac structure and function have been investigated previously, these results suggests that frailty may be a better predictor of cardiovascular changes in the aging mouse model than chronological age.

4.5 Changes in ventricular myocyte structure and contractile function in relation to frailty and age

It is well established in various mammals, including humans, that advanced age is associated with cardiomyocyte hypertrophy (Olivetti *et al.*, 1995; Grandy & Howlett, 2006; Howlett, 2010). Indeed, the results of this study showed that ventricular myocyte length, width, and area all significantly increased in cells from oldest animals when compared to cells from younger mice. Interestingly, cells from the middle-aged mice were significantly shorter when compared to those from young animals. This may be due to differences in sample size between the three age groups, as the youngest and oldest age groups had a larger sample size compared to the middle-aged group. Therefore, additional experiments in animals in the middle-aged group are required to determine whether this difference remains.

Changes in ventricular myocyte dimensions are also evident in frail mice when compared to less frail mice. Results clearly show that cell length, width, and area were graded by the animal's frailty index score. Ventricular myocyte hypertrophy is a major contributor to LV remodeling (van Empel & De Windt, 2004). Several studies have shown that cellular apoptosis increases with age in rodent models (Tevzadze *et al*., 2005; Karkala *et al.*, 2010). This is initially compensated for by reactive hypertrophy in response to cell loss, whereby the surviving cardiomyocytes increase in size to preserve cardiac function (van Empel & De Windt, 2004). As apoptosis continues in aging hearts, myocyte hypertrophy can no longer keep pace and heart failure develops (Nadal-Ginard *et al.*, 2003). Results from this study shows that both age and frailty are predictors of cellular hypertrophy in the mouse model. However, cellular hypertrophy is actually graded by

increasing frailty scores. Mice from both frail groups had larger cell sizes compared to the control group, whereas only cells from the oldest mice were significantly larger than cells from the youngest group. This suggests that frailty is a better predictor of changes in cellular dimensions than age. Nonetheless, both age and frailty can be regarded as important factors in assessing cardiomyocyte morphology and the vulnerability to adverse events such as heart failure.

Previous studies have also shown that advanced age is linked to contractile dysfunction in ventricular myocytes (Grandy & Howlett, 2006; Howlett, 2010). Lim *et al.* (2000) showed that cell shortening is reduced in aged mouse ventricular myocytes compared to young adult cells. Furthermore, peak Ca^{2+} transient amplitudes are also smaller in aged myocytes (Lim *et al.*, 2000). This study investigated the contractile function of individual ventricular myocytes paced at 2 Hz. Results showed that cell shortening did not differ with respect to age. However, peak Ca^{2+} transient amplitudes were significantly smaller in cells from the oldest group compared to young myocytes. This finding is consistent with previous studies in cells from aged mice (Lim *et al.*, 2000). Interestingly, frailty was not a good predictor in changes in cardiac contractile function. Only the myocytes from the moderately frail group showed a decline in cell shortening. This effect was not seen when comparing the most frail mice to the control group. Furthermore, concentrations of diastolic Ca^{2+} and peak Ca^{2+} transient amplitudes were similar across all three frailty groups. These results suggest that frailty and age were not strong predictor of changes in cardiomyocyte contractile function in this study.

The findings in this study are novel, as the impact of frailty on cardiomyocyte function has not been previously investigated in longitudinal studies. The first study to

investigate the link between frailty and cardiomyocyte function used a small sample size in a cross-sectional study (Parks *et al.*, 2012). Parks *et al.* (2012) found that cell shortening was reduced in myocytes from frail mice when compared to non-frail cells. Interestingly, Parks *et al.* (2012) also did not observe any changes in peak Ca^{2+} transient amplitudes. The discrepancies between the results of the present study and the previous study may be due to the differences in FI scores in the mice used. Mice used for this study had frailty ranging from 0 to 0.38 while mice used by Parks *et al.* (2012) were markedly more frail, with frailty scores between 0.31 and 0.52. Therefore, it is possible that mice used in this study are simply not frail enough to observe clear differences in cardiomyocyte contractile function. It is possible that, as mice in this cohort become older and more frail, changes in cardiomyocyte function will become more evident.

4.6 Contractile responses and Ca^{2+} concentrations following acute application of β-adrenergic stimulation in cardiomyocytes from frail and less frail animals

Various studies have previously investigated the effects of β-adrenergic receptor stimulation in aged cardiomyocytes (Xiao *et al.*, 1994; Farrell & Howlett, 2007; Farrell & Howlett, 2008). Ventricular myocytes from aged animals showed a decrease in their ability to augment contractions and Ca^{2+} transients in comparison to younger animals following stimulation by catecholamines (Xiao *et al.*, 1994; Farrell & Howlett, 2007; Farrell & Howlett, 2008). This is the first study to examine the effect of β-adrenergic stimulation in relation to frailty. Results of this study showed that, upon exposure to the β-adrenergic agonist isoproterenol, fractional shortening significantly increased in myocytes from the moderately frail group. Interestingly, fractional shortening was not significantly increased

by isoproterenol treatment in myocytes from the frail group. Both groups showed an increase in Ca^{2+} transient amplitude in response to isoproterenol. These results suggest that there are no changes in Ca^{2+} loading following β-adrenergic stimulation in relation to frailty. However, the differences in fractional shortening may warrant further investigations.

Farrell & Howlett (2008) reported an age-associated decrease in adenylyl cyclase activity in ventricular myocytes from rats. Adenylyl cyclase stimulates the conversion of ATP to cAMP, which in turn activates PKA (Bers, 2002). Activation of PKA phosphorylates various targets in the EC-coupling pathway, including troponin I on the myofilaments (Bers, 2002; Li *et al.*, 2000). Phosphorylation of troponin I decreases Ca^{2+} sensitivity of the myofilaments (Layland *et al.*, 2005). Therefore, an age-related decrease in adenylyl cyclase may result in a smaller increase in peak contractions in response to β-adrenergic stimulation. This age-associated decline may also be linked to frailty, where animals with high frailty may have a reduction in adenylyl cyclase activity. However, further investigations are required to determine whether frailty is linked to the adenylyl cyclase pathway.

Acute application of isoproterenol also showed that, while systolic Ca^{2+} levels rose, diastolic Ca^{2+} concentrations were not affected by drug treatment in either frailty groups. Nonetheless, isoproterenol did induce signs of Ca^{2+} overload such as increased spontaneous activity and cell death. Interestingly, the incidence of spontaneous activity in ventricular myocytes was similar in moderately frail and frail mice. These results suggest that myocytes from frail animals are not more sensitive to Ca^{2+} overload induced by isoproterenol treatment. However, the incidence of cell death was slightly higher in

ventricular myocytes from the frail group when compared to the moderately frail group, and may warrant further investigation. It is important to note that the sample size in this portion of the study is relatively small, and additional experiments involving application of isoproterenol to ventricular myocytes could provide more insight to the link between frailty and Ca^{2+} sensitivity. Moreover, although mice used in these experiments were divided into the moderately frail and frail group, the mean FI scores for each group were not markedly different. The mean FI score for the moderately frail group was 0.275 while the frail group had a mean FI score of 0.333. Future experiments using mice with a wider range of frailty scores may yield more prominent differences in Ca^{2+} sensitivity with respect to frailty. The inclusion of mice with very low frailty scores also could be informative.

4.7 Limitations

The present study quantified frailty in a longitudinal study using the mouse model. Frailty was quantified using the clinical FI previously developed by Whitehead *et al.* (2014). This is the first longitudinal study to assess frailty in an animal model. Longitudinal studies require lengthy time periods spanning the individual's entire lifespan. However, data collected in this present study only account for the first 15 months of the mice's life cycle. Previous cross-sectional animal studies as well as human studies have shown that frailty increases exponentially age (Parks *et al.*, 2012; Whitehead *et al.*, 2014; Mitnitski *et al.*, 2005). This is also evident in the present study. Therefore, it is expected that mice in this cohort will experience significant increases in their FI scores as they reach senescence. The differences in their biological health will have greater variability as the mice age. It may be during senescence that changes cardiac morphology and function

become even more evident between frail and less-frail mice and risks of adverse outcomes to stressors may be more profound.

This study also investigated whether frailty can predict changes in cardiac morphology and function, both *in vivo* and at the cellular level, better than chronological age. While M-mode echocardiography provides important insights to the changes in morphology and contractile function in relation to frailty, there are other age-associated changes that can be assessed *in vivo*. A possible addition to this current study would be to assess LV diastolic function in relation to frailty. Numerous studies have shown adverse changes in LV function with increasing age in both human and animal models (Svealv *et al.*, 2006; Dai & Rabinovitch, 2009; Hacker *et al.*, 2006). Investigating whether frailty predicts LV diastolic dysfunction would contribute to a wider understanding of frailty and cardiac function. Additionally, performing echocardiography on the mouse model requires substantial precision due to the small size of the mouse heart. A minute movement in the position of the transducer on the mouse heart can affect structural and functional measurements. Therefore, it would also be ideal to standardize echocardiography measurements to either body weight or tibia length to allow for more accurate comparisons in *in vivo* morphology and function between mice. Furthermore, studies in individual cardiomyocytes are integral to understanding fundamental changes in relation to frailty at the cellular level. Previous studies on frailty and cardiomyocytes showed that fractional shortening decreased as frailty increased (Parks *et al.*, 2012). Those changes were not as apparent in this study. However, the oldest mice used in the Parks *et al.* (2012) study were much more frail than those used in this current study. Mice used for this study had frailty ranging from 0 to 0.38 while mice used by Parks *et al.* (2012) had frailty scores between

0.31 and 0.52. Therefore, as the cohort used in our study becomes older and more frail, changes in cardiomyocyte function may become more evident.

Finally, the majority of data used in this study was collected from male mice. The cohort used for the longitudinal assessment of frailty was all males. Some females were used in *in vivo* and myocyte field stimulation experiments. However, female mice were not included in the longitudinal portion of the study. Whether there are sex-differences in frailty has only been investigated in cross-sectional studies in mice (Parks *et al.*, 2012; Whitehead *et al.*, 2014). Both the current study and previous work (Parks *et al.* 2012; Whitehead *et al.*, 2014) found no sex-differences in mice. Interestingly, human studies have shown that females are more frail compared to males (Puts *et al.*, 2005). Thus, further longitudinal studies using both male and female mice may be required to determine whether there are sex-differences in frailty and whether frailty develops at the same rate in both sexes.

4.8 Summary

The present study demonstrates that frailty increases with age in the mouse model. Changes in cardiac morphology and contractile function in relation to frailty and age are summarized in Table 4.1. As frailty increases, LV internal diameter increased while fractional shortening and ejection fraction declined. At the cellular level, frailty was associated with cardiomyocyte hypertrophy, where cells from frail animals were larger than those from less frail animals. There was also evidence that cell shortening decreased with frailty, but no changes in Ca^{2+} transient amplitudes and diastolic Ca^{2+} levels were evident.

Table 4.1. Summary of changes in cardiac morphology and function in relation to frailty and age.

	Frailty	Age
In Vivo		
IVS	↔	↔
LVPW	↔	↔
LVID	↑	↔
Heart Rate	↔	↔
Fractional Shortening	↓	↔
Ejection Fraction	↓	↔
Ventricular Myocytes		
Cell Length	↑	↑ & ↓
Cell Width	↑	↑
Cell Area	↑	↑
Fractional Shortening	↓	↔
Ca^{2+} Transients	↔	↓
Diastolic Ca^{2+}	↔	↔

This is the first study to quantify frailty in a longitudinal study in an animal model using a large cohort. The results of this study demonstrate that a simple, non-invasive clinical FI can be used to quantify frailty in aging mice. Furthermore, this study showed that frailty is a better predictor of changes in cardiac morphology and function than chronological age in mice. These findings may have important clinical implications, where frailty may be a better indicator of the cardiovascular status of older adults and used to more accurately assess risks of cardiovascular treatments and procedures.

4.9 Future Work

This is the first longitudinal study of frailty in the animal model. Results from this study provided evidence that frailty can predict age-associated changes in cardiac structure and function. In fact, results suggest that frailty is a better predictor of these changes than chronological age. However, this study focused on the early portion of the mouse's lifespan, and future frailty assessments as well as *in vivo* and cellular experiments are required to support these findings. This study followed the frailty scores of the cohort up approximately 15 months of age. It is critical that frailty assessments are continued as the mice reach the latter portion of their lives. Frailty was initially developed to account for the heterogeneity in health status in the older population. Thus, the strength of the frailty index will be more evident in predicting cardiovascular changes and adverse outcomes as the mice reach senescence.

Additionally, this study assessed the relationship between frailty, age, and cardiovascular changes. In this study, frailty and age were regarded as independent

variables. However, this study as well as previous studies in both human and animal models showed that frailty is correlated with age (Parks *et al.*, 2012; Whitehead *et al.*, 2014). The present study and Whitehead *et al.* (2014) showed that frailty increases exponentially with age. Therefore, future studies incorporating both frailty and age in evaluating changes in cardiac morphology and contractile function would prove invaluable. For example, using multiple regression analysis would provide insight to the relationships between cardiovascular changes and age or frailty independently and also evaluate the interactions between frailty and age.

Finally, this study predominantly used male mice. Studies of frailty in human have suggested that females are more frail than males, however, these findings remain controversial (Mitnitski *et al.*, 2002; Yang *et al.*, 2010; Kulminski *et al.*, 2007). Cross-sectional studies in animal models suggest there are no sex-differences in frailty (Parks *et al.*, 2012; Whitehead *et al.*, 2014). Future longitudinal studies using both male and female animals may help assess if there are sex differences in frailty and whether frailty develops at the same rate.

References

[1]Abramowitch, S.D., Feola, A., Jallah, Z., Moalli, P.A. (2009). Tissue mechanics, animal models, and pelvic organ prolapse: a review. *European Journal of Obstetrics, Gynecology, and Reproductive Biology*, *144 Suppl 1*, S146–58.

[2]Afilalo, J. (2011). Frailty in Patients with Cardiovascular Disease: Why, When, and How to Measure. *Current Cardiovascular Risk Reports*, *5*(5), 467–472.

[3]Afilalo, J., Alexander, K.P., Mack, M.J., Maurer, M.S., Green, P., Allen, L.A., Popma, J.J., Ferrucci, L., Forman, D. E. (2014). Frailty assessment in the cardiovascular care of older adults. *Journal of the American College of Cardiology*, *63*(8), 747–62.

[4]Apell, H.-J., & Karlish, S. J. (2001). Functional Properties of Na,K-ATPase, and Their Structural Implications, as Detected with Biophysical Techniques. *Journal of Membrane Biology*, *180*(1), 1–9.

[5]Baumgartner, R.N., Waters, D.L., Gallagher, D., Morley J.E., Garry, P.J. (1999). Predictors of skeletal muscle mass in elderly men and women. *Mech Ageing Dev, 107*(2), 123-36.

[6]Bergman, H., Ferrucci, L., Guralnik, J., Hogan, D.B., Hummel, S., Karunananthan, S., Wolfson, C. (2007). Frailty: an emerging research and clinical paradigm--issues and controversies. *The Journals of Gerontology. Series A, Biological Sciences and Medical Sciences*, *62*(7), 731–737.

[7]Berne, R.M., Levy, M.N. (1997). Cardiovascular Physiology. Mosby-Year Book, Inc. St. Louis, USA.

[8]Bers, D.M. (2001). Excitation-Contraction Coupling and Cardiac Contractile Force. Kluwer Academic Press, Dordrecht, Netherlands.

[9]Bers, D.M. (2002). Cardiac excitation-contraction coupling. *Nature*, *415*, 198-205.

[10]Bers, D.M. (2008). Calcium cycling and signaling in cardiac myocytes. *Annual Review of Physiology*, *70*, 23–49.

[11]Biernacka, A., Frangogiannis, N.G. (2011). Aging and cardiac fibrosis. *Aging Dis, 2*(2), 158-173.

[12]Birkeland, J.A., Sejersted, O.M., Taraldsen, T., & Sjaastad, I. (2005). EC-coupling in normal and failing hearts. *Scandinavian Cardiovascular Journal*, *39*(1-2), 13–23.

[13]Blackwell, B.N., Bucci, T.J., Hart, R.W., Turturro, A. (1995). Longevity, Body Weight, and Neoplasia in Ad Libitum-Fed and Diet-Restricted C57BL6 Mice Fed NIH-31 Open Formula Diet. *Toxicologic Pathology*, *23*(5), 570–582.

[14]Boockvar, K.S., Meier, D.E. (2014). Palliative Care for Frail Older Adults "There Are Things I Can't Do Anymore That I Wish I Could . . .", *296*(18), 2245–2254.

[15]Brayton, C. (2007). Spontaneous diseases in commonly used inbred mouse strains. *The mouse in biomedical research.* 2nd ed. Elsevier, Academic Press, Amsterdam, 623-718.

[16]Brayton, C., Justice, M., Montgomery, C.A. (2001). Evaluating Mutant Mice: Anatomic Pathology. *Veterinary Pathology*, *38*(1), 1–19.

[17]Cacciatore, F., Abete, P., Mazzella, F., Viati, L., Della Morte, D., D'Ambrosio, D., Gargiulo, G., Testa, G., De Santis, D., Galiza G., Ferrara, N., Rengo, F. (2005). Frailty predicts long-term mortality in elderly subjects with chronic heart failure. *European Journal of Clinical Investigation*, *35*(12), 723–30.

[18]Cesari, M., Penninx, B.W.J.H., Newman, A.B., Kritchevsky, S.B., Nicklas, B.J., Sutton-Tyrrell, K., Rubin, S.M., Ding, J., Simonsick E.M., Harris, T.B., Pahor, M. (2003). Inflammatory markers and onset of cardiovascular events: results from the Health ABC study. *Circulation*, *108*(19), 2317–22.

[19]Chatterjee, K., Massie, B. (2007). Systolic and diastolic heart failures: differences and similarities. *J Cardiac Failure, 13*(7), 569-576.

[20]Clegg, A., Trust, D.M. (2011). CME Geriatric medicine The frailty syndrome. *Clinical Medicine*, *11*(1), 72–75.

[21]Clegg, A., Young, J., Iliffe, S., Rikkert, M.O., Rockwood, K. (2013). Frailty in elderly people. *Lancet*, *381*(9868), 752–62.

[22]Collerton, J., Martin-Ruiz, C., Davies, K., Hilkens, C.M., Isaacs, J., Kolenda, C., Parker, C., Dunn, M., Catt, M., Jagger, C., von Zglinicki, T., Kirkwood, T. B. L. (2012). Frailty and the role of inflammation, immunosenescence and cellular ageing in the very old: cross-sectional findings from the Newcastle 85+ Study. *Mechanisms of Ageing and Development*, *133*(6), 456–66.

[23]Dai, D.-F., Chen, T., Johnson, S.C., Szeto, H., Rabinovitch, P.S. (2012). Cardiac aging: from molecular mechanisms to significance in human health and disease. *Antioxidants & Redox Signaling*, *16*(12), 1492–526.

[24]Dai, D.-F., Rabinovitch, P.S. (2009). Cardiac Aging in Mice and Humans: the Role of Mitochondrial Oxidative Stress. *Trends Cardiovasc Med*, *19*(7), 213–220.

[25]De Vries, N.M., Staal, J.B., van Ravensberg, C.D., Hobbelen, J.S.M., Olde Rikkert, M.G.M., Nijhuis-van der Sanden, M.W.G. (2011). Outcome instruments to measure frailty: a systematic review. *Ageing Research Reviews*, *10*(1), 104–14.

[26]Defensor, E.B., Corley, M.J., Blanchard, R.J., Blanchard, D.C. (2012). Facial expressions of mice in aggressive and fearful contexts. *Physiology & Behavior*, *107*(5), 680–5.

[27]Dhingra, N., & Guttman-Yassky, E. (2014). A possible role for IL-17A in establishing Th2 inflammation in murine models of atopic dermatitis. *The Journal of Investigative Dermatology*, *134*(8), 2071–4.

[28]Drazner, M.H. (2011). The progression of hypertensive heart disease. *Circulation*, *123*(3), 327–34.

[29]Fabiato, A. (1985). Time and calcium dependence of activation and inactivation of calcium-induced release of calcium from the sarcoplasmic reticulum of a skinned canine cardiac Purkinje cell. *The Journal of General Physiology*, *85*(2), 247–89.

[30]Fahlström, A., Yu, Q., Ulfhake, B. (2011). Behavioral changes in aging female C57BL/6 mice. *Neurobiology of Aging*, *32*(10), 1868–80.

[31]Fares, E., Howlett, S.E. (2010). Effect of age on cardiac excitation-contraction coupling. *Clinical and Experimental Pharmacology & Physiology*, *37*(1), 1–7.

[32]Farrell, S.R., Howlett, S.E. (2007). The effects of isoproterenol on abnormal electrical and contractile activity and diastolic calcium are attenuated in myocytes from aged Fischer 344 rats. *Mechanisms of Ageing and Development*, *128*(10), 566–73.

[33]Farrell, S.R., Howlett, S.E. (2008). The age-related decrease in catecholamine sensitivity is mediated by beta(1)-adrenergic receptors linked to a decrease in adenylate cyclase activity in ventricular myocytes from male Fischer 344 rats. *Mechanisms of Ageing and Development*, *129*(12), 735–44.

[34]Ferrucci, L., Penninx, B.W.J.H., Volpato, S., Harris, T.B., Bandeen-Roche, K., Balfour, J., Leveille, S.G., Fried, L.P., Guralnic, J.M. (2002). Change in muscle strength explains accelerated decline of physical function in older women with high interleukin-6 serum levels. *Journal of the American Geriatrics Society*, *50*(12), 1947–54.

[35]Foltz, C.J., Ullman-Cullere, M.H. (1999). Guidelines for assessing the health and condition of mice. *Lab Anim, 28,* 28-32.

[36]Fried, L.P., Tangen, C.M., Walston, J., Newman, A.B., Hirsch, C., Gottdiener, J., Seeman, T., Tracy, R., Kop, W.J., Burke, G., McBurnie, M.A. (2001). Frailty in older adults: evidence for a phenotype. *The Journals of Gerontology. Series A, Biological Sciences and Medical Sciences*, *56*(3), M146–56.

[37]Frigerio, M., Roubina, E. (2005). Drugs for left ventricular remodeling in heart failure. *Am J Cardiol, 96,* 10-18.

[38]Frommeyer, G., Eckardt, L., Milberg, P. (2012). Calcium handling and ventricular tachyarrhythmias. *Wiener Medizinische Wochenschrift (1946)*, *162*(13-14), 283–6.

[39]Fulop, T., Larbi, A., Witkowski, J.M., McElhaney, J., Loeb, M., Mitnitski, A., Pawelec, G. (2010). Aging, frailty and age-related diseases. *Biogerontology*, *11*(5), 547–63.

[40]Gelatt, K.N. (1997). Visual disturbance: where do I look? *J Small Anim Pract, 38,* 328-335.

[41]Gradman, A.H., Alfayoumi, F. (2006). From left ventricular hypertrophy to congestive heart failure: management of hypertensive heart disease. *Progress in Cardiovascular Diseases. 48*(5), 326-341.

[42]Grandy, S.A., Howlett, S.E. (2006). Cardiac excitation-contraction coupling is altered in myocytes from aged male mice but not in cells from aged female mice. *Am J Physiol Heart Circ Physiol*, 2362–2370.

[43]Grundy, E.M.D. (2003) The epidemiology of aging. In: Tallis R., Fillit H. (eds). *Brocklehurst's Textbook of Geriatric Medicine and Gerontology,* 6th edn. Churchill Livingstone, London.

[44]Hacker, T.A., Mckiernan, S.H., Douglas, P.S., Wanagat, J., Aiken, J.M., Timothy, A. (2006). Age-related changes in cardiac structure and function in Fischer 344 x Brown Norway hybrid rats. *Am J Physiol Heart Circ Physiol*, *290*, 304–311.

[45]Herfarth, H. (2002). IL-10 therapy in Crohn's disease: at the crossroads. *Gut*, *50*(2), 146–147.

[45]Heuberger, R.A. (2011). The frailty syndrome: a comprehensive review. *Journal of Nutrition in Gerontology and Geriatrics*, *30*(4), 315–68.

[47]Hogan, D.B., MacKnight, C., Bergman, H. (2003). Models, definitions, and criteria of frailty. *Aging Clin Exp Res, 15*(3), 1-29.

[48]Hove-Madsen, L., Bers, D.M. (1993). Sarcoplasmic reticulum Ca2+ uptake and thapsigargin sensitivity in permeabilized rabbit and rat ventricular myocytes. *Circulation Research*, *73*(5), 820–828.

[49]Howlett, S.E. (2010). Age-associated changes in excitation-contraction coupling are more prominent in ventricular myocytes from male rats than in myocytes from female rats. *Am J Physiol Heart Circ Physiol*, 659–670.

[50]Howlett, S.E., Nicholl, P.A. (1992). Density of 1,4-dihydropyridine receptors decreases in the hearts of aging hamsters. *J Med Cell Cardiol, 24,* 885-894.

[51]Howlett, S.E., Rockwood, K. (2013). New horizons in frailty: ageing and the deficit-scaling problem. *Age and Ageing*, *42*(4), 416–23.

[52]Kakarla, S.K., Rice, K.M., Katta, A., Paturi, S., Wu, M., Kolli, M., Keshavarzian, S., Manzoor, K., Wehner, P.S., Blough, E.R. (2010). Possible molecular mechanisms underlying age-related cardiomyocyte apoptosis in the F344XBN rat heart. *The Journals of Gerontology. Series A, Biological Sciences and Medical Sciences*, *65*(2), 147–55.

[53]Katz, A.M., Reuter, H. (1979). Cellular calcium and cardiac cell death. *Am J Cardiol, 44,* 188-190.

[54]Kentish, J.C., McCloskey, D.T., Layland, J., Palmer, S., Leiden, J.M., Martin, A.F., Solaro, R.J. (2001). Phosphorylation of Troponin I by Protein Kinase A Accelerates Relaxation and Crossbridge Cycle Kinetics in Mouse Ventricular Muscle. *Circulation Research*, *88*(10), 1059–1065.

[55]Knollmann, B.C., Katchman, A.N., Franz, M.R. (2001). Monophasic action potential recordings from intact mouse heart: validation, regional heterogeneity, and relation to refractoriness. *Journal of Cardiovascular Electrophysiology*, *12*(11), 1286–94.

[56]Knollmann, B.C., Kirchhof, P., Sirenko, S.G., Degen, H., Greene, A.E., Schober, T., Mackow, J.C., Fabritz, L., Potter, J.D., Morad, M. (2003). Familial hypertrophic cardiomyopathy-linked mutant troponin T causes stress-induced ventricular tachycardia and Ca^{2+}-dependent action potential remodeling. *Circulation Research*, *92*(4), 428–36.

[57]Knollmann, C., Schober, T., Petersen, A.O., Sirenko, S.G., Franz, M.R. (2006). Action potential characterization in intact mouse heart : steady-state cycle length dependence and electrical restitution. *Am J Physiol Heart Circ Physiol*, *0575*, 614–621.

[58]Koller, K., Rockwood, K. (2013). Frailty in older adults: implications for end-of-life care. *Cleveland Clinic Journal of Medicine*, *80*(3), 168–74.

[59]Kulminski, A., Ukraintseva, S.V., Akushevich, I., Arbeev K.G., Land, K., Yashin, A.I. (2007). Accelerated accumulation of health deficits as a characteristic of aging. *Exp Gerontol, 42,* 963-970.

[60]Lakatta, E.G., Levy, D. (2003). Arterial and Cardiac Aging: Major Shareholders in Cardiovascular Disease Enterprises: Part II: The Aging Heart in Health: Links to Heart Disease. *Circulation*, *107*(2), 346–354.

[61]Lakatta, E.G., Sollott, S.J. (2002). Perspectives on mammalian cardiovascular aging: humans to molecules. *Comparative Biochemistry and Physiology. Part A, Molecular & Integrative Physiology*, *132*(4), 699–721.

[62]Langford, D.J., Bailey, A.L., Chanda, M.L., Clarke, S.E., Drummond, T.E., Echols, S., Glick, S., Ingrao, J., Klassen-Ross, T., LaCroix-Fralish, M.L., Matsumiya, L., Sorge, R.E., Sotocinal, S.G., Tabaka, J.M., Wong, D., van den Maagdenberg, A.M.J.M., Ferrari, M.D., Craig, K.D., Mogil, J.S. (2010). Coding of facial expressions of pain in the laboratory mouse. *Nature Methods*, *7*(6), 447–9.

[63]Layland, J., Solaro, R.J., Shah, A.M. (2005). Regulation of cardiac contractile function by troponin I phosphorylation. *Cardiovasc Res, 66*(1), 12-21.

[64]Lee, D.H., Buth, K.J., Martin, B.-J., Yip, A.M., Hirsch, G.M. (2010). Frail patients are at increased risk for mortality and prolonged institutional care after cardiac surgery. *Circulation*, *121*(8), 973–8.

[65]Lehmann, K., Schmidt, K.F., Löwel, S. (2012). Vision and visual plasticity in ageing mice. *Restorative Neurology and Neuroscience*, *30*(2), 161–78.

[66]Li, H., Manwani, B., Leng, S.X. (2011). Frailty, inflammation, and immunity. *Aging and Disease*, *2*(6), 466–73.

[67]Li, L., Chu, G., Kranias, E.G., Bers, D. M. (1998). Cardiac myocyte calcium transport in phospholamban knockout mouse: relaxation and endogenous CaMKII effects. *The American Journal of Physiology*, *274*(4 Pt 2), H1335–47.

[68]Li, L., Desantiago, J., Chu, G., Kranias, E.G., Bers, D.M. (2000). Phosphorylation of phospholamban and troponin I in beta-adrenergic-induced acceleration of cardiac relaxation. *American Journal of Physiology. Heart and Circulatory Physiology*, *278*(3), H769–79.

[69]Lim, C.C., Apstein, C.S., Colucci, W.S., Liao, R. (2000). Impaired cell shortening and relengthening with increased pacing frequency are intrinsic to the senescent mouse cardiomyocyte. *Journal of Molecular and Cellular Cardiology*, *32*(11), 2075–82.

[70]Lim, C.C., Liao, R., Varma, N., Apstein, C.S. (1999). Impaired lusitropy-frequency in the aging mouse: role of Ca(2+)-handling proteins and effects of isoproterenol. *The American Journal of Physiology*, *277*(5 Pt 2), H2083–90.

[71]Liu, H., Graber, T.G., Ferguson-Stegall, L., Thompson, L.V. (2013). Clinically relevant frailty index for mice. *J Gerontol A Biol Sci Med Sci,* first published online December 13, 2013, doi:10.1093/Gerona/glt188.

[72]Liu, S.J., Wyeth, R.P., Melchert, R.B., Kennedy, R.H. (2000). Aging-associated changes in whole cell K(+) and L-type Ca(2+) currents in rat ventricular myocytes. *American Journal of Physiology. Heart and Circulatory Physiology*, *279*(3), H889–900.

[73]Loscalzo, J., Libby, O., Epstein, J. (2012). Basic Biology of the Cardiovascular System. In Harrison's Principles of Internal Medicine (New York, McGraw-Hill).

[74]Marx, S.O., Reiken, S., Hisamatsu, Y., Jayaraman, T., Burkhoff, D., Rosemblit, N., Marks, A.R. (2000). PKA phosphorylation dissociates FKBP12.6 from the calcium release channel (ryanodine receptor): defective regulation in failing hearts. *Cell*, *101*(4), 365–76.

[75]Meijis, M.F.L., Bots, M.L., Vonken, E-J.A., Cramer, M-J.M., Melman, P.G., Velthuis, B.K., van der Graaf, Y., Mali, W.P.Th.M., Doevendans, P.A. (2007). Rationale and design of the SMART heart study. *Neth Heart J, 15*(9), 295-298.

[76]Mitnitski, A.B., Mogilner, A.J., Rockwood, K. (2001). Accumulation of deficits as a proxy measure of aging. *TheScientificWorld*, *1*, 323–36.

[77]Mitnitski, A., Song, X., Skoog, I., Broe, G.A., Cox, J.L., Grunfeld, E., Rockwood, K. (2005). Relative fitness and frailty of elderly men and women in developed countries and their relationship with mortality. *J Am Geriatr Soc, 53*, 2184-2189.

[78]Mitnitski A.B., Mogilner, A.J., MacKnight, C., Rockwood, K. (2002). The mortality rate as a function of accumulated deficits in a frailty index. *Mech Ageing Dev, 123,* 1457-1460.

[79]Nadal-Ginard, B., Kajstura, J., Leri, A., Anversa, P. (2003). Myocyte death, growth, and regeneration in cardiac hypertrophy and failure. *Circulation Research, 92,* 139-150.

[80]Newman, A.B., Gottdiener, J.S., Mcburnie, M.A., Hirsch, C.H., Kop, W.J., Tracy, R., Walston, J.D., Fried, L.P. (2001). Associations of subclinical cardiovascular disease with frailty. *The Journals of Gerontology. Series A, Biological Sciences and Medical Sciences*, *56*(3), M158–66.

[81]Olivetti, G., Quaini, F., Lagrasta, C., Ricci, R., Tiberti, G., Capasso, J.M., Anversa, P. (1992). Myocyte cellular hypertrophy and hyperplasia contribute to ventricular wall remodeling in anemia-induced cardiac hypertrophy in rats. *The American Journal of Pathology*, *141*(1), 227–39.

[82]Ottenbacher, K.J., Ottenbacher, M.E., Ottenbacher, A.J., Acha, A.A., Ostir, G.V. (2006). Androgen treatment and muscle strength in elderly men: A meta-analysis. *Journal of the American Geriatrics Society*, *54*(11), 1666–73.

[83]Parks, R.J., Fares, E., Macdonald, J.K., Ernst, M.C., Sinal, C.J., Rockwood, K., Howlett, S.E. (2012). A procedure for creating a frailty index based on deficit accumulation in aging mice. *The Journals of Gerontology. Series A, Biological Sciences and Medical Sciences*, *67*(3), 217–27.

[84]Percy, D.H., Barthold, S.W. (2007). Pathology of laboratory rodents and rabbits. 3rd ed. Ames, IA: Wiley-Blackwell.

[85]Public Health Agency of Canada (2009). 2009 Tracking heart disease and stroke in Canada. Retrieved from http://www.phac-aspc.gc.ca/publicat/2009/cvd-avc/report-rapport-eng.php.

[86]Purser, J.L., Kuchibhatla, M.N., Fillenbaum, G.G., Harding, T., Peterson, E.D., Alexander, K.P. (2006). Identifying frailty in hospitalized older adults with significant coronary artery disease. *Journal of the American Geriatrics Society*, *54*(11), 1674–81.

[87]Puts, M.T., Lips, P., Deeg, D.J. (2005). Sex differences in the risk of mortality independent of disability and chronic diseases. *Journal of the American Geriatrics Society, 53*(1), 40-47.

[88]Rockwood, K., Fox, R.A., Stolee, P., Robertson, D., Beattie, B.L. (1994). Frailty in elderly people: an evolving concept. *CMAJ : Canadian Medical Association Journal = Journal de l'Association Medicale Canadienne*, *150*(4), 489–95.

[89]Rockwood, K., Hogan, D.B., MacKnight, C. (2000). Conceptualisation and measurement of frailty in elderly people. *Drugs & Aging*, *17*(4), 295–302.

[90]Rockwood, K., Mitnitski, A. (2007). Frailty in relation to the accumulation of deficits. *The Journals of Gerontology. Series A, Biological Sciences and Medical Sciences*, *62*(7), 722–7.

[91]Rockwood, K., Mitnitski, A. (2011). Frailty defined by deficit accumulation and geriatric medicine defined by frailty. *Clinics in Geriatric Medicine*, *27*(1), 17–26.

[92]Rockwood, K., Mitnitski, A., Song, X., Steen, B., Skoog, I. (2006). Long-term risks of death and institutionalization of elderly people in relation to deficit accumulation at age 70. *Journal of the American Geriatrics Society*, *54*(6), 975–9.

[93]Rockwood, K., Song, X., Mitnitski, A. (2011). Changes in relative fitness and frailty across the adult lifespan : evidence from the Canadian National Population. *CMAJ :*

Canadian Medical Association Journal = Journal de l'Association Medicale Canadienne, *183*(8), 487–494.

[94]Rodriguez, P., Kranias, E.G. (2005). Phospholamban: a key determinant of cardiac function and dysfunction. *Arch Mal Coeur Vaiss, 98,* 1239-1243.

[95]Scriven, D.R., Dan, P., Moore, E.D. (2000). Distribution of proteins implicated in excitation-contraction coupling in rat ventricular myocytes. *Biophysical Journal*, *79*(5), 2682–91.

[96]Shamliyan, T., Talley, K.M.C., Ramakrishnan, R., Kane, R.L. (2013). Association of frailty with survival: a systematic literature review. *Ageing Research Reviews*, *12*(2), 719–36.

[97]Shiga, A., Nakagawa, T., Nakayama, M., Endo, T., Iguchi, F., Kim, T.S., Naito, Y., Ito, J. (2005). Aging effects on vestibulo-ocular responses in C57BL/6 mice: comparison with alteration in auditory function. *Audiology & Neuro-Otology*, *10*(2), 97–104.

[98]Simmler, M., Zwaenepoel, I., Verpy, E., Guillaud, L., Elbaz, C., Petit, C., Panthier, J. (2000). Twister mutant mice are defective for otogelin, a component specific to inner ear acellular membranes, *Mammalian Genome, 11*, 961–966.

[99]Singh, M., Rihal, C.S., Lennon, R.J., Spertus, J.A., Nair, K.S., Roger, V.L. (2011). Influence of frailty and health status on outcomes in patients with coronary disease undergoing percutaneous revascularization. *Circulation. Cardiovascular Quality and Outcomes*, *4*(5), 496–502.

[100]Singh, M., Stewart, R., White, H. (2014). Importance of frailty in patients with cardiovascular disease. *European Heart Journal*, *35*(26), 1726–1731.

[101]Sjaastad, I., Wasserstrom, J.A., Sejersted, O.M. (2003). Heart failure- a challenge to our current concepts of excitation-contraction coupling. *J Physiol, 546*(1)*,* 33-47.

[102]Statistics Canada (2011). The Canadian population in 2011: Age and sex. Retrieved from http://www12.statcan.ca/census-recensement/2011/as-sa/98-311-x/98-311-x2011001-eng.cfm.

[103]Strozik, E., Festing, M.F.W. (1981). Whisker trimming in mice. *Laboratory Animals*, *15*(4), 309–312.

[104]Sumukadas, D., Jenkinson, F., Witham, M.D. (2009). Associations and consequences of hypophosphataemia in older hospitalised women. *Age and Ageing*, *38*(1), 112–5.

[105]Trammell, R.A., Cox, L., Toth, L.A. (2012). Markers for heightened monitoring, imminent death, and euthanasia in aged inbred mice. *Comp Med, 62,* 172-178.

[106]Ten Eick, R.E., Baumgarten, C.M., Singer, D.H. (1981). Ventricular dysrhythmia: membrane basis or of currents, channels, gates, and cables. *Prog Cardiovasc Dis, 24*, 157-188.

[107]Tevzadez, N., Rukhadze, R., Dzidziguri, D. (2005). The age related changes in cell cycle of mice cardiomyocytes. *Georgian Med News, 128,* 87-90.

[108]Torres-González, E., Bueno, M., Tanaka, A., Krug, L.T., Cheng, D.S., Polosukhin, V.V., Sorescru, D., Lawson, W.E., Blackwell, T.S., Rojas, M., Mora, A.L. (2012). Role of endoplasmic reticulum stress in age-related susceptibility to lung fibrosis. *American Journal of Respiratory Cell and Molecular Biology*, *46*(6), 748–56.

[109]Turturro, A., Witt, W.W., Lewis, S., Hass, B.S., Lipman, R.D., Hart, R.W. (1999). Growth curves and survival characteristics of the animals used in the Biomarkers of Aging Program. *The Journals of Gerontology. Series A, Biological Sciences and Medical Sciences*, *54*(11), B492–501.

[110]Ullman-Cullere, M.H., Foltz, C.J. (1999). Body condition scoring: a rapid and accurate method for assessing health status in mice. *Lab Anim Sci, 49,* 319-323.

[111]Valdivia, H.H., Kaplan, J.H., Ellis-Davies, G.C., Lederer, W.J. (1995). Rapid adaptation of cardiac ryanodine receptors: modulation by Mg2+ and phosphorylation. *Science, 267,* 1997-2000.

[112]van Empel, V.P.M., De Windt, L.J. (2004). Myocyte hypertrophy and apoptosis: a balancing act. *Cardiovasc Res, 63*(3), 487-499.

[113]Van Meer, P., Raber, J. (2005). Mouse behavioural analysis in systems biology. *Biochem J, 389(*3), 593-610.

[114]Van Winkle, T.J., Balk, M.W. (1986). Spontaneous corneal opacities in laboratory mice. *Lab Anim Sci, 36,* 248-255.

[115]Visser, M., Pahor, M., Taaffe, D.R., Goodpaster, B.H., Simonsick, E.M., Newman, A.B., Nevitt, M., Harris, T.B. (2002). Relationship of interleukin-6 and tumor necrosis factor-alpha with muscle mass and muscle strength in elderly men and women: the Health ABC Study. *The Journals of Gerontology. Series A, Biological Sciences and Medical Sciences*, *57*(5), M326–32.

[116]Walker, K.E., Houser, S.R. (1993). Age associated changes in membrane currents. *Cardiovascular Research*, (85), 1968–1977.

[117]Walston, J., Fedarko, N., Yang, H., Leng, S., Beamer, B., Espinoza, S., Lipton, A., Zheng, H., Becker, K. (2008). The physical and biological characterization of a frail mouse model. *The Journals of Gerontology. Series A, Biological Sciences and Medical Sciences*, *63*(4), 391–8.

[118]Wang, Q.-D., Pernow, J., Sjöquist, P.-O., Rydén, L. (2002). Pharmacological possibilities for protection against myocardial reperfusion injury. *Cardiovascular Research*, *55*(1), 25–37.

[119]Waters, D.L., Brooks, W.M., Qualls, C.R., Baumgartner, R.N. (2000). Skeletal muscle mitochondrial function and lean body mass in healthy exercising elderly. *Mech Ageing Dev, 124*(3), 301-309.

[120]Whitehead, J.C., Hildebrand, B.A., Sun, M., Rockwood, M.R., Rose, R.A., Rockwood, K., Howlett, S.E. (2014). A Clinical Frailty Index in Aging Mice: Comparisons With Frailty Index Data in Humans. *The Journals of Gerontology. Series A, Biological Sciences and Medical Sciences*, 1–12.

[121]Wolf, N.S., Li, Y., Pendergrass, W., Schmeider, C., Turturro, A. (2000). Normal mouse and rat strains as models for age-related cataract and the effect of caloric restriction on its development. *Experimental Eye Research*, *70*(5), 683–92.

[122]Wong, A.A, Brown, R.E. (2007). Age-related changes in visual acuity, learning and memory in C57BL/6J and DBA/2J mice. *Neurobiology of Aging*, *28*(10), 1577–93.

[123]Wu, L., Zhang, L., Ai, Z., Zou, L., Zhu, Y., Bao, Y., Li, J., Kang, S., Fan, H., Zhang, D., Fan, L., Liu, Z., Li, J. (2012). Association between risk factors and left ventricular remodeling in middle-aged and aged population: a community-based study. *J Hypertens, 30,* 1862-1873.

[124]Xiao, R., Spurgeon, H.A., Connor, F.O., Lakatta, E.G. (1994). Age-associated Changes in β-Adrenergic Modulation Excitation-Contraction Coupling Rat Cardiac. *Journal of Clinical Investigation*, *94*, 2051–2059.

[125]Xing, S., Tsaih, S., Yuan, R., Svenson, K.L., Jorgenson, L.M., So, M., Paigen, B.J., Korstanje, R. (2009). Genetic influence on electrocardiogram time intervals and heart rate in aging mice. *Am J Physiol Heart Circ Physiol, 296,* 1907–1913.

[126]Xu, A., Narayanan, N. (1998). Effects of aging on sarcoplasmic reticulum Ca2+-cycling proteins and their phosphorylation in rat myocardium. *The American Journal of Physiology*, *275*(6 Pt 2), H2087–94.

[127]Yang, Y., Lee, L.C. (201). Dynamics and heterogeneity in the process of human frailty and aging: evidence from the U.S. older adult population. *J Gerontol N Psychol Sci Soc Sci, 65,* 246-255.

[128]Yuan, C., Chen, W.-X., Zhu, J.-S., Chen, N.-W., Lu, Y.-M., Ou, Y.-X., Chen, H.-Q. (2013). IL-10 treatment is associated with prohibitin expression in the Crohn's disease intestinal fibrosis mouse model. *Mediators of Inflammation*, *2013*, 617145.

[129]Zhang, J., McDonald, K.M. (1995). Bioenergetic consequences of left ventricular remodeling. *Circulation, 92,* 1011-1019.

[130]Zhang, J., Yan, H., Löfgren, S., Tian, X., Lou, M.F. (2012). Ultraviolet radiation-induced cataract in mice: the effect of age and the potential biochemical mechanism. *Investigative Ophthalmology & Visual Science*, *53*(11), 7276–85.

Appendix A: Publications

Portions of this thesis have been published as follows:

Publications

Whitehead, J.C., Hildebrand, B.A., **Sun, M.**, Rockwood, M.R., Rose, R.A., Rockwood, K., Howlett, S.E. (2014). A Clinical Frailty Index in Aging Mice: Comparisons With Frailty Index Data in Humans. *The Journals of Gerontology. Series A, Biological Sciences and Medical Sciences*, 1–12.

Appendix B: Copyright permission letters

OXFORD UNIVERSITY PRESS LICENSE TERMS AND CONDITIONS

Aug 18, 2014

This is a License Agreement between Michael H Sun ("You") and Oxford University Press ("Oxford University Press") provided by Copyright Clearance Center ("CCC"). The license consists of your order details, the terms and conditions provided by Oxford University Press, and the payment terms and conditions.

All payments must be made in full to CCC. For payment instructions, please see information listed at the bottom of this form.

License Number	3439690627694
License date	Jul 31, 2014
Licensed content publisher	Oxford University Press
Licensed content publication	Journals of Gerontology - Series A: Biological Sciences and Medical Sciences
Licensed content title	A Clinical Frailty Index in Aging Mice: Comparisons With Frailty Index Data in Humans:
Licensed content author	Jocelyne C. Whitehead, Barbara A. Hildebrand, Michael Sun, Michael R. Rockwood, Robert A. Rose, Kenneth Rockwood, Susan E. Howlett
Licensed content date	06/01/2014
Type of Use	Journal/Magazine
Requestor type	Academic/Educational institute
Format	Electronic
Portion	Figure/table
Number of figures/tables	3
Will you be translating?	No
Author of this OUP article	Yes